

Molecular and metabolic characterization of  
assimilate uptake and storage product synthesis in  
*Brassica napus*

Von der Naturwissenschaftlichen Fakultät der  
Gottfried Wilhelm Leibniz Universität Hannover

zur Erlangung des Grades  
Doktorin der Naturwissenschaften  
(Dr. rer. nat.)

genehmigte Dissertation  
von  
Diplom – Biologin Christina König  
geboren am 03.03.1987 in Nauen

2017

Referentin/Referent: Dr. habil. Hardy Rolletschek

Korreferentin/Korreferent: Prof. Dr. Hans-Peter Braun

Tag der Promotion: 17.01.2017

## Zusammenfassung

Das bessere Verständnis um die Transport- und Anreicherungsprozesse von Metaboliten und Speicherreserven in Samen von *Brassica napus* ist ein wesentlicher Bestandteil aktueller Forschung. In dieser Arbeit wurde ein experimenteller Aufbau etabliert, der es erlaubt, den Fluss von Saccharose von maternalem Gewebe bis in den Samen zu verfolgen (mit Hilfe von  $^{13}\text{C}$  markiertem Substrat). Es konnte gezeigt werden, wie Zucker (und andere Assimilate) in frühen Stadien der Entwicklung durch den Funinkulus und die Samenschale in den Samen eindringen und sich anschließend gleichmäßig über das flüssige Endosperm im Samen verteilen. Entgegen vieler Vermutungen, gab es keine Hinweise über einen Transport der Saccharose zum Embryo über den Suspensor. Des Weiteren konnten organspezifische Unterschiede in metabolischer Aktivität, im Vergleich von flüssigem Endosperm sowohl zum Embryo als auch der Samenschale mit zellularisiertem Endosperm, aufgezeigt werden. Diese Daten repräsentieren wichtige Erkenntnisse um den generellen Samenmetabolismus und die Aufnahme von Assimilaten besser zu verstehen.

Ein weiterer wichtiger Bestandteil meiner Arbeit war die Charakterisierung von transgenen Linien von *B. napus*, welche eine Reduzierung der PEPC Enzymaktivität sowie eine massiv reduzierte Speicherproteinanreicherung anstrebten. Der erhaltene samenspezifische Phänotyp erleichterte die Identifizierung vieler wichtiger Änderungen auf metabolischer und genetischer Ebene. Die Samen der transgenen Linie zeigen einen Ausgleich im Proteingehalt, indem sie andere Proteinmengen, vor allem Oleosin2, für das fehlende Napin und Cruciferin erhöhen. Dies führt zu Änderungen in genetischen und zellulären Prozessen, die sich unter anderem in sehr ungewöhnlichen zellulären Membranstrukturen äußern. Entgegen vorangegangener Hypothesen, führte die Verringerung im Speicherproteingehalt zu einem erniedrigten Lipidgehalt im Samen mit etwas geänderten Fettsäureprofil. Die Analyse der transgenen Pflanzen führte zu neuen Einsichten im Kohlenhydratstoffwechsel und den Kontrollmechanismen für die Samen-zusammensetzung. Die gewonnenen Erkenntnisse sind Teil zukünftiger Projekte.

Schlagerworte: Rapssamen, Lipidstoffwechsel, Speicherproteine,  $^{13}\text{C}$  – Isotopenmarkierung, Oleosin

## Abstract & Summary

Understanding the delivery and accumulation processes of metabolites and storage reserves in seeds of *Brassica napus* is in the focus of modern research. In this work an experimental setup was established, tracing the flow of sucrose from maternal source tissues toward the seed (feeding of  $^{13}\text{C}$  labelled substrate). It is demonstrated how sugars (and other assimilates) travel through the funiculus, and then disperse through the seed coat and then evenly spread through the liquid endosperm during early stages of development. Against the expectations, no indications were found for movement of sucrose to the embryo via the suspensor. Furthermore, spatial differences in metabolic activity could be unraveled for the endosperm in comparison to both embryo and seed coat/aleurone layer. These data present important findings for general understanding of seed metabolism and assimilate uptake. Further important aim of my work was the characterization of transgenic lines of *B. napus* with reductions in PEPC enzyme activity and impaired storage protein accumulation. The observed seed-specific phenotype identified distinct molecular and metabolic rearrangements. Seeds of transgenic plants rebalance their protein content, with oleosin2 being one of the main substituents for the loss in napins and cruciferins. This caused changes in molecular and cellular processes including the appearance of very unusual membrane structures. Against previous hypothesis, the transgenic modulation of seeds, caused a lower lipid content with slightly changed fatty acid profile. The analysis of transgenic plants led to novel insights into carbon partitioning and control mechanisms for seed composition. These will be followed up in future work.

Keywords: Rapeseed, lipid metabolism, Seed storage proteins,  $^{13}\text{C}$  Isotope labelling, oleosin

## Table of contents

<b>Zusammenfassung .....</b>	<b>3</b>
<b>Abstract &amp; Summary .....</b>	<b>4</b>
<b>Table of contents .....</b>	<b>5</b>
<b>Abbreviations .....</b>	<b>7</b>
<b>List of figures.....</b>	<b>9</b>
<b>Tables directory .....</b>	<b>11</b>
<b>1. Introduction .....</b>	<b>13</b>
<b>2. Aims of this work.....</b>	<b>21</b>
<b>3. Methods and Material.....</b>	<b>22</b>
<b>4.1 Results Part I - The use of <sup>13</sup>C labelling to unravel sucrose uptake in developing oilseed rapeseed .....</b>	<b>34</b>
4.1.1 Establishing a procedure that allows <sup>13</sup> C-label uptake of seeds under near <i>in vivo</i> conditions .....	34
4.1.2 Test for various sugar substrates .....	35
4.1.3 The uptake of label is equal in all seeds along the silique.....	36
4.1.4 Use of <sup>13</sup> C labelling to follow sucrose uptake and metabolism in developing seeds .....	38
4.1.5 Label transfer along metabolic pathways differs among seed organs .....	39
4.1.6 Visualisation of <sup>13</sup> C-sucrose uptake in developing seeds of <i>B. napus</i> .....	42
4.1.7 Using <sup>13</sup> C - sucrose labelling to compare high-oil and low oil lines.....	43
<b>4.2 Results Part II - Characterisation of a transgenic <i>B. napus</i> plants with knockdown of PEPC-Napin-Cruciferin .....</b>	<b>45</b>
4.2.1 Analysis of down-regulation efficiency in the transgenic lines .....	45
4.2.1.1 The down-regulation of <i>cruciferin</i> , <i>napin</i> and <i>pepc</i> in embryos at 30 days after pollination .....	45
4.2.1.2 The down-regulation of <i>napins</i> and <i>cruciferins</i> shows a developmental pattern .....	47
4.2.2 The low level of down-regulation of PEPC transcripts is reflected in enzyme activity measurements .....	48
4.2.3 Characterisation of major seed traits .....	49
4.2.4 Evaluating the transgenic effect on embryo metabolism.....	51
4.2.4.1 Steady-state metabolite levels .....	51

4.2.4.2 Fatty acid profile of embryos at 30 DAP.....	53
4.2.5 Proteomics studies .....	53
4.2.5.1 Staining of protein storage vacuoles indicates less soluble protein .....	53
4.2.5.2 Quantification of total soluble protein using IEF SDS –PAGE .....	54
4.2.5.3 Mass spectrometry analysis and outcome of the proteomics study.....	55
4.2.6 Transcriptomics - Impact of the triple knockdown on gene expression pattern of embryo .....	58
4.2.6.1 General aspects .....	58
4.2.6.2 Transcript abundance of storage proteins.....	60
4.2.6.3 Rebalancing of amino acid demands in transgenic plants.....	60
4.2.6.4 No significant changes in PEPC transcript abundance in transcriptomics.....	61
4.2.6.5 No significant increase in transcript abundance of oleosins in the embryo of the transgenic line BCS580 .....	61
4.2.6.6 Transcriptomics revealed changes in sulfur metabolism.....	62
4.2.7 Further analysis of transgenic plants .....	63
4.2.7.1 Transgenic plants show a reduction in sulphur content.....	63
4.2.7.2 Transgenic seeds show a delayed germination.....	63
4.2.7.3 Respiratory activity does not differ between transgenic and wildtype plants .....	64
4.2.7.4 Transgenic and wildtype embryos have similar photosynthetic activity at physiological light conditions.....	65
4.2.8 Histology – demonstrating an extraordinary phenotype .....	67
4.2.9 The obtained phenotype in triple knockdown lines is probably not related to the low reduction in PEPC .....	69
4.2.9.1 Low down-regulation effect in <i>pepc</i> knockdown lines .....	69
4.2.9.2 The PEPC enzyme activity was not affected in embryos of <i>pepc</i> knockdown lines.....	70
4.2.9.3 Mature seeds of PEPC knockdown plants do not show any changes in seed traits .....	70
<b>5.1 Discussion PART I.....</b>	<b>71</b>
<b>5.2 Discussion PART II .....</b>	<b>75</b>
<b>6 Outlook .....</b>	<b>86</b>
<b>Supplement .....</b>	<b>87</b>
<b>References.....</b>	<b>100</b>
<b>Appendix.....</b>	<b>119</b>

## Abbreviations

ABI3	ABA-Insensitive3
ACCase	Acetyl-CoA carboxylase
acetyl-CoA	Acetyl coenzyme A
AP2/EREB	APETALA2/Ethylene Responsive Element Binding-like
ATP	adenosine triphosphate
cDNA	complementary DNA
DE	differentially expressed genes
DAP	days after pollination
DGAT	diacylglycerol acyltransferase
DHB	2,5-dihydroxybenzoic acid
DNA	deoxyribonucleic acid
DW	dry weight
EA-IRMS	elemental analyzer - isotope ratio mass spectrometer
ER	endoplasmatic reticulum
ETR	electron transport rate
FA	fatty acids
FUS3	transcription factor FUSCA3
G3P	glycerol-3-phosphate
GO	gene ontology
GPD1	glycerol-3-phosphate dehydrogenase
GUS	$\beta$ -Glucuronidase
HOLL	high oleic and low linolenic acids varieties
ICP-OES	inductively coupled plasma optical emission spectroscopy
IEF/SDS – PAGE	Isoelectric focusing/ sodium dodecyl sulfate - polyacrylamide gel electrophoresis

KAS	3-ketoacyl-ACP synthase
LC/MS	liquid chromatography–mass spectrometry
LEAR	low Erucic Acid Rapeseed-
MALDI–FT–ICR	matrix-assisted laser desorption/ionization - Fourier transform ion cyclotron reso- nance
mRNA	messenger ribonucleic acid
NAD <sup>+</sup>	nicotinamide adenine dinucleotide; oxidized form
NADH	nicotinamide adenine dinucleotide; re- duced form
NADPH	nicotinamide adenine dinucleotide phos- phate; reduced form
napA	napin A
NMR	nuclear magnetic resonance
PAM	pulse-amplitude modulation
PCR	polymerase chain reaction
PDC	pyruvate dehydrogenase complex
PEP	phosphoenolpyruvate
RNA	ribonucleic acid
RNAi	RNA interference
SAM	sequence alignment/map format
SD	standard deviation
SSP	seed storage protein
TAG	triacylglycerol
TD-NMR	time-domain NMR
TEM	transmission electron microscopy
TN	total nitrogen content
WTS	wild type segregant



## List of figures

Figure 1: The stages (I – V) of <i>B. napus</i> seed development based on embryo shape and age .....	16
Figure 2: Schematic overview over TAG synthesis in the embryo. ....	18
Figure 3: Silique incubation .....	35
Figure 4: Differences in <sup>13</sup> C-carbon uptake per mg seed.....	36
Figure 5: Distribution of seed weight and isotope abundance in seeds along the silique .....	37
Figure 6: Uptake of labeled <sup>13</sup> C sucrose into either silique or seed.....	37
Figure 7: Label uptake of seed organs.....	39
Figure 8: The level of <sup>13</sup> C-labelled metabolites in seed coat, endosperm and embryo ..	41
Figure 9: Mass spectrometry imaging of <sup>13</sup> C sucrose uptake into seeds. ....	43
Figure 10: Uptake of <sup>13</sup> C sucrose in two distinct rapeseed lines.. ....	43
Figure 11: Sucrose synthase mRNA expression level and enzyme activity in two contrasting rapeseed lines1. ....	44
Figure 12: Transcript level changes displayed as log2fold changes of <i>cruciferin</i> (A), <i>napin</i> (B) and <i>pepc</i> (C) isoforms in transgenic lines and corresponding wild type segregants (WTS).....	46
Figure 13: Transcript level changes displayed as log2fold change of napin and cruciferin isoforms. ....	47
Figure 14: Measurement of the Vmax PEPC enzyme activity in μmol/g fresh weight per minute of transgenic lines (light grey bars) compared to their corresponding WTS (black bars). ....	48
Figure 15: Overview on major seed traits at maturity.. ....	50
Figure 16: Steady state metabolite levels in embryos of transgenic and WTS plants measured by liquid chromatography/mass spectrometry.....	52
Figure 17: Fatty acid composition of embryos .....	53
Figure 18: Staining of protein vacuoles with 0.1% Ponceau - (A) or 0.02% Comassie solution (B).....	54
Figure 19: Overview on the calculation of protein spot volume difference in the Comassie gels based on three replicates per line and the generation of an overlay image. ....	55
Figure 20: Proteome structure of cruciferin chains obtained after separation for pI and kDa in WTS BCS581 and transgenic line BCS580 as well as the published separation of cruciferin chains (Nietzel et al., 2013).....	58
Figure 21: Overview over differential expression of genes in 36 categories, that show higher (red) or lower (blue) abundance in the transgenic line BCS580 compared to the wildtype line BCS581. ....	59
Figure 22: GO ontology mapping of the reads regarding biological processes overrepresented in the embryo of the transgenic line BCS580 compared to the WTS BCS581. ....	59

Figure 23: Calculated amino acid demands for protein synthesis in the transgenic line BCS580 compared to the WTS based on differential expression of genes, obtained from the RNA Seq data. ....	61
Figure 24: The total sulphur content in seeds (30 DAP) was measured by inductively coupled plasma optical emission spectroscopy (ICP-OES).....	63
Figure 25: Time curve of germination of seeds from transgenic (BCS580) and WTS (BCS581) plants taken from the same batch (growth period). Seeds were .....	64
Figure 26: Respiration rates measured as uptake of O <sub>2</sub> . (see methods for details) values are means ± SD (n = 5). ....	64
Figure 27: Gradients in <i>B. napus</i> seed photosynthesis measured by the Imaging-PAM Chlorophyll Fluorometer.....	66
Figure 28: TEM - Histology of outer cotyledon cells of seeds (50 DAP).....	67
Figure 29: Immunostaining of cotyledons at almost mature stage of development (50 DAP). ....	68
Figure 30: Transcript level changes displayed as log <sub>2</sub> fold change of <i>pepc</i> genes in embryos of the <i>pepc</i> single knockdown line and corresponding wildtype.. ....	69
Figure 31: Measurement of the V <sub>max</sub> PEPC enzyme activity in μmol/g fresh weight per minute of <i>pepc</i> single transgenic lines (grey) compared to their corresponding wildtype (dark grey bars). ....	70
Figure 32: Measurement of the lipid content as % of dry weight of intact mature seeds of the three <i>pepc</i> single transgenic lines and their corresponding WTS. ....	70

## Supplemental Figures

Figure S 1: Uptake of <sup>15</sup> N glutamine into 1 mg of siliques or seeds that were incubated in a solution containing 20mM of <sup>15</sup> N gklutamine for 24 to 96 hours.....	91
Figure S 2: Starch content in % of the seed dry weight in mature seeds of all tested transgenic lines.....	91
Figure S 3: Starch content in mg per g embryo dw at 37 DAP .....	92
Figure S 4: Temporal expression profile of oleosins in transgenic lines compared to their wildtype. ....	92

## Tables directory

Table 1: The primers used for quantitative real – time PCR analysis of PEPC, napins and cruciferins in <i>B. napus</i> embryos .....	26
Table 2: Concentrations of metabolites in the distinct seed organs given in mM and measured using LC/MS.....	40
Table 3: Top 10 proteins, that show a higher abundance in the transgenic line BCS580 .....	56
Table 4: Top 10 proteins, that show a lower spot volume in the transgenic line BCS580 .....	57
Table 5: Overview over differential expressed genes related to sulfur metabolism and transport.....	62

## Supplemental Tables

Table S 1: Filtered Masses and potentials of MS/MS transitions in negative mode. DP Declustering Potential, EP Entrance Potential, CE Collision Energy, CXP Collision Cell Exit Potential.....	87
Table S 2: Primers used for Oleosin real-time PCR .....	90
Table S 3: Proteins with higher spot volume in the transgenic line (BCS580) .....	93
Table S 4: Proteins with lower spot volume in the transgenic line (BCS580) .....	94
Table S 5: Amino acid sequences of seed storage proteins .....	98
Table S 6: Seed relevant traits for the tested PEPC single transgenic line (grayed) and the corresponding WTS.....	99



## 1. Introduction

In the family of *Brassicaceae*, oilseed rape (*Brassica napus* L.) is the most popular cultivated crop worldwide. *B. napus* ssp. *napus* includes winter and spring oilseed, fodder and vegetable rape forms, and ranks third in the global consumption of vegetable oils after oil palm and soybean oils (<http://www.statista.com>). Rapeseed oil is highly nutritional food oil and provides the raw materials for biodiesel production. The oil content ranges from 40 to 50% and the residual meal is rich in protein and used mainly for animal feed and human food. Rapeseed is mostly produced for low erucic and low glucosinolate varieties or so-called canola (Canadian oil low acid) quality. It contains the lowest level of saturated fatty acids and is recommended as healthy fatty acid profile. This composition maintains the balance of blood cholesterol and prevents heart disease risks (Gillingham *et al.*, 2011). Due to the remarkable increase of oilseed rape production in recent years it has become a focus for breeding and molecular genetics.

### 1.1 *B. napus* as a target of crop improvement

#### 1.1.1 Breeding success in oilseed rape

Advanced breeding programs aiming to produce edible rapeseed oil with low erucic acid as well as glucosinolates (Low Erucic Acid Rapeseed- LEAR) have greatly influenced the increase of oilseed rape production (Snowdon *et al.*, 2007). More challenging was the breeding of high oleic and low linolenic acids varieties (HOLL). These are lower in saturated lipids and thus favorable for food productions (Mailer 2009). As a result of *B. napus* breeding, Canola (Canadian oil) quality was originally produced which include all LEAR varieties that contain very low amounts of erucic acid (< 2%; Kimber and McGregor 1995). In addition to edible oils, oilseed rape has advanced applications to produce biodiesel as a source of energy and rape meal for livestock feed having high protein amount (Snowdon *et al.*, 2007).

### 1.1.2 Genetic engineering of *B. napus* to improve crop quality

With the development of genetic engineering and transgene production, there have been many efforts toward improving crop or seed products. The main focus in rapeseed has been the elevation of triacylglycerol (TAG) levels inside the seed and the modification of fatty acid composition (Dyer and Mullen, 2008; Napier, 2007). The main strategies for increasing plant lipids either interfere in the fatty acid biosynthesis pathway by up-regulation of relevant enzymes, increasing TAG assembly or preventing TAG breakdown (which occurs at the end of seed maturation by targeting TAG lipases and  $\beta$ -oxidation). One successful approach used the overexpression of fatty acid synthesis related genes like diacylglycerol acyltransferase (DGAT) in seeds (Weselake *et al.*, 2008; Jako *et al.*, 2001). Previous experiments with developing seeds of *B. napus* have suggested that DGAT activity may have a substantial effect on carbon flow into seed oil (Perry and Harwood, 1993; Perry *et al.*, 1999). Upregulation of DGAT in seeds resulted in an increase of lipid content of up to 14% (Jako *et al.*, 2001). Another study showed that an overexpression of acetyl-coenzyme A carboxylase in *B. napus* resulted in 6% seed oil increase (Roesler *et al.*, 1997). A much higher increase in oil content of up to 40% in *B. napus* could be achieved when overexpressing the *glycerol-3-phosphate dehydrogenase* GPD1 (Vigeolas *et al.*, 2007). Approaches that try to block TAG breakdown at the end of seed maturation have used suppression of *Sugar-dependent 1* (SDP1), which is a specific lipase for the first step of TAG catabolism during seed germination (Eastmond *et al.*, 2006). The RNAi suppression of SDP1 led to an increase in seed oil content of up to 8% in *B. napus* and up to 30% in *Jatropha curcas* (Kelly *et al.*, 2013; Kim *et al.*, 2014). More recent approaches have discovered the advantages of combining different genetic targets in one approach. For example, a combined overexpression of *dgat* and *wril* in *Nicotiana benthamiana* transient leaf expression system resulted in TAG levels exceeding those expected from an additive effect (Vanhercke *et al.*, 2013). Another push and pull strategy in *A.thaliana* showed that even a stack of three genes - a combined overexpression of *dgat* and *wril* and a down-regulation of *sdp1* led to an increase in seed lipid content (van Erp *et al.*, 2014).

## 1.2 *Brassica napus* seed development

In the life cycle of plants, seed production is an essential process for plant reproduction. Male and female gametes are produced during meiosis within the anthers and ovaries. In angiosperm, the fusion of male and female gametes in a double fertilization event produces a single-cell diploid zygote (the embryo) and the triploid endosperm. The embryo consists of embryonic axis with shoot and root poles required for seedling growth and development, and two (inner and outer) cotyledons. The cotyledons in the mature seed contain high levels of storage products such as proteins and lipids (West and Harada, 1993; Möller and Weijers, 2009, Borisjuk *et al.*, 2013). The production of storage reserves in the embryo is highly dependant on assimilate supply from maternal tissues. In the early stages of seed development, sugars (sucrose) enter the seed and are converted to hexoses via invertases located in the endosperm. This is connected with water uptake and volume increase. At a certain time point, the embryo switches from cell division to cell expansion, and sucrose is primarily used to build up storage reserves (Baud *et al.*, 2002; Hill *et al.*, 2003). To understand the development of the embryo inside the seed, it is crucial to unravel the pathways of nutrient supply from maternal tissues and subsequent metabolism inside the seed. There is evidence that the pod becomes the main photosynthetically active source for assimilate delivery from maternal tissue during later development (there is significant leaf senescence before and during seed filling). Thus, the pod is not only protection against adverse external influences (Mendham and Salisbury, 1995). But also the seed organs themselves have distinct functions during development. The triploid endosperm is consumed during embryogenesis but plays an important role in providing carbon resources (Hill *et al.*, 2003); it also contributes to seed size control and correct anatomical structure (Borisjuk *et al.*, 2013). For *Arabidopsis* and *Lepidium* spp. it was shown that the endosperm undergoes a cellularization process that begins in the micropylar region and spreads to central and chalazal region (e.g. Brown *et al.*, 1999, Debeaujon *et al.*, 2000, Nguyen *et al.*, 2000, Windsor *et al.*, 2000). Also in mature *B. napus* seeds, the endosperm is depleted to a single aleurone layer (Müller *et al.*, 2006). Consequently after maturation the embryo is entirely filling the whole seed (figure 1). The contribution of the seed-coat (testa) to the metabolism of *B. napus* seeds has not been studied extensively; there are some studies focussing on the biosynthesis of flavonoids (Auger *et al.*, 2010). The seed coat is the maternal tissue that channels sugars from the source to the embryo and there is evidence that carbon flow

from the maternal photosynthetic active tissue is facilitated by the seed coat (King *et al.*, 1997; Sheen *et al.*, 1999; Weber *et al.*, 1995; Wobus and Weber, 1999).

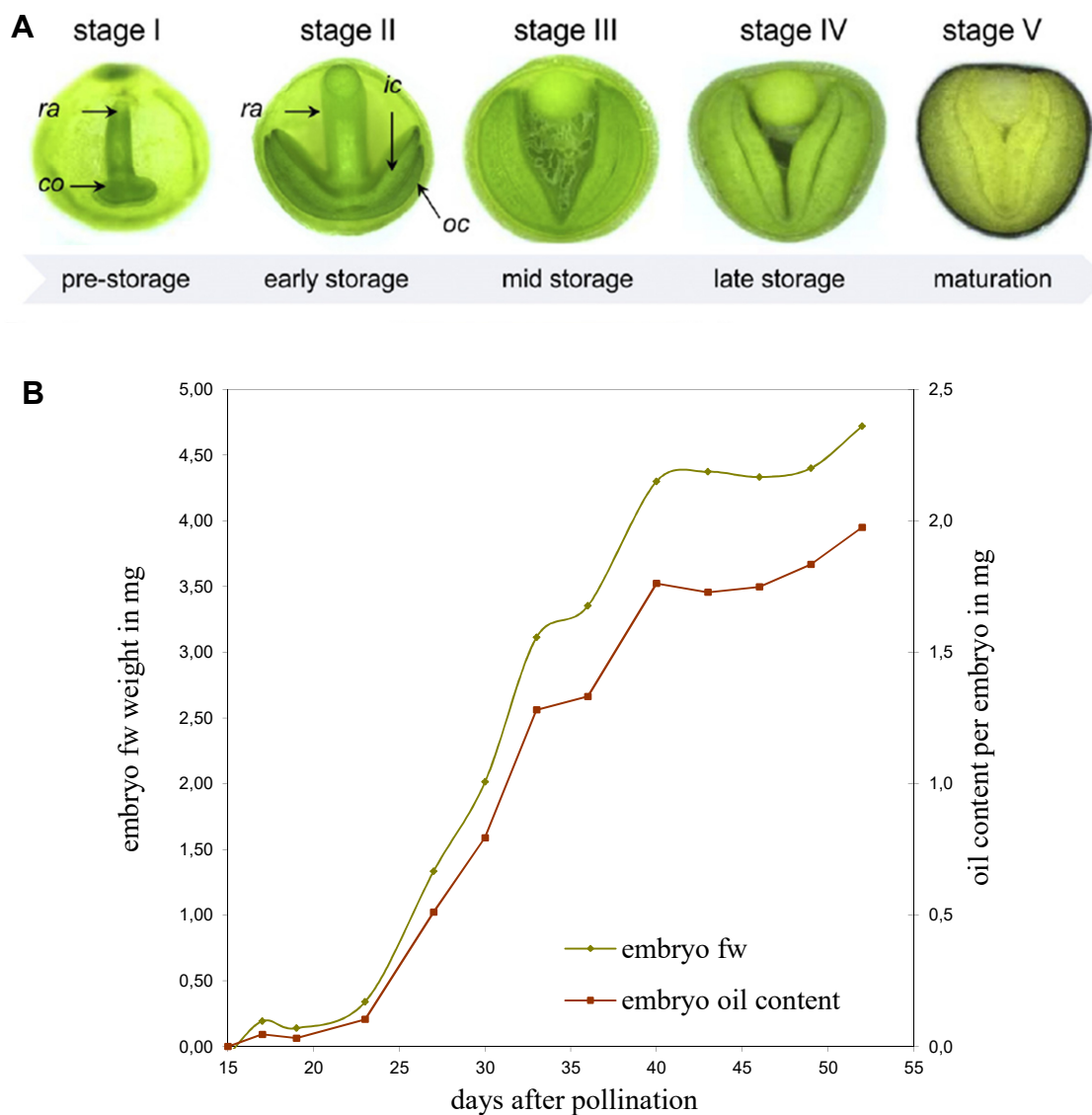


**Figure 1:** The stages (I – V) of *B. napus* seed development based on embryo shape and age (A; taken from Borisjuk *et al.*, 2013) and the increase in seed oil content with increasing embryo fresh weight during development (B). ra - radicle, co - cotyledons, ic - inner cotyledon, oc - outer cotyledon



## 1.3 Main seed storage components

### 1.3.1 Lipids

The seed of *B. napus* has several ways to store carbon and energy (to be used upon germination). One of the major sources for high-density energy are lipids, mostly triacylglycerols (TAG). These may account for up to 50% of mature seed dry weight (Baud *et al.*, 2002; O'Neill *et al.*, 2003). In germinating seedlings, TAG is broken down through  $\beta$ -oxidation to yield acetyl-CoA for energy production and gluconeogenesis (Theodoulou & Eastmond, 2012). The distinct functions and the value of seed oil is mainly dependant on the fatty acid composition of the TAGs. *B. napus* mainly consist of primarily five different FA, the saturated 16:0 and 18:0, the monounsaturated 18:1 and the polyunsaturated 18:2 and 18:3 (carbons:double bonds). The generation of TAGs occurs mainly in the embryo, which has to import sucrose and further degraded via phosphoenolpyruvate (PEP) and the (mostly cytosolic) glycolytic pathway (figure 2). Next, PEP is imported into the plastids and irreversibly converted to pyruvate by plastidic pyruvate kinase (Andre *et al.*, 2007; Baud *et al.*, 2007). Subsequently, acetyl-CoA is produced by the pyruvate dehydrogenase complex (PDC) in an oxidative decarboxylation reaction (Lutziger and Oliver, 2000; Lin *et al.*, 2003). The first enzyme of *de novo* fatty acid synthesis is ACCase, which initiates the ATP-dependent carboxylation of acetyl-CoA to form malonyl-CoA in the plastids (Turnham and Northcote, 1983; Harwood, 1996, Sasaki and Nagano, 2004). In particular this reaction is believed to be a key regulatory step in fatty acid biosynthesis (Thelen and Ohlrogge, 2002). There is evidence, that the production of malonyl-CoA by ACCase is regulated and represents a rate-limiting step for fatty acid biosynthesis in plants (Post-Beittenmiller *et al.*, 1991, 1992; Roughan, 1997). The substrate for the following sequential two carbon elongation is catalyzed by different 3-ketoacyl-ACP synthase (KAS) enzymes. FA synthesis up to 18 carbons and one double bond takes place within the plastid (Li-Beisson *et al.*, 2010). The fatty acids are then transferred to the cytoplasm. The final assembly of TAG takes place in the endoplasmatic reticulum (ER). Biosynthesis of TAG mainly occurs via the Kennedy or glycerol-3-phosphate (G3P) pathway in which three acyl chains are esterified to a glycerol backbone (Kennedy, 1961). Several pathways interconnected with TAG biosynthesis have been described in maturing oilseeds, including the generation of membrane phospholipids (Bates *et al.*, 2009; Bates *et al.*, 2011). Storage of TAG occurs in specialized organelles, the oil bodies in the cytosol. TAGs in the oil bodies are surrounded by a

phospholipid monolayer (Yatsu and Jacks, 1972). This monolayer also contains proteins, making up about 4% of the total oil body weight. Among these proteins, oleosins are the most abundant ones (Huang, 1992; Tzen and Huang, 1992; Tauchi-Sato *et al.*, 2002). The regulation of TAG synthesis has been elucidated to a large extent. For *A. thaliana* there are several transcriptional regulatory factors known that play an important role in lipid synthesis in oilseeds (Baud and Lepiniec, 2009). Especially WRINKLED1, a transcription factor of the AP2/EREB family, has been shown to control genes involved in sugar transfer/breakdown (glycolysis), fatty acid biosynthesis and TAG assembly (Cernac and Benning, 2004). Also FUS3, ABI3 and LEC2, as well as the transcriptional activator LEC1, have been shown to be master regulators of seed development and reserve product accumulation (Santos-Mendoza *et al.*, 2008).

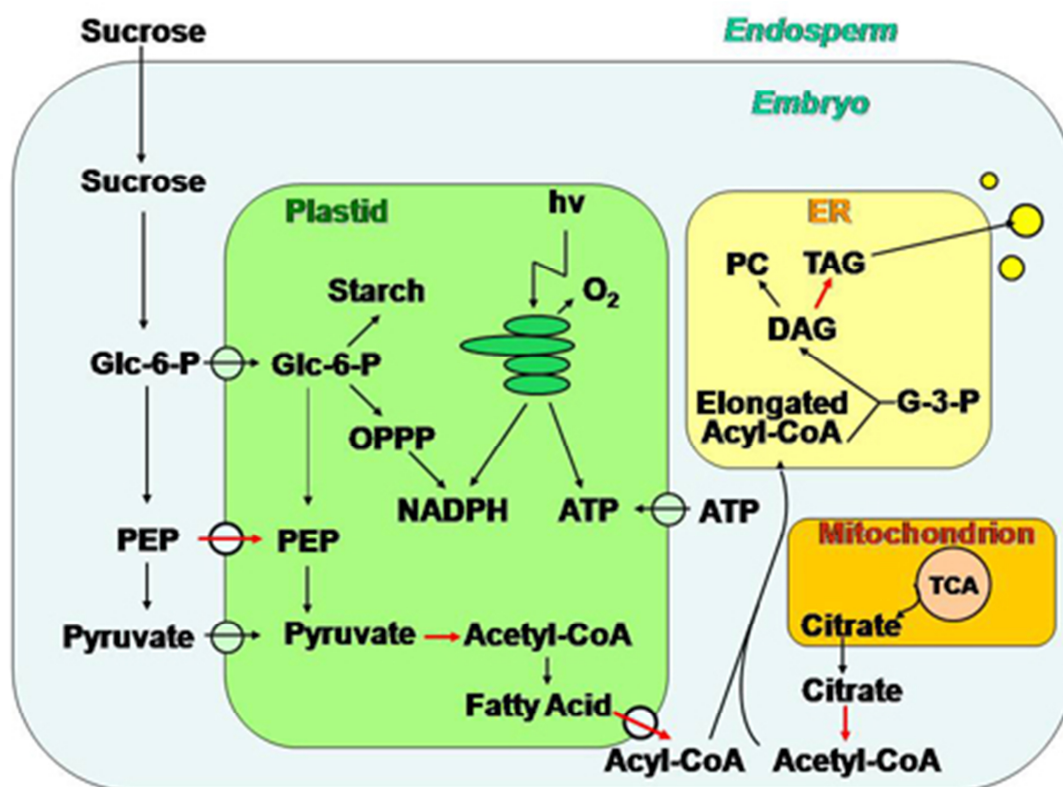


**Figure 2:** Schematic overview over TAG synthesis in the embryo. Taken from <http://www3.botany.ubc.ca/kunst/oil.htm>; modified from Hills M.J. (2004) Control of storage product synthesis in seeds. *Current Opinion in Plant Biology* Volume 7, Issue 3, Pages 302–308.

### 1.3.2 Storage proteins

In *B. napus* the major seed storage proteins are cruciferins (12S globulins) and napins (2S albumins), which account for 60% and 20%, respectively, of total protein in mature seeds (Crouch & Sussex, 1981). These storage proteins serve as an important nitrogen and carbon source during germination and are rapidly degraded. The main synthesis phase of the napins and cruciferins occurs following embryo expansion at ~25-30 days after pollination (DAP). Both storage proteins are synthesized as precursors, which are transported to the vacuoles via the ER and the Golgi apparatus. These vacuoles then form protein bodies and the precursors are further processed to the final napins and cruciferins (Chrispeels *et al.*, 1982; Rödin *et al.*, 1990). The expression of the corresponding genes in the tissues of the embryo is concisely controlled and can be considered as an important characteristic of seed maturation (Gutierrez *et al.*, 2007). Studies in *Arabidopsis* have shown that the regulation of seed storage proteins is mainly enforced by B3 and bZIP transcription factors, which bind to cis-elements in the promotor regions of the seed storage protein (SSP) (Ellerstrom *et al.*, 1996; Ezcurra *et al.*, 1999; Ezcurra *et al.*, 2000; Nakabayashi *et al.*, 2005; Suzuki *et al.*, 2005). Overall there is only little knowledge about mutants with defects in SSP-encoding genes. Due to the large gene redundancy, single mutants often lack a phenotype (Kohno-Murase *et al.*, 1994). The structure of the cruciferin complex of *B. napus* has recently been shown to possess a unique octameric barrel-like structure, optimized for maximal storage of amino acids within minimal space. Each subunit consisting of an  $\alpha$ - and  $\beta$ -chain linked by a disulfide bond, which are present in various isoforms (Nietzel *et al.*, 2013). In *B. napus*, five different cruciferins exist, that belong to three different families. In contrast, the 2S albumins form a heterodimer, built by a large and small peptide, that are linked by a disulfide bond (Krebbbers *et al.*, 1988; Guerche *et al.*, 1990).

During seed maturation of *B. napus*, besides accumulation of nutritional seed storage proteins, seeds also accumulate other proteins such as oleosins. As mentioned before, these are small hydrophobic proteins proposed to function in maintaining the structural integrity of oil bodies and serving as a recognition signal for lipase binding during oil mobilization in seedlings (Lee *et al.*, 1991; Huang, 1996, Hsieh and Huang, 2004; Siloto *et al.*, 2006; Wilfling *et al.*, 2013). Studies also show a possible role in oil body stability (Leprince *et al.*, 1998; Shimada *et al.*, 2008) and in the regulation of oil body repulsion (Heneen *et al.*, 2008), preventing the fusion of oil bodies into a single

organelle (Schmidt and Herman, 2008). In *A. thaliana* the major oleosins found in developing seeds are OLE1 (At4g25140), OLE2 (At5g40420), and OLE4 (At3g01570) (Jolivet *et al.*, 2004).

### 1.3.3 Carbohydrates

In seeds of *B. napus*, starch plays an important role as a transiently stored seed component (Andriotis *et al.*, 2010). Studies suggest that starch accumulation is functionally linked to cell division and differentiation of the embryo (Andriotis *et al.*, 2010). In embryos of early to mid storage phase high starch deposition was associated with cell growth; starch content later declined during later stages when lipid accumulation occurs (Borisjuk *et al.*, 2013). In mature seeds, starch is nearly absent.

## **2. Aims of this work**

### **I. Unravel the pathway and characteristics of sucrose uptake and subsequent metabolism in developing *B. napus* seeds**

As the understanding of assimilate and sugar delivery from maternal source organs to the seed/embryo still remains fragmentary, one aim of this study was to investigate how sugars are provided to the developing embryo. This needed to establish a method which delivers  $^{13}\text{C}$  - labelled sugars toward seed/embryo in a procedure which closely mimics maternal sugar supply *in vivo*. This method should then be used to investigate the temporal and tissue-specific distribution as well as subsequent metabolism of sugars. It eventually aimed to unravel potential functions and metabolic contributions of the various seed organs.

### **II. Characterization of transgenic *B. napus* plants with seed-specific modulation of storage activity (knockdown of PEPC + Napin + Cruciferin)**

Previous work has suggested that a combined down-regulation of PEPC and the major storage proteins (napin and cruciferin) might shift storage activity from proteins towards lipids, resulting in higher oil content of mature seeds. Transgenic plants have been generated to test this hypothesis. My aim was to characterize these transgenic plants, in particular relevant seed traits including storage compounds and potential metabolic shifts. To this end, a combined analysis of the transcriptome, the proteome and the metabolome was performed as well as various physiological assays were done using the developing embryo. This part of work aimed to elucidate control mechanisms for storage metabolism.

### 3. Methods and Material

#### 3.1 Plant material and growth conditons

If not stated otherwise, *B. napus* plants were grown in a glasshouse with 16 h light: 8 h dark, 250  $\mu\text{mol}$  photosynthetically active radiation  $\text{m}^{-2}$ ,  $\text{s}^{-1}$ , at 22°C and 60% relative humidity. Plant growth was restricted to the main stem and two lateral stems, side shoots were removed upon emergence. Flowers were tagged on the day of anthesis. Plants used in these experiments were either natural accessions derived from the IPK Gatersleben genebank (CR3231, CR3170, Reston) or provided by the company Bayer-Crop Science (BCS transgenic lines and corresponding wild type segregants).

#### 3.2 Silique culture and isotope labelling

For isotope labelling experiments, siliques from *B.napus* were harvested, cut with scalpel and immediately placed in the solution containing  $\frac{1}{4}$  Murashige and Skoog medium, 2mM MES and a pH of 5,6. Additionally an appropriate quantity of labelled compounds - as a sugar source either  $^{13}\text{C}_{12}$  - sucrose or  $^{13}\text{C}_6$  – glucose (Campro Scientific; Berlin, Gemany) – was used. In some experiments as a nitrogen source,  $^{15}\text{N}$  glutamine was used (Campro Scientific; Berlin, Gemany).The incubation time varied for the different experiments and is described in each chapter, if not differentially mentioned, incubation conditions were similar to the growth conditions. At the end of the incubation, seeds were removed from the siliques; embryos were rapidly dissected and frozen at -80°C or dried at 70°C until further analysis. The measurement of  $^{13}\text{C}/^{15}\text{N}$  label in the carbon and nitrogen fraction was carried out using dried, pulverized plant material by an elemental analyzer coupled to an isotope ratio mass spectrometer (EA-IRMS; Elementar Analysensysteme GmbH, Hanau, Germany).

#### 3.3 Germination

Mature seeds were sprinkled on three 10 cm diameter glass-microfiber filter discs (Whatman GF/A paper) wetted with 1.0 ml sterilized water and placed in 10 cm diameter Petri-dishes, which were sealed with Parafilm, packaged in aluminum foil and put in a growth chamber (23°C, 14h light of 100  $\mu\text{E m}^{-2}\text{s}^{-1}$ ). Germination was followed and germinated seeds were counted.

### **3.4 Measurements of seed components**

#### **3.4.1 Calculation of the protein content based on the measurement of the total nitrogen content**

The protein content was calculated on the basis of nitrogen content, which was measured using an elemental analyzer - Vario Micro Cube (EA-IRMS; Elementar Analysensysteme GmbH, Hanau, Germany). Thoroughly dried samples were ground and weighted in thin zinc foils to enhance combustion with pure oxygen. High purity helium is used as carrier gas. The resulting gases CO<sub>2</sub> and NO<sub>x</sub> (the latter is further reduced to N<sub>2</sub>) are brought to a defined pressure/volume state and are passed to a gas chromatographic system. Blank values are taken from empty zinc foils. Acetanilide was used as a standard for calibration with known C (71.09 %) and N (10.36 %) content. The obtained N content of the samples was multiplied with the factor 5.7 (Sosulski and Imafidon, 1990) to yield total protein content in the analysed sample. This approach is based on two assumptions that seed carbohydrates and lipids do not contain nitrogen, and that nearly all of the nitrogen in the seed is present as amino acids in proteins.

#### **3.4.2 Measurement of Starch**

Seeds were ground in a Retsch TissueLyser (Quiagen GmbH, Hilden, Germany) and dried overnight at 70°C to remove traces of water. 20 mg of seed powder were used for extraction and mixed throughoutly with 1 ml 80% ethanol and then incubated for 30 minutes at 60°C. After centrifugation at 13.000 rpm for 10 minutes, the supernatant was removed and the pellet mixed with 500 µl 80% ethanol. The subsequent incubation and centrifugation was repeated twice. The yielded pellet was rinsed with distilled water and taken for starch extraction. For starch extraction, the remaining pellet was suspended in a solution containing 0.5 M KOH and incubated at 95°C shaking for 1 h, followed by the adjustment of the pH to 5-7 using 5 N hydrochloric acid. 20 µl of this sample were then mixed with 100 µl of amyloglucosidase buffer (100 mM tri sodium citrate dihydrate pH 4.6 and amyloglucosidase 75 U/ml) and incubated for 30 minutes shaking at 60 °C. To measure the starch content, in a cuvette, the prepared starch extract together with 750 µl of the measurement buffer (100mM imidazole pH 6.9, 5mM MgCl<sub>2</sub>, 2 mM NAD and 1 mM ATP) and 2 µl of glucose – 6 – phosphate – dehydrogenase were mixed and after 10 minutes the absorbance was measured at 340 nm to yield a baseline value. Subsequently 10 µl of hexokinase (diluted 1:1) was added and after an incubation time

of 25 minutes the second measurement at 340 nm was carried out. From the difference in absorbance, one can calculate the amount of starch present in the sample.

### **3.4.3 Total seed lipid and fatty acid measurement**

Lipid content in mature seeds of *B. napus* cultivars was measured in a low-field TD-NMR machine for high-throughput measurements (Minispec mq60 Bruker BioSpin GmbH, Rheinstetten, Germany). The NMR instrument has proton frequency of 60 MHz (1.4 T). The applied pulse sequence was set as described previously in Rolletschek et al. (2015). Fatty acid composition was assessed by gas chromatography, following a procedure with transesterification as in Borisjuk et al. (2013a).

## **3.5 Enzyme assays**

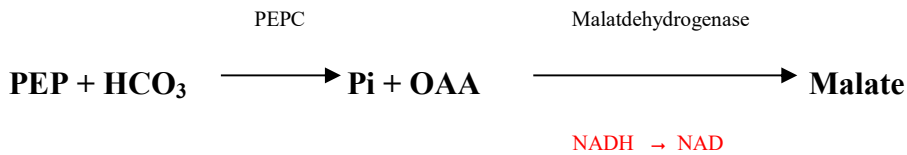
### **3.5.1 Preparation of plant enzyme extracts**

For the preparation of enzyme extracts, samples of frozen seeds were preweight and ground in liquid nitrogen using prechilled mortar and pistil. To the powder 3x extraction buffer containing 100 mM MOPS, 10 mM MgCl<sub>2</sub>, 1 mM EDTA, 1 mM EGTA, 2 mM DTT, 1 mM PMSF adjusted to a pH of 7.4 was immediately added. The mixture was then transferred to a prechilled 2 ml reaction tube and kept on ice. In a centrifuge cooled to 4°C, the sample was spun at maximum speed for 5 minutes and the supernatant was transferred to a fresh prechilled tube on ice. The extract was then either used for prompt measurement or frozen at -80°C for longer storage.



### 3.5.2 Measurement of phosphoenolpyruvate carboxylase enzyme activity

The measurement of the PEPC enzyme activity is based on the following reaction:



The reaction buffer contained the following substrates: 25 mM TRIS, 5 mM MgCl<sub>2</sub>, 2 mM DTT, 1 mM KHCO<sub>3</sub>, 0.2mM NADH, 5 mM Glu-6-P and was adjusted to pH 8.0 using hydrochloric acid. All enzymes and samples should be kept on ice. If the buffer was used for measurement, to 20 ml of buffer 14,4 µl malate dehydrogenase was added. Immediately before the start of the measurement 50mM phosphoenolpyruvate (PEP) was added to start the reaction. Each sample was measured twice in parallel. The decline in absorbance at 340 nm was monitored and activity was then calculated as µmol/g fresh weight \* min.

## 3.6 Methods for transcriptome analysis

### 3.6.1 RNA extraction and RNA-sequencing

Total RNA was extracted from various tissues at different stages following the instruction manual of the Spectrum™ Plant Total RNA Kit (Sigma-Aldrich Chemie GmbH, Germany), as and it was then treated with RNase-free DNaseI (NEW ENGLAND Biolabs, Ipswich, MA, USA) to remove any contaminating DNA. A 1 µg aliquot of total RNA extracted from the embryo material was converted to single stranded cDNA using a RevertAid First Strand cDNA Synthesis kit (ThermoScientific, Germany). A 100 ng template of this cDNA provided the template for a qPCR based on the SYBR® Green PCR Master Mix (Invitrogen, Germany). The necessary primers, designed with Primer3 software (<http://primer3.ut.ee>) to generate an amplicon size of 150–200 bp, targeted mainly the 3'-UTR of the selected genes (three pairs of primers per gene). The specificity and amplification efficiency of each primer pair was checked by means of running standard curves with melting curves. The quantitative real-time PCR conditions were as follows: 95°C for 1 min; 40 cycles of 95°C for 30 s, 55°C for 30 s, 72°C for 30 s; and 72°C for 10 min for the final extension. The primers used for real-time PCR are listed in

Table. Each assay comprised three biological replicates, each of which was repeated three times. Relative transcript abundances were estimated using the  $2^{-\Delta\Delta C_t}$  method (Livak and Schmittgen, 2001). The chosen reference sequence for normalization purposes was the housekeeping gene ubiquitin carrier protein 9 (UBC9). Means were statistically compared using the Students' *t*-test. Primer sequences used in qPCR are listed in Table 1.

**Table 1:** The primers used for quantitative real – time PCR analysis of PEPC, napins and cruciferins in *B. napus* embryos

<b>Gene name</b>	<b>Sequence 5' → 3'</b>
PEPC 3 fwd	AACCTCCACATGCTGCAAGA
PEPC 3 rev	TACAATGCAGCGATCCCAGG
PEPC 2 fwd	TGGTGTTTCGCTAAAGGAGATCC
PEPC 2 fwd	TCGCCTTCAAGCAGATCCTT
PEPC 1 fwd	ACCTAGGAGATGGTGCTGGT
PEPC 1 fwd	TCTCCATAGCTTCACCATCGG
Napin4 fwd	TTCCTTCTCACCAACGCCTC
Napin4 rev	ACTACCGGACTGCATTGCCT
Napin3 fwd	GCCACTTTGTGTTTGCCCAA
Napin3 rev	GCTAACTTGCGGGATGTTGC
Napin2 fwd	CCTTCTCACCAATGCCTCCA
Napin2 rev	ACTACCGGACTGCATTGCCT
Cruciferin 1 fwd	GTCAAAACGCGATGGTGCTT
Cruciferin 1 rev	CCGGAAGTTCGCTTGTTG
Cruciferin 2 fwd	GGTGACGGATAACCTCGAT
Cruciferin 2 rev	ACGTAGAGAACCGCGTTTGA
Cruciferin 4 fwd	TAACGCGATGGTCAGCACTT
Cruciferin 4 rev	TCTCCTCGATCAACTGGGGT
UBC9 fwd	TGGCTTTTAGGACGAAGGTG
UBC9 rev	AAGATGTCGAGGCAGATGCT

### 3.6.2 Library construction and sequencing

The samples for transcriptome analysis were prepared using an Illumina kit following the manufacturer's instructions. Briefly, beads with Oligo(dT) were used to isolate poly(A) mRNA from the total RNA. Fragmentation buffer was added in order to convert mRNA into short fragments. Taking these short fragments as templates, random hexamer-priming was used to synthesize the first-strand cDNA. The second-strand cDNA was synthesized using buffer, dNTPs, RNaseH, and DNA polymerase I. Short fragments were purified with the QiaQuick PCR extraction kit and resolved with EB buffer for end repair and for addition of poly(A). Subsequently, the short fragments were connected with sequencing adapters. Following agarose gel electrophoresis, the suitable fragment fraction was selected for PCR amplification. Finally, the library was sequenced using Illumina HiSeq™ 2500 (100bp, paired-end).

### 3.6.3 Transcription estimation

High-throughput sequencing reads of the six samples were aligned against *B. napus* transcripts using bowtie2 (Langmead and Salzberg, 2012). Paired reads alignments; only paired end alignments were counted. To assess the alignment quality we extracted statistical information provided by bowtie2 in the SAM-format output (“mapping quality”). Accordingly, for 87% of the read alignments there is less than 1% probability that the alignment does not correspond to the read's true point of origin in the genome. Read alignment to 101,040 predicted *B. napus* transcripts resulted in detectable transcription for 67885 of the *B. napus* protein encoding genes (67%). In addition, DE analysis was repeated after aggregation of all *B. napus* read counts into a new gene set based on the orthology relations to *A. thaliana*. Accordingly, 99.5% of the *B. napus* level reads were aggregated into 19062 Arabidopsis genes, while only 0.5% of read counts were associated with 1591 *B. napus* genes that are left without orthology relation.

We assembled a draft transcriptome-wide collection of 222,331 (average length 1452 bp) putative cDNA sequences by aligning RNA-seq reads to the genome references of diploid progenitors *Brassica rapa* and *Brassica oleracea* using the splice-aware aligner TopHat (v2.0.8b) (Trapnell *et al.*, 2009) and subsequently applying the Cufflinks (v 2.0.2) reference annotation based transcript assembly (Roberts *et al.*, 2011). Reads that did not align to the reference genomes were assembled separately using Trinity (trinityrnaseqr20130814) (Grabherr *et al.*, 2011). Gene expression estimation was

subsequently done by using RSEM (Li and Dewey, 2011) which deconvolutes expression coming from very similar sequences such as homeologs. Expression estimates from splicing isoforms were summarized to a gene-level transcript per million and inferred gene-specific read counts.

#### **3.6.4 Differential transcription**

The `estimateSizeFactors` and `estimateDispersions` functions in the DESeq package v1.12.1 ([www.bioconductor.org](http://www.bioconductor.org)) using default parameters were run for the normalization of the RNA-seq read count data. The negative binomial test implemented in DESeq was used to assess differential expression between the two genotypes. Variance stabilizing transformation (`varianceStabilizingTransformation` function in the `vsn` package v3.28.0) was performed on the normalized expression estimates.

#### **3.6.5 Data visualization using mapman software and AgriGO**

The MapMan visualization tool (<http://mapman.gabipd.org>) was used for the functional characterization of differential expressed transcripts. The threshold for significance was set to  $p < 0.01$  with a minimum  $\log_2$  (fold change) of 2. Differentially expressed transcripts that exhibited similarity to annotated *A. thaliana* genes, but showed an opposing trend in expression level were sorted out for further analysis. To assess the affiliation of the differentially expressed genes to a certain gene ontology (GO), the web based software AgriGO was used (<http://bioinfo.cau.edu.cn/agriGO/>).

### **3.7 Comparative proteomics of the *B. napus* embryo**

#### **3.7.1 Phenolic extraction of proteins and two dimensional (2D) IEF/SDS PAGE**

Total soluble proteins were extracted from the embryos according to Colditz *et al.* (2004) and Lorenz *et al.* (2014). For the analysis embryos aged 30 DAP from three different plants each, were separated from the seeds and immediately frozen in liquid nitrogen and subsequently homogenized using a bead mill. Pulverized samples of the embryos were then homogenized in extraction buffer (700 mM sucrose, 500 mM Tris, 50 mM EDTA, 100 mM KCl, 2% (v/v)  $\beta$ -mercaptoethanol and 2 mM PMSF, pH adjusted to 8.0). Then, saturated phenol (pH 6.6/7.9; Amresco, Solon, USA) was added. After several rounds of centrifugation proteins were precipitated with 100 mM ammonium acetate in methanol at -20 °C over night. In total 18 mg protein pellet per sample were resuspended in 350  $\mu$ l resuspension buffer (8 M urea, 2 M thiourea, 2% (w/v) CHAPS, 100 mM DTT, 12  $\mu$ l/ml DeStreak-reagent, 0.5% (v/v) IPG-buffer pH 3-11 NL, GE Healthcare, Freiburg, Germany) and directly loaded onto an IPG strip (18 cm pH 3-11 NL, GE Healthcare, Freiburg, Germany). Isoelectric focussing was performed as described in Mihr and Braun (2003) using the IPGphor system (GE Healthcare, Freiburg, Germany). Prior to second gel dimension, IPG strips were equilibrated for 15 minutes with DTT solution (30 % (v/v) glycerol, 50 mM Tris-HCl pH 8.8, 6 M urea, 2 % (w/v) SDS, bromophenol blue, 1% DTT) followed by equilibration with iodoacetamide solution (30 % (v/v) glycerol, 50 mM Tris-HCl pH 8.8, 6 M urea, 2 % (w/v) SDS, bromophenol blue, 2.5% iodoacetamide) for another 15 minutes. Then, IPG strips were fixed horizontally onto 12 % acrylamide SDS gels. The gel run was performed for 18 h at 30 mA per gel using the Biorad Protean IIXL gel system (Biorad, München, Germany).

#### **3.7.2 Gel staining procedure**

All two-dimensional gels were fixed with 10% (v/v) acetate in 40% (v/v) methanol for 90 minutes and stained with Coomassie Blue CBB G-250 (Merck, Darmstadt, Germany) as described by Neuhoff *et al.* (1990, 1985).

### 3.7.3 Quantitative gel analysis and mass spectrometry

Coomassie colloidal stained gels were first scanned and then analysed by using the Delta2D Software 4.3 (Decodon, Greifswald, Germany) according to Berth *et al.* (2007) and Lorenz *et al.* (2014). In total 1124 spots were detected automatically, though minor corrections of obvious gel disturbances were performed manually. The analyses of changes in protein abundances in the embryos were based on protein identifications by mass spectrometry (MS). Tryptic digestion and MS analysis was performed according to Klodmann *et al.* (2010) using the EASY-nLC System (Proxeon) coupled to a Micro-TOF-Q II mass spectrometer (Bruker Daltonics, Bremen, Germany). Identification of proteins was carried out using the MASCOT search algorithm ([www.matrixscience.com](http://www.matrixscience.com)) against the SwissProt ([www.uniprot.org](http://www.uniprot.org)) database.

## 3.8 Metabolite Measurements

### 3.8.1 Steady state metabolite analysis

Metabolic intermediates were extracted and measured by liquid chromatography coupled to mass spectrometry as detailed in previous studies (Hay *et al.*, 2014). The identity of the various compounds was verified by comparison of their mass and retention time with those of authenticated standards. External calibration was applied for all compounds using these standards.

### 3.8.2 Isotope enriched metabolite extraction and analysis

For analysis of  $^{13}\text{C}$  - labelled target analytes frozen material (seed coat/embryo) were homogenized in 1.5 mL microcentrifuge tubes (Eppendorf, Hamburg, Germany) by manual grinding with a pestle. After homogenization, the samples were extracted with 0.2 mL 1:1 (v/v) methanol/chloroform containing 2.5 nmol Acephate<sup>®</sup> (Sigma Aldrich, Germany) as internal standard in a Retsch TissueLyser (Quiagen GmbH, Hilden, Germany) for 180 s at 1800 strokes-1 (racks precooled at  $-80^{\circ}\text{C}$ ). 0.1 ml water was added and vortexed, followed by centrifugation at 2000 g for 5 min (to achieve two separate layers). The main part of the upper water/methanol layer (ca. 0.15 ml) was filtered with Vivaclear centrifugal filters (0.8  $\mu\text{m}$  pore size, SatoriusStedim biotech, Göttingen, Ger-

many) at 2000 g for 2 min. Endosperm was diluted 10-fold with water/methanol 1:1 (incl. int. Std.) and filtered. Samples were analyzed in an LC-MS/MS system (Dionex Ultimate 3000 RSLC, Dionex, Sunnyvale, CA, USA and API 4000, Applied Biosystems, Ontario, Canada). The methods were performed as Hydrophilic interaction chromatography with an aminopropyl column (Luna NH<sub>2</sub>, 250 mm x 2 mm, particle size 5 µm, Phenomenex, Torrance, CA). Carbohydrates and organic acids were measured in negative mode with varying eluent gradients. Injection volume was 2 µl. The LC eluents were: Solvent A, 20mM ammonium acetate + 20mM ammonium hydroxide in 95:5 water:acetonitrile, pH 9.45; Solvent B: acetonitrile. The gradients in the negative mode to determine the metabolites are as follows: t = 0, 75% B; t = 8 min, 70% B; t = 22 min, 0% B; t = 32 min, 0% B; t = 33.5 min, 75% B; t = 44 min, 75% B. The gradients in the positive mode to determine the metabolites are as follows: t = 0, 80% B; t = 6 min, 75% B; t = 14 min, 0% B; t = 24 min, 0% B; t = 25 min, 80% B; t = 35 min, 80% B. Nitrogen was used as a curtain gas, nebulizer gas, heater gas and collision gas. The ion spray voltage was set to -4000V, the capillary temperature was 450°C and the dwell time for all compounds was 25 ms.

### 3.8.3 Visualisation of sugars in MALDI-ICP- MS measurements

Incubated seeds were typically flash frozen in liquid nitrogen to prevent enzymatic degradation or analyte migration, and then stored at -80°C. Subsequently samples were cryosectioned (most commonly used method to prepare plant tissue slices). The thickness of most plant sections in current MSI studies is about 50 µm and was also used in this study (Peukert *et al.*, 2012). Carboxymethyl cellulose (CMC) (Goto-Inoue *et al.*, 2012) has been successfully employed as MSI-compatible embedding medium. Thaw-mounting is usually used to attach tissue sections acquired by cryosectioning. Thaw mounted samples are usually dried within a desiccator at a reduced pressure (Lee *et al.*, 2012; Boughton *et al.*, 2015). For ionisation 2,5-dihydroxybenzoic acid (DHB) was used as a matrix applied with TM Spray (50mg/mL, 1200mm/min, 150uL/min, 30°C, 1.5mm/0.75mm, 4 passes).

### 3.9 Investigation of photosynthesis and respiration rates

For that purpose non-invasive optical oxygen microsensor spots of the company Pre-Sens (Regensburg, Germany) were used. This system measures the partial pressure of dissolved & gaseous oxygen and thus allows to follow the O<sub>2</sub> consumption of a sample over time (according to Borisjuk *et al.*, 2013). The photosynthetic activity, measured as operation efficiency of photosystem II, was measured using PAM fluorescence (according to Borisjuk *et al.*, 2013).

### 3.10 Histology

#### 3.10.1 Staining of protein storage vacuoles

Sections of embryos were either stained with Ponceau or Coomassie following the protocol of Kang *et al.* (2002). For the Ponceau staining, 0.1% Ponceau S (w/v) was dissolved in 5% acetic acid (w/v) (according to the manufacturer Sigma). The microscope slides were placed on a heating plate (60°C) and covered with the staining solution. After 2 minutes, the slides were carefully rinsed with distilled water and dried.

#### 3.10.2 Immunostaining of curciferins, napins and oleosin

Isolated embryos were fixed for 2 h in 2% (w/v) paraformaldehyde and 2.5% (v/v) glutaraldehyde in phosphate buffer 0.1 M, pH 7.4. Following fixation, the embryos were washed with phosphate buffer 0.1 M, pH 7.4, for 10 min, resuspended in 1% (w/v) paraformaldehyde for 2 h, and rinsed three times with phosphate buffer. Embryos were post-fixed for 2 h with 1% (w/v) osmium tetroxide containing 0.8% (w/v) potassium hexacyanoferrate prepared in phosphate buffer, followed by four washes with deionized water and sequential dehydration in acetone. All procedures were performed at 4°C. Samples were embedded in Spurr's resin and polymerized at 60°C for 48 h. Ultrathin sections (0.5 µm) were obtained with a diamond knife (45°, Diatome) and were mounted on a 8-well-microscope slide and dried at 60°C. The microscope slides were placed in a wet chamber containing a blocking buffer. After 20 minutes, the blocking buffer was removed and the slides were washed with washing buffer (0.5% (v/v) Tween 20 in phosphate-buffered saline) for 2 minutes. Next, the primary antibody was placed onto the slides and incubated for 45 minutes at 37°C. After five washing steps, the slide was kept in the dark for 30 minutes incubated with the second fluorescence antibody at 37°C. The subsequent steps were carried out under low illumination. The slides were again washed



---

five times with washing buffer and moistened with antifade. The slides were then sealed with a cover slip and fixugum. The slides were examined transmission electron microscope. Embryos from three individual plants were used in each analysis.

## 4.1 Results Part I - The use of $^{13}\text{C}$ labelling to unravel sucrose uptake in developing oilseed rapeseed

### 4.1.1 Establishing a procedure that allows $^{13}\text{C}$ -label uptake of seeds under near *in vivo* conditions

Previous work has demonstrated that *in vitro* culture of developing embryos is well suited to perform stable isotope labelling and metabolic flux analysis (Schwender *et al.*, 2004, 2006, 2008). However, this procedure also has some limitations, and causes growth patterns which differ from the *in planta* situation (Borisjuk *et al.*, Plant Cell 2013). My work aimed to setup a procedure, where the developing seed/embryo has not to be isolated for subsequent *in vitro* cultivation, but rather receives nutrients/assimilates/water via the funiculus from maternal tissues (Chan and Belmonte, 2013; Khan *et al.*, 2015), thereby mimicking the *in planta* situation. To achieve this, the procedure for incubating intact siliques in buffer containing nutrients and ( $^{13}\text{C}/^{15}\text{N}$ -labelled) sugars/amino acids described previously by Morley-Smith *et al.* (2008) was evaluated and further refined. Siliques of *B. napus* were cut from plants using a scalpel and immediately placed in a solution that contained 100mM sucrose (figure 3B). Seeds of siliques that were either kept in culture or grown *in planta* in the greenhouse were harvested at the same time points and the embryo weight was determined. As shown in figure 3A, after one week of incubation the weight increase was about 0.5 mg dry weight; embryo weights were comparable between *in planta* and *in silique-culture* grown ones. Embryos grown *in silique-culture* for four days did not reveal any signs of anatomical aberrations (as observed under *in vitro* culture; see Borisjuk *et al.*, 2013) (figure 3C). Over the entire incubation period, siliques took up water and nutrients from the incubation media and looked healthy.

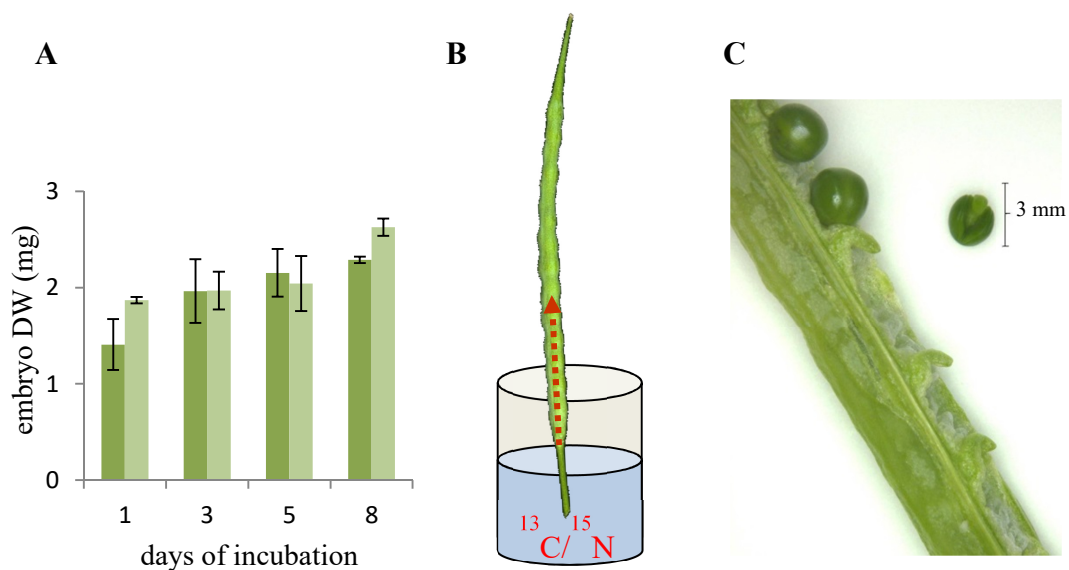


**Figure 3:** Silique incubation – (A) Comparison of dry weight of embryos grown in planta (light green) versus those grown in silique culture (dark green). (B) Schematic view of the experimental setup of silique incubation. (C) The embryos inside incubated siliques grow with similar dynamics as in planta. (siliques at 30 DAP, incubated for 4 days).

#### 4.1.2 Test for various sugar substrates

We incubated 30 days old siliques in a solution containing 100mM of either fully labelled  $^{13}\text{C}$ -sucrose or  $^{13}\text{C}$ -glucose. Following incubation for 2, 4, 8, and 24 hours, seeds were taken off from the siliques and dried at  $70^{\circ}\text{C}$ . The amount of total carbon and the  $^{13}\text{C}$ -fraction was measured using EA-IRMS. The results in figure 4 demonstrate, that the incubation in  $^{13}\text{C}$  sucrose gives a 10-fold higher labelling ( $^{13}\text{C}$  abundance) as compared to  $^{13}\text{C}$  glucose. The preferential sucrose uptake corresponds to the fact that sucrose is also the natural (phloem) substrate for sugar supply toward seeds. It should thus be used for efficient label transfer into the seed.

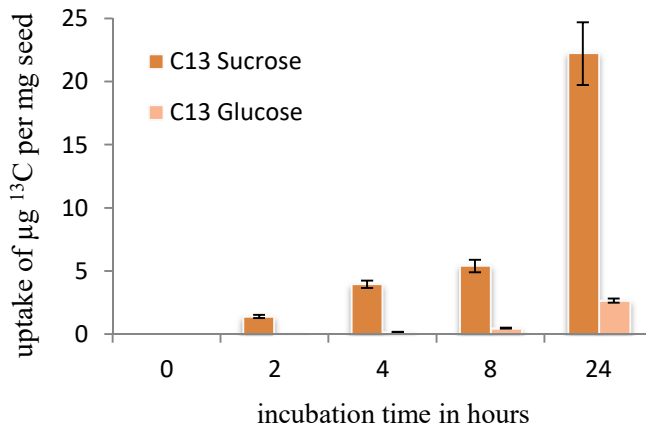


**Figure 4:** Differences in  $^{13}\text{C}$ -carbon uptake per mg seed after incubation of siliques in a solution containing either 100 mM  $^{13}\text{C}$  sucrose or  $^{13}\text{C}$  glucose. The age of the incubated siliques was 30 DAP.

#### 4.1.3 The uptake of label is equal in all seeds along the silique

We further tested if the position of seeds inside the silique has an effect on the uptake of labelled assimilates. Siliques were incubated for 24 hours and then each seed (from top to bottom) was analysed with respect to dry weight and  $^{13}\text{C}/^{15}\text{N}$  label abundance. We observed that neither seed weight nor uptake of label ( $^{13}\text{C}$  sucrose and  $^{15}\text{N}$  glutamine) was dependent on the position of the seed inside the silique (figure 5).

In an additional experiment, siliques were incubated for four days and samples of both seeds and siliques were taken every 24 hours, followed by analysis of  $^{13}\text{C}/^{15}\text{N}$  label abundance. As shown in figure 6, siliques don't show a significant increase in label abundance after 24 hours while seeds continue to accumulate label. After three days of incubation, seeds have incorporated about 3-fold higher amounts of labelled sucrose than siliques. The same results were observed when using  $^{15}\text{N}$  - glutamine as nitrogen source (see Supplement).

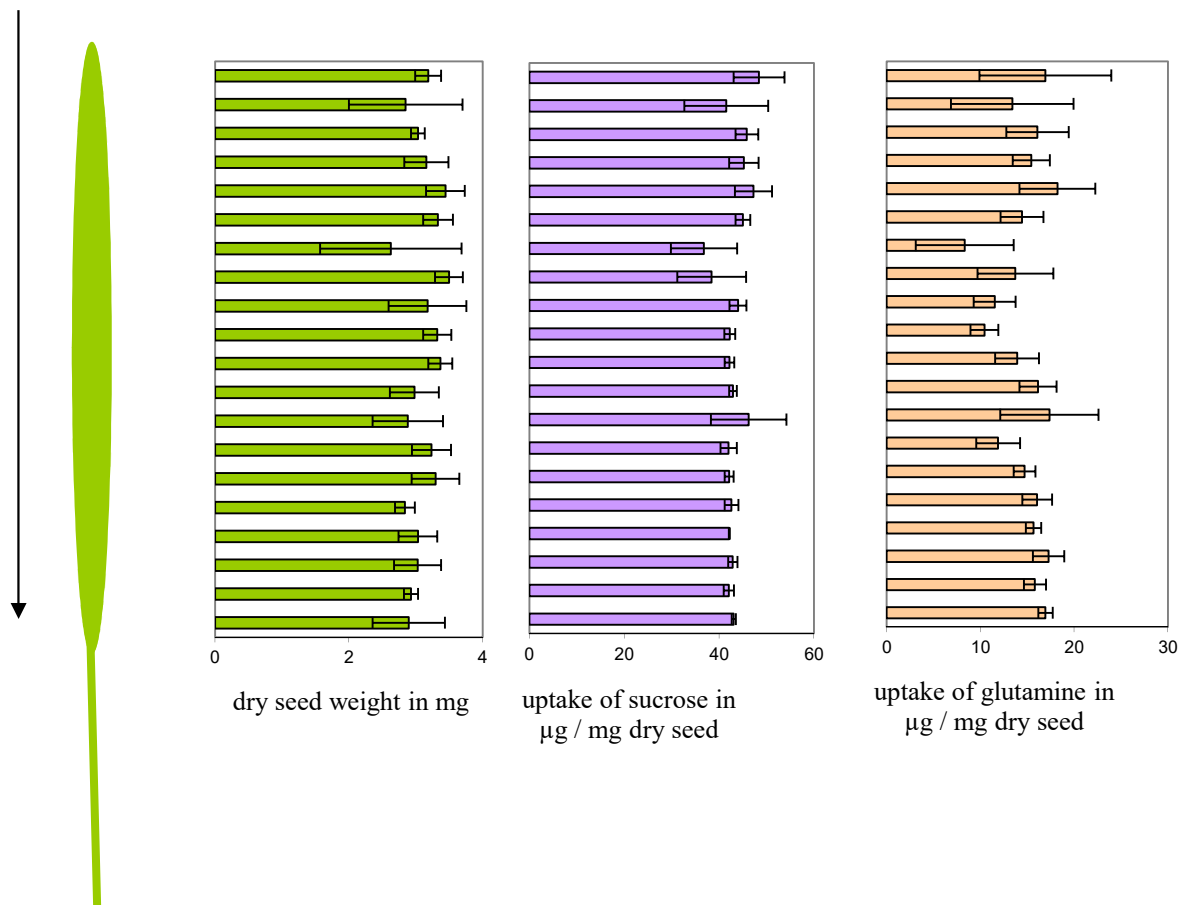
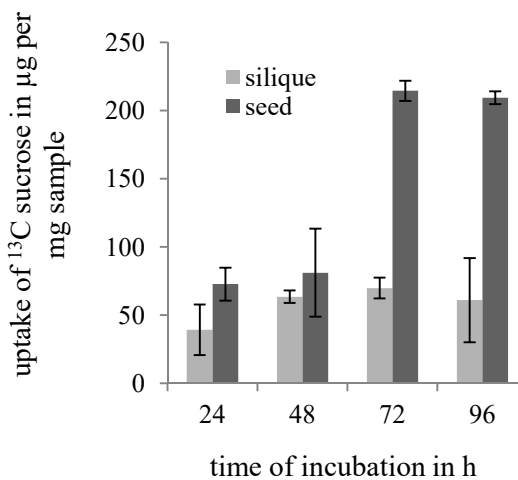


**Figure 5:** Distribution of seed weight and isotope abundance in seeds along the silique (30 DAP) after incubation in a solution containing 100mM fully labelled sucrose and 50mM fully labelled glutamine.

**Figure 6:** Uptake of labeled  $^{13}\text{C}$  sucrose into either silique or seed over a time period of 4 days. For the incubation 100 mM  $^{13}\text{C}$  sucrose were added to the media.



#### 4.1.4 Use of $^{13}\text{C}$ labelling to follow sucrose uptake and metabolism in developing seeds

In the following experiment, we separated the seed into three organ fractions: embryo, seed coat (which includes the attached cellular endosperm/aleurone) and the non-cellular, liquid endosperm. Siliques (with seeds in early-cotyledon stage; ~21 DAP) were incubated. This stage of seed development was chosen because the massive expansion of the embryo has just started and the liquid endosperm is about to decline but can still be sampled separately from the other fractions. The uptake of labelled compounds in the distinct organs was measured using EA-IRMS. The results in figure 7 show that the seed coat/aleurone is the component which initially takes up most of the  $^{13}\text{C}$  label (sucrose), followed by the liquid endosperm fraction and the embryo. The seed coat represents the tissue where sucrose enters the seeds. Following 4 hours of incubation, a steady increase in label abundance in the liquid endosperm was visible. After 24 hours, the highest accumulation of  $^{13}\text{C}$  label was found here, corresponding to around 60  $\mu\text{g}$  per whole organ. At that time point, the seed coat/aleurone had incorporated about 50  $\mu\text{g}$  and the embryo around 15  $\mu\text{g}$ . The increase of label in embryo started around 6 hours after incubation in a steady manner. A similar pattern was observed for the uptake of  $^{15}\text{N}$  glutamine (see Supplemental data).

A

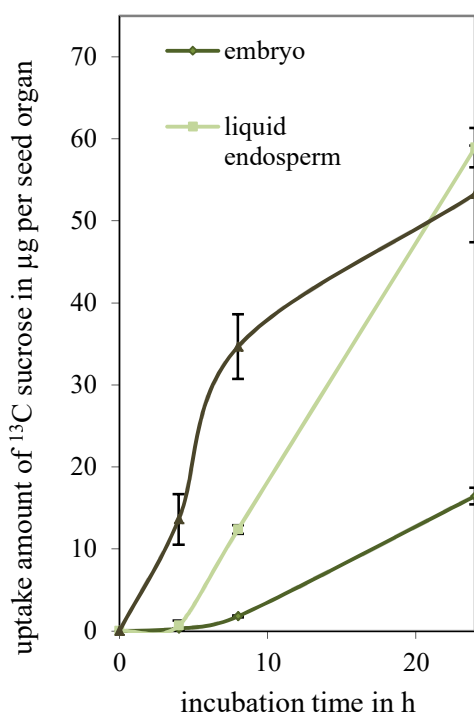
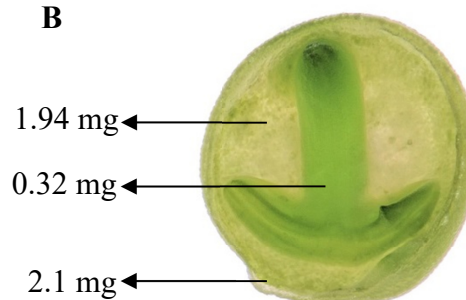


**Figure 7:** Label uptake of seed organs. (A) Accumulation of  $^{13}\text{C}$  label inside the distinct seed organs. (B) The fresh-weight contribution of seed coat/aleurone, liquid endosperm and embryo to the total seed fresh-weight.

B



#### 4.1.5 Label transfer along metabolic pathways differs among seed organs

Besides the calculation of total sucrose uptake in the seed fractions, we also applied mass spectrometry to follow label transfer among some metabolic intermediates (sucrose, hexoses, hexose-P, PEP, malate, citrate). In general, the hexose concentration in the seed coat/aleurone layer and embryo was rather low while the liquid endosperm was the hexose storage pool of the seed. The concentration of sucrose was nearly comparable between embryo and liquid endosperm. Because of the higher volume of the endosperm, the total amount of sucrose in the liquid endosperm was much higher than that of the embryo. Thus, the liquid endosperm is also the main sucrose storage organ in the seed. The seed coat/aleurone layer accumulated similar concentrations of sucrose and hexoses. The liquid endosperm showed a nearly balanced hexose to sucrose ratio, whereas in the embryo the sucrose to hexose ratio was much higher (table 2). The levels of hexose-P were similar between the organs and the concentration was in all cases rather low (0.7-2.9 mM). The concentration of malate was similar in embryo and liquid endosperm but lower in seed coat/aleurone. Citrate showed lowest concentration in the liquid endosperm followed by seed coat/aleurone layer and embryo. PEP levels were highest in embryo.

**Table 2:** Concentrations of metabolites in the distinct seed organs given in mM and measured using LC/MS.

	Concentration of metabolites		
	seed coat / aleurone	liquid endosperm	embryo
sucrose mM	$12.45 \pm 8.3\%$	$60.77 \pm 8.8\%$	$49.75 \pm 6.9\%$
hexoses mM	$7.01 \pm 4.2\%$	$85.9 \pm 6.1\%$	$3.75 \pm 6.7\%$
hexose-P mM	$0.74 \pm 5.5\%$	$1.39 \pm 6.5\%$	$2.93 \pm 0.5\%$
malate mM	$7.49 \pm 0.6\%$	$26.88 \pm 9.0\%$	$24.78 \pm 7.2\%$
citrate mM	$4.71 \pm 7.8\%$	$1.43 \pm 2.3\%$	$10.3 \pm 5.8\%$
PEP mM	$0.01 \pm 5.2\%$	$0.01 \pm 3.7\%$	$0.04 \pm 9.5\%$

We also calculated the labeled proportion for each metabolite (figure 8). All metabolites showed the first significant enrichment in  $^{13}\text{C}$  abundance in the pools of the seed coat/aleurone layer (already after 4 hours of incubation). This again corresponds to the fact that  $^{13}\text{C}$  sucrose is taken up by the seed coat first. In contrast, the embryo did not show labeling in intermediates at four hours of incubation, and the liquid endosperm only displayed a slight enrichment in the labelling of sucrose, glucose, hexose phosphates and citrate. After 24 hours of incubation, a clear label in the sucrose pool as well as other metabolites was visible in all three seed organs. In general only very few of the entered label was detectable in the hexose pool (which corresponds to earlier findings by Morley-Smith *et al.*, 2008).



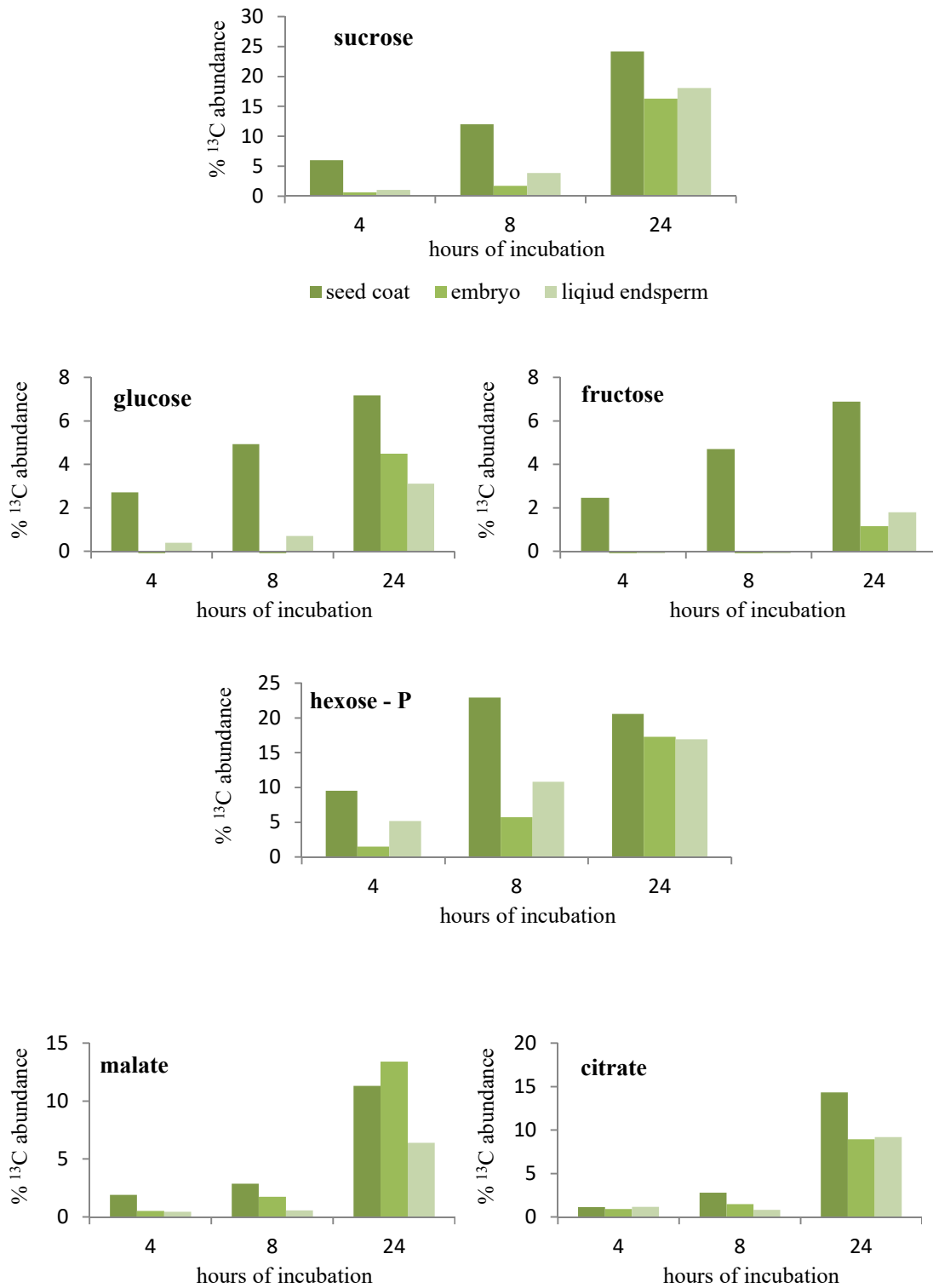


**Figure 8:** The increase in  $^{13}\text{C}$ -labelled metabolites in seed coat, endosperm and embryo after an incubation time of either 4, 8 or 24 hours in a solution containing 100 mM  $^{13}\text{C}$ -sucrose shown in % of total metabolite in the compartment.

#### 4.1.6 Visualisation of $^{13}\text{C}$ -sucrose uptake in developing seeds of *B. napus*

Previous data clearly indicated a flow of sucrose from the seed coat towards both liquid endosperm and (finally) to the embryo. In collaboration with the group of Prof. Dr. Ute Rössner (Metabolomics Unit, Melbourne/Australia), we applied MALDI-FT-ICR-MS to visualize the pathway for sugar uptake inside the seeds. This method enables to specifically detect  $^{13}\text{C}$ -labelled sugars with spatial resolution. Seeds, that were previously incubated in  $^{13}\text{C}$  sucrose-containing media, were sectioned, mounted on glass slides (figure 9 A&D) and after applying DHB as a suitable matrix the slides were measured using a Bruker Solarix XR instrument. As shown in the figure 9 B & E, unlabeled disaccharides like sucrose, maltose and lactose (identical sum formula:  $\text{C}_{12}\text{H}_{22}\text{O}_{11}$ ) were detectable in all seed compartments. Figure A-C further show, that the pattern for  $^{13}\text{C}$  sucrose uptake can clearly be followed: At two hours after the start of incubation, the  $^{13}\text{C}$ -sucrose was detectable in the branch point of funiculus and started to spread towards the inner cells. After three hours, the  $^{13}\text{C}$ -sucrose was already spread evenly through the first third of the seed. Notably, label accumulated in the aleurone layer and liquid endosperm, but was not detectable in either suspensor or embryo.

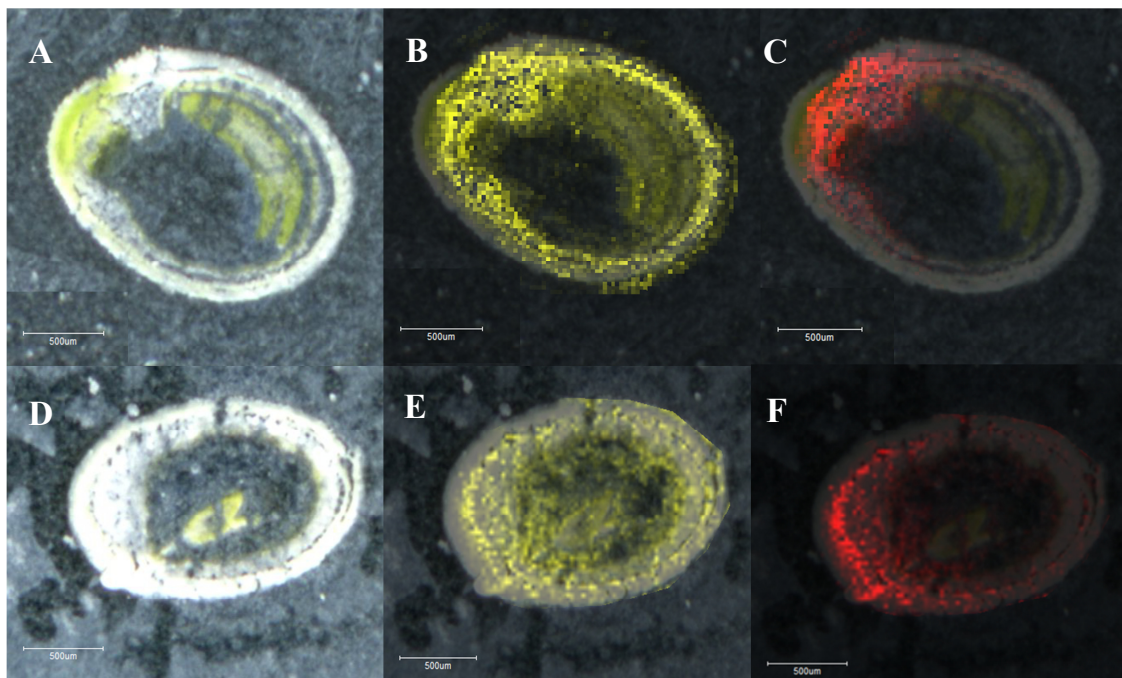


**Figure 9:** Mass spectrometry imaging of  $^{13}\text{C}$  sucrose uptake into seeds. Seed sections (30  $\mu\text{m}$ ) of *B. napus* at 15 DAP (A, B, C) and 12 DAP (D, E, F); measurements were done using MALDI-FT-ICR-MS. Matrix: DHB, TM Spray, 50mg/mL, 1200mm/min, 150uL/min, 30C, 1.5mm/0.75mm, 4 passes. The seeds were previously incubated in a solution containing 100mM  $^{13}\text{C}$  sucrose for either 60 minutes (A, B, C) or 120 minutes (D, E, F). A and D show the section through the seed, B and E show the distribution of unlabeled disaccharides with the sum formula of  $\text{C}_{12}\text{H}_{22}\text{O}_{11}$ , pictures C and F show the distribution of  $^{13}\text{C}$  sucrose in the seed section (previous page).

#### 4.1.7 Using $^{13}\text{C}$ - sucrose labelling to compare high-oil and low oil lines

A further aim of my work was to demonstrate that the silique culture is applicable to analyse contrasting genotypes of oilseed rape. To this end, I used two rapeseed accessions (CR3170 and CR3231) which have been previously characterised (Schwender *et al.*, 2014): CR3231 shows an increased starch accumulation and a decreased lipid content in comparison to CR3170. I applied the silique incubation approach to see if potential differences in uptake and metabolism of labelled sugars can be detected. We incubated siliques as described above, separated the seeds and measured the  $^{13}\text{C}$  label abundance. As shown in figure 10, there was evidence for a higher uptake of  $^{13}\text{C}$  sucrose of about 20% in the high-oil line CR3170.

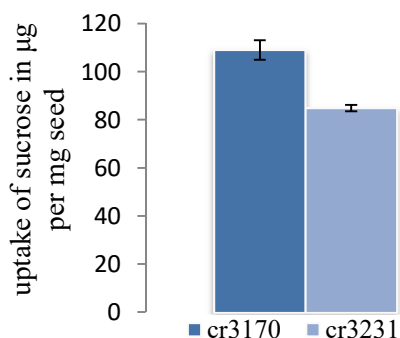


**Figure 10:** Uptake of  $^{13}\text{C}$  sucrose in two distinct rapeseed lines. The uptake of  $^{15}\text{N}$  labelled glutamine and  $^{13}\text{C}$  labelled sucrose after 24 hours of incubation in a solution containing either 50mM  $^{15}\text{N}$  glutamine or 100 mM  $^{13}\text{C}$  sucrose. Siliques used for incubation: 30 DAP.

In previous work, Schwender and colleagues could demonstrate that the high-oil line CR3170 differed in flux pattern around the hexose pool/hexose-P/glycolysis (Schwender *et al.*, 2015). In own preliminary experiments, there was a hint to a faster sucrose breakdown in the high-oil line CR3170: when measuring the  $^{13}\text{C}$  labelled fractions of some central metabolites, we observed a higher isotope label in hexoses and hexose-P in high-oil line CR3170 (data not shown). To show the faster sucrose uptake and turnover rates in the high-oil line CR3170, we measured enzyme activity of sucrose

synthase and the mRNA expression levels of *sucrose synthase 2* (which is the main isoform in seeds at 30 DAP) in the two rapeseed lines. As shown in figure 11, we observed a two-fold higher enzyme activity in high-oil line CR3170 and additionally ~50% increase in mRNA abundance of *sucrose synthase 2*.

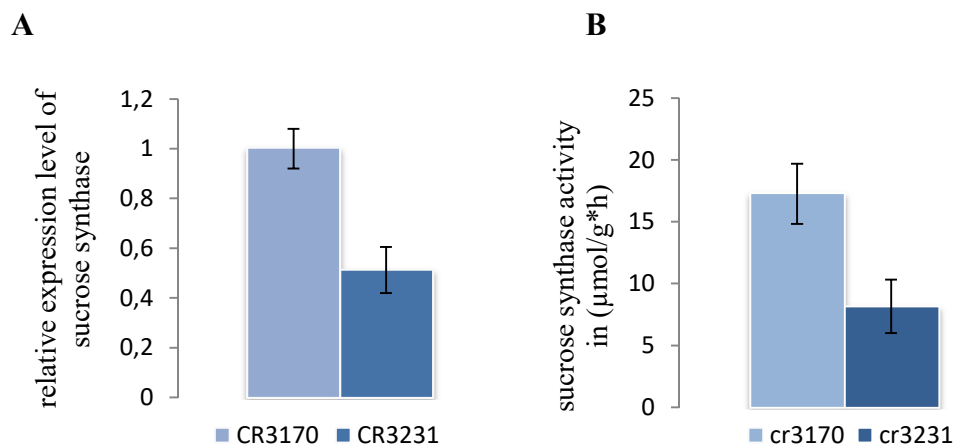


**Figure 11:** Sucrose synthase mRNA expression level and enzyme activity in two contrasting rapeseed lines. (A) The sucrose synthase activity (in  $\mu\text{mol/g}\cdot\text{h}$ ) of high-oil line CR3170 in comparison to low-oil line CR3231; (B) mRNA expression level of Sucrose Synthase 2 of high-oil line CR3170 in comparison to low-oil line CR3231.

## 4.2 Results Part II - Characterisation of a transgenic *B. napus* plants with knockdown of PEPC-Napin-Cruciferin

### 4.2.1 Analysis of down-regulation efficiency in the transgenic lines

#### 4.2.1.1 The down-regulation of *cruciferin*, *napin* and *pepc* in embryos at 30 days after pollination

The plants analysed in this study were generated and provided by Bayer CropScience within the frame of previous collaborations. Transgenic lines have been generated as double haploids. The down-regulation constructs of *B. napus napin2* and *cruciferin* (targeting mostly the p1, p2 and p3 chain) were both set under the *B. napus napinA* promoter, which is known to be active throughout the seed storage phase. The down-regulation construct for *pepc* (in particular targeting *pepc1* and *pepc2*) was set under two different promoters. For the lines BCS 566, 568, 570, 572 and 574 the promoter *FatB4* was used. In the lines BCS 576, 578, 580 the constructs were set under the promoter *Ole1At*. It was previously shown that both promoters confer seed-specific expression with slightly different activity patterns (Borisjuk *et al.*, unpublished data). Based on the measurement of GUS activity in a fluorimetric assay, it was shown, that the *Ole1At* promoter is active in all seed tissues during development, with increasing amount in the embryo tissues during maturation. The *fatB4* promoter is mainly active in the cotyledons and shows a stable expression level during development. In later stages of seed storage initiation and maturation the activity of the *fatB4* promoter reached only 50% of the activity measured for *Ole1At*. For each transgenic line, a corresponding wild type segregant (WTS) was available for analysis. To assess down-regulation efficiency of *cruciferin*, *napin* and *pepc* transcript, three isoforms were chosen each, because of their prediction to be highly abundant in seeds. Primers used for this analysis were generated by sequence alignment to *B. napus* sequences (provided by BAYER Crop Science, confidential). All tested *cruciferin* isoforms were strongly down-regulated, ranging around a log<sub>2</sub> fold change from -2 to -6. This implies a change in *cruciferin* transcripts from 8 to 70 fold. The tested isoform *cruciferin3* shows the strongest down-regulation in all tested transgenic lines. The strongest rate in down-regulation was observed in the transgenic lines BCS568, followed by BCS572, BCS578 (figure 12A). The strongest down-regulation in the transgenic lines was achieved for *napins*, ranging around a log<sub>2</sub> fold

change from -3 to -7, which implies a reduction in transcript amounts from 8 to 700 fold. The down-regulation was similar for all tested isoforms. The strongest down-regulation was observed in the transgenic lines BCS570, followed by BCS568, BCS580 (figure 12B). Figure 12C shows, that for all transgenic lines, the downregulation of the tested *pepc* isoforms was rather low, with the efficiency of down-regulation ranging a log2fold change around -1, which means a fold change of 0.5. This indicates a rather weak reduction of transcript amount (~50%).

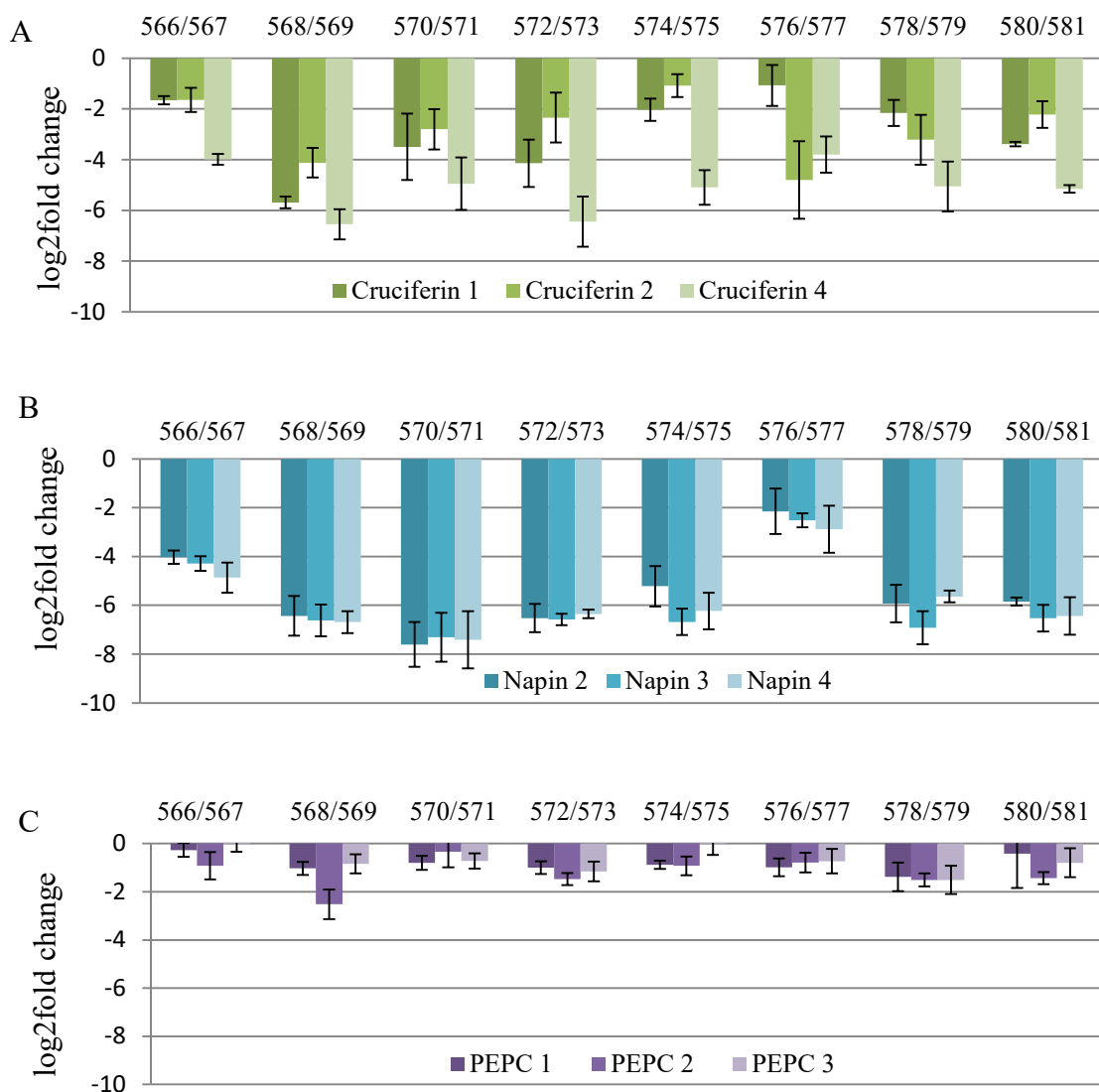


**Figure 12:** Transcript level changes displayed as log<sub>2</sub>fold changes of *cruciferin* (A), *napin* (B) and *pepc* (C) isoforms in transgenic lines and corresponding wild type segregants (WTS). Total RNA was extracted from the embryos of 30-days-old seeds and the transcript levels of the genes were analyzed by quantitative real-time PCR. The expression level was normalized to that of *BnUBC9*. Values are mean  $\pm$  SD (n = 3).

#### 4.2.1.2 The down-regulation of *napins* and *cruciferins* shows a developmental pattern

To assess the expression profile of the *napA* promoter (and thus the time point, when the down-regulation effect for the storage proteins napin and cruciferin in the embryo might be at maximum), we isolated the RNA of *B. napus* embryos at six different time points during development and performed a quantitative real-time PCR. We chose the line BCS580 and its WTS BCS581 as an example for all other transgenic lines. The degree of down-regulation of *napins* and *cruciferins* is shown as log<sub>2</sub>fold expression change. As shown in figure 13, the expression levels of *cruciferin* and *napin* isoforms show a similar developmental profile. The strongest down-regulation for the tested isoforms of napins and cruciferins in the transgenic plants was reached between 35 and 47 days after pollination. This corresponds to the main storage phase in seeds. At 45 days after pollination, the log<sub>2</sub>fold change of the napin isoforms was about -10, which means a more than 1000-fold decrease in transcript abundance. At the same time point also the expression values for cruciferins was lowest with a log<sub>2</sub> fold change of around -6, giving a 60-fold decrease in transcript abundance.

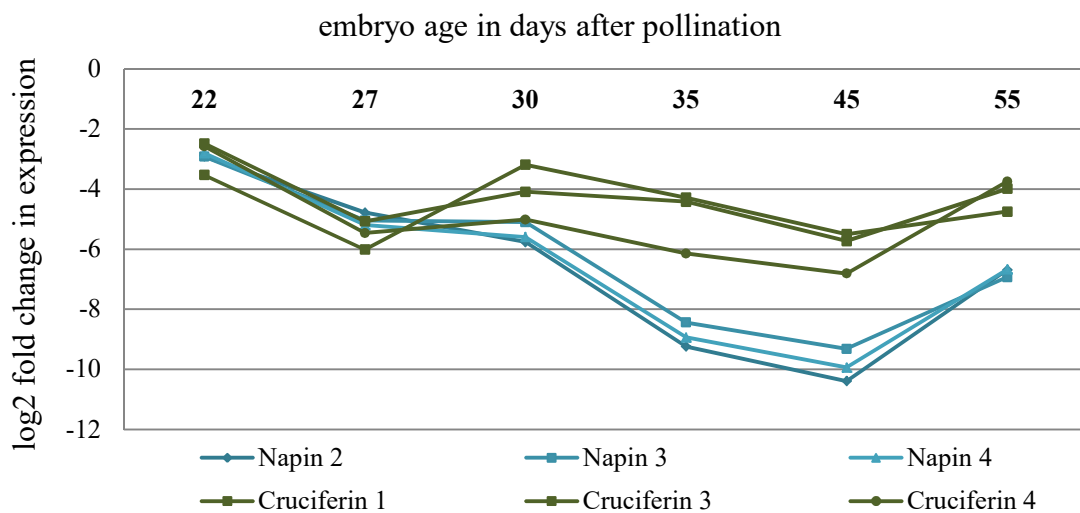


**Figure 13:** Transcript level changes displayed as log<sub>2</sub>fold change of napin and cruciferin isoforms. Total RNA was extracted from the embryos at different developmental time points (22, 27, 30, 35, 45, 55 DAP); transcript levels of the genes were analyzed by quantitative real-time PCR. The expression level was normalized to that of *BnUBC9*. Values are mean  $\pm$  SD (n = 9).

#### 4.2.2 The low level of down-regulation of PEPC transcripts is reflected in enzyme activity measurements

To show whether the low down-regulation of the *pepc* transcripts in transgenic plants was reflected on the protein/activity level, the maximum catalytic activity of the PEPC enzyme was measured using a spectrophotometric assay (figure 14). The measurements were carried out with embryo material, previously used also for real-time PCR analysis. The results show that a significant reduction in PEPC activity could only be obtained for the two lines: 570 (versus WTS 571) and 580 (versus WTS 581). These results correspond to the low level of down-regulation of PEPC transcripts obtained in the real-time PCR analysis. The line BCS580 and its corresponding wildtype were chosen for further analysis.

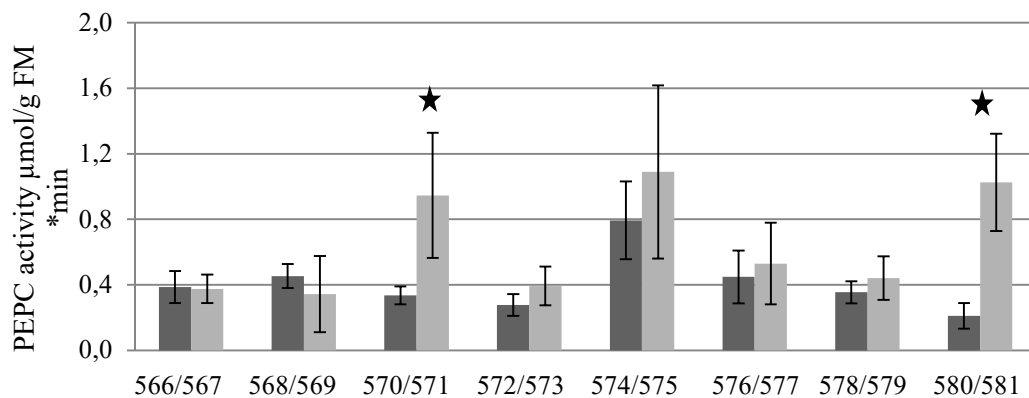


**Figure 14:** Measurement of the Vmax PEPC enzyme activity in  $\mu\text{mol/g}$  fresh weight per minute of transgenic lines (light grey bars) compared to their corresponding WTS (black bars). Stars indicate statistical significance determined by student's T-Test ( $p=0.01$ ). Values are mean  $\pm$  SD ( $n=6$ ).



### 4.2.3 Characterisation of major seed traits

All transgenic plants and corresponding WTS were grown at IPK greenhouse (in total 16 lines with 5 plants each). After maturation, the seeds of all plants were harvested and weighted. To investigate the effect of down-regulation of major storage proteins in the mature seeds of transgenic plants, various seed traits were analysed. Total lipid content was measured non-invasively using TD-NMR. As shown in figure 15A, the total lipid content in transgenics was significantly decreased compared to the WTS plants. Mature seeds of transgenics showed an average ~15% reduction in lipid content. Total protein content in mature seeds was analysed as total nitrogen content (TN\*5.7) using elemental analysis, and, alternatively, using near-infrared spectroscopy). Our data indicate that the levels of protein in mature seeds of transgenic lines are reduced by ~10 % as compared to corresponding WTS (figure 15B). However, mature seeds of the transgenic plants reached dry weights similar to those of WTS (figure 15C). In contrast to the WTS, the transgenic lines showed a continuously higher fibre content of about 25 % (figure 15D). In mature seeds, starch was equally low (<2 % of DW) in all tested lines, though the difference in starch content varied between the transgenic lines and their corresponding wildtype (supplemental data, figure S2). However, the embryos of the transgenic line BCS580, which we later focussed on, stored about 30% less transient starch compared to the WTS (supplemental data, figure S3).

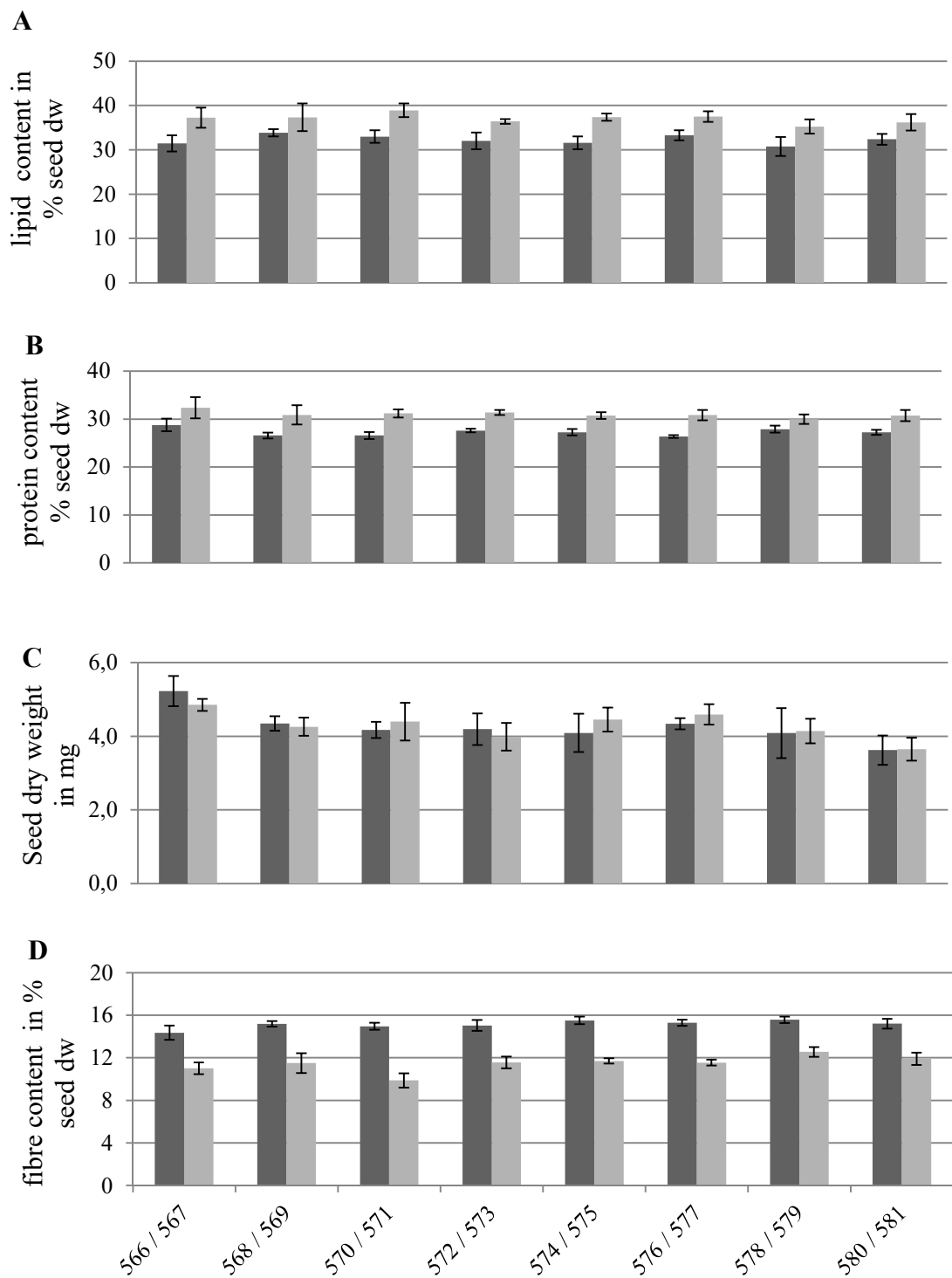


**Figure 15:** Overview on major seed traits at maturity. (A) Measurement of the total lipid content as % of seed dry weight (dw). Values are mean  $\pm$  SD (of about 10 seeds per 3 different batches). (B) Protein content in % of seed dw; Values are mean  $\pm$  SD (of about 10 seeds per 3 different batches). (C) Dry weight of mature seeds in mg; values are mean  $\pm$  SD (n = 60-90). (D) Fibre content in % of seed dw. Values are mean  $\pm$  SD (n = of about 10 seeds per 3 different batches).

#### **4.2.4 Evaluating the transgenic effect on embryo metabolism**

##### **4.2.4.1 Steady-state metabolite levels**

The use of the liquid chromatography/mass spectrometry (LC/MS) enabled the quantification of 79 metabolites, representative of embryo's central metabolism. Work was done under supervision of Dr. Nicolas Heinzl (IPK Gatersleben). For analysis, three biological and three technical replicates each were used; embryo material was isolated from greenhouse grown plants at 30 DAP. Overall, our analysis revealed rather few changes in steady state levels of metabolic intermediates (figure 16). Major statistically significant changes were visible for some free amino acids (glutamine, arginine, valine, tryptophane, proline, serine, histidine, methionine and aspartic acid). Further differences were apparent for the organic acids oxaloacetate and malate (participating in both TCA cycle and amino acid metabolism). There was also a change for glucose-1-phosphate with higher abundance in the transgenic plants.

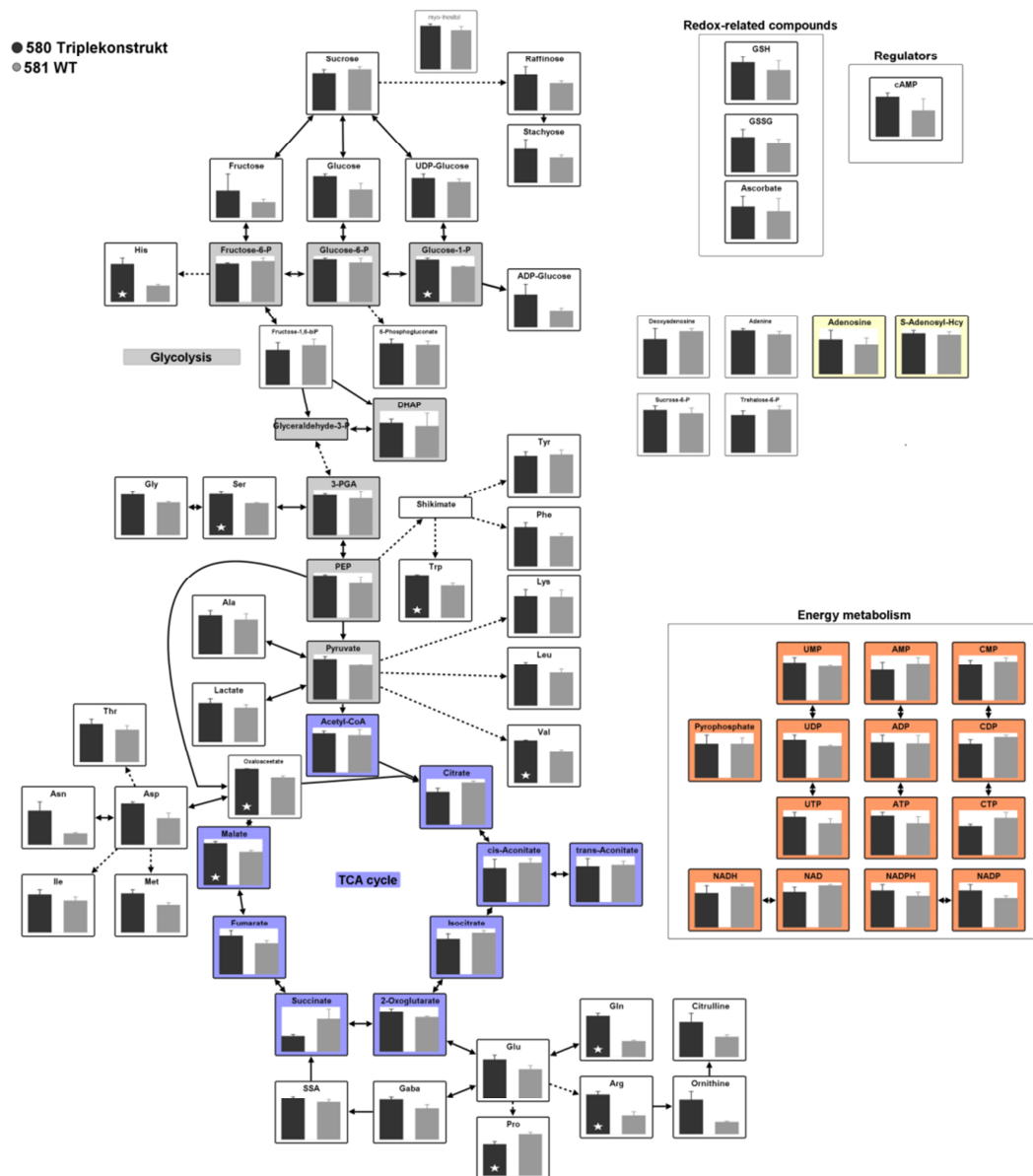


**Figure 16:** Steady state metabolite levels in embryos of transgenic and WTS plants measured by liquid chromatography/mass spectrometry. The standard error was calculated from measurements taken from five technical replicates per each of three biological replicates. Asterisks indicate means differing significantly ( $p < 0.05$ , t-test) between both genotypes.

#### 4.2.4.2 Fatty acid profile of embryos at 30 DAP

We aimed to investigate if the decrease in lipid content in seeds of transgenics is accompanied by changes in the fatty acid (FA) profile. As shown in figure 17, the most abundant FA in embryos of WTS were oleic acid (~55%), linoleic acid (~25%) and linolenic acid (~10%). In transgenics, lower percentage of oleic acid (~35%) in favour of more unsaturated linoleic (~40%) and linolenic acid (~15%) were detected. The remaining FA did not show any significant changes in abundance.

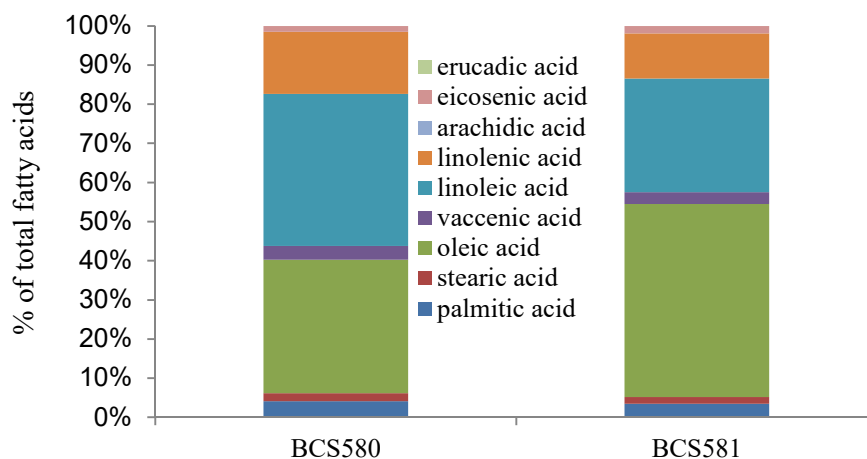


**Figure 17: Fatty acid composition** of embryos; fatty acids were extracted from the embryos of 30-days-old seeds and analysed by gas chromatography. Values are mean  $\pm$  SD (n = 3).

#### 4.2.5 Proteomics studies

##### 4.2.5.1 Staining of protein storage vacuoles indicates less soluble protein

We performed staining of storage proteins in sections of outer cotyledons of embryos isolated at 37 DAP. The results for staining with Ponceau and with Commassie are shown in figure 18. Staining in the WTS BCS581 indicated the presence of protein vacuoles with accumulation of soluble proteins. In contrast, there were hardly visible protein storage vacuoles in the transgenic line BCS580.

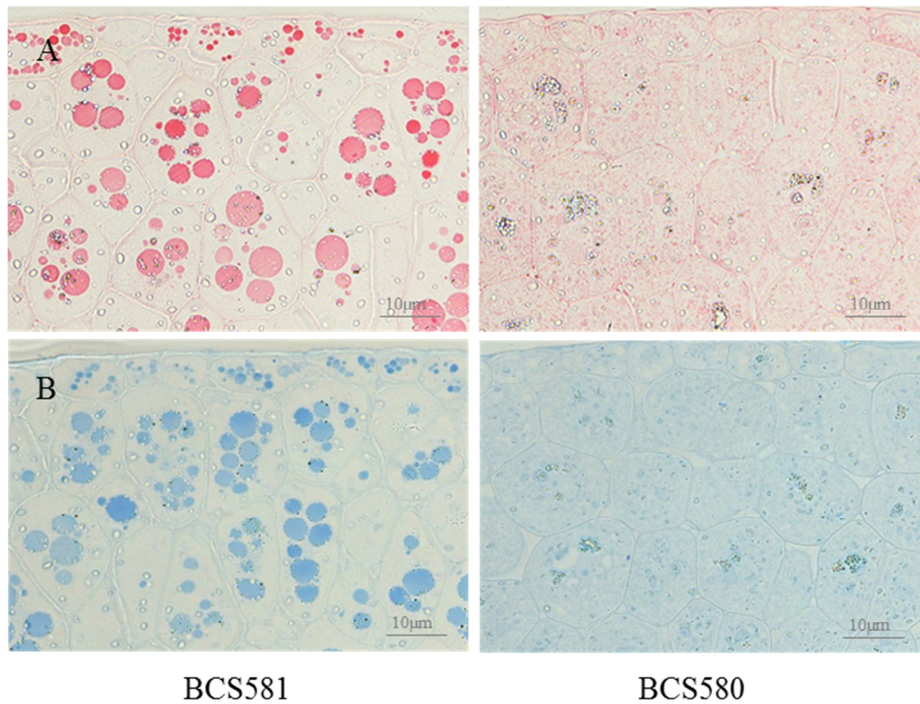


**Figure 18:** Staining of protein vacuoles with 0.1% Ponceau - (A) or 0.02% Coomassie solution (B). Sections were obtained from outer cotyledons of embryos at 37 DAP of transgenic line BCS580 and the WTS BCS581.

#### 4.2.5.2 Quantification of total soluble protein using IEF SDS –PAGE

To investigate the molecular pattern of protein accumulation, a proteomics approach was initiated in collaboration with Prof. Hans Peter Braun (Leibniz University Hannover, Institute of Plant Genetics). Embryos of three independent plants of the transgenic line and the corresponding WTS were harvested at 30 DAP. Protein isolation and the subsequent steps were carried out under supervision of Dr. Christin Lorenz. Three gels were run per line; Coomassie staining revealed a good and proper separation of the protein spots (figure 19). Software evaluation was carried out by generating an overlay image, originating from all 3 gels run per line. Subsequently the two resulting representative gels were compared and spot volume differences were monitored. The threshold to distinguish between higher and lower abundant proteins was set to a change in normalized relative spot volume of  $\geq 1.5$  and a high significance of Student's t-test: p-value 0.01. In total, we could identify 1124 spots of which 109 were differentially expressed. The embryos of transgenic line BCS580 showed an increase in spot volume for 40 spots, whereas the volume of 69 spots was significantly decreased as compared to the WTS BCS581.

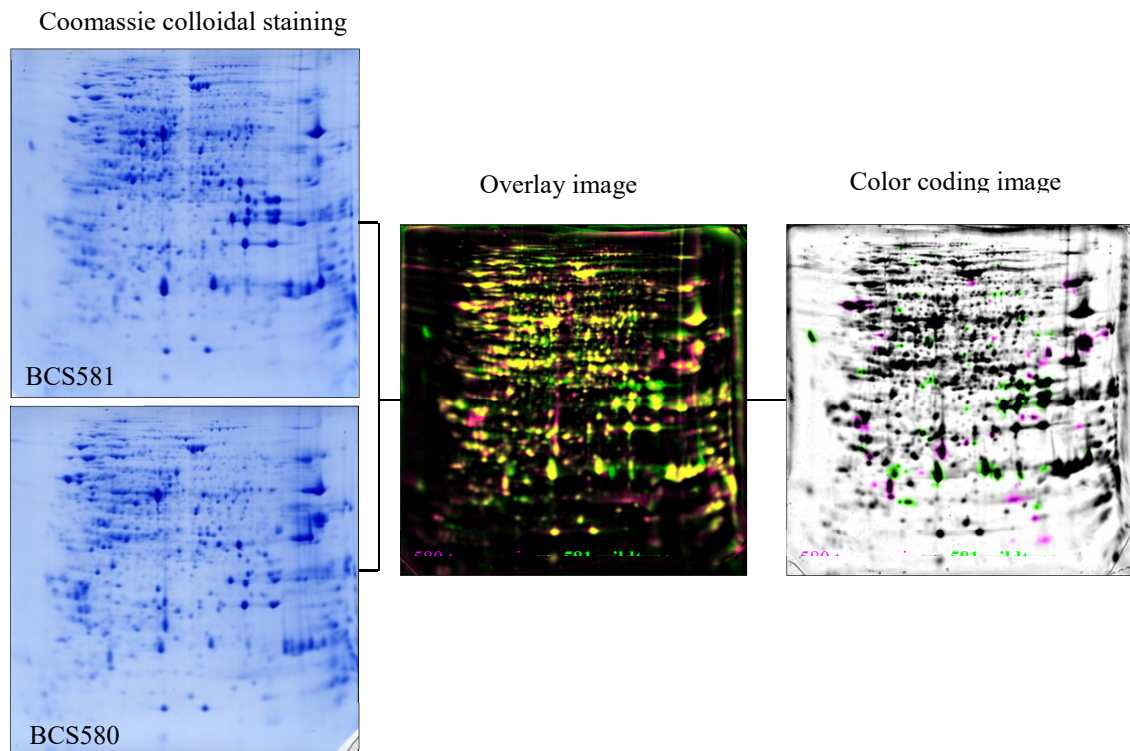


**Figure 19:** Overview on the calculation of protein spot volume difference in the Coomassie gels based on three replicates per line and the generation of an overlay image. Black spots in the color coding image indicate equal abundance of protein spot volume. The pink colour shows the spots with higher protein abundance and the green colored spots feature a lower spot volume in the transgenic embryos versus the WTS.

#### 4.2.5.3 Mass spectrometry analysis and outcome of the proteomics study

Based on the colour coding image (figure 19), the protein spots with differential volumes were picked and analysed using mass spectrometry. We were able to identify 49 proteins with higher abundance in the transgenic line BCS580 out of the 40 picked spots. For the lower abundant proteins in BCS580 we could identify 165 proteins out of 69 picked spots (see Supplemental data). The top-ten candidates, that either showed a higher or lower protein spot volume in the transgenic line BCS580 are shown in Table 3 and 4. It became apparent that oleosin 2 seems to be the storage protein that highly substitutes the loss of napins and cruciferins in the embryos of transgenic, with an average 6-fold increase in protein abundance compared to the WTS. Biotin carboxyl carrier protein 2 (BCCP2) showed an about 5-fold increased amount in the transgenics; this protein is a component of the acetyl coenzyme A carboxylase complex (ACCase). Amongst the top-ten candidates we also found EF-1 alpha, which appears to have a volume in-

crease of nearly four-fold compared to WTS; this protein is known to be essential for protein synthesis. There are several proteins that showed a spot volume increase of 2-2.5 (see Supplemental table), which indicates an enrichment in protein abundance about 2-fold. Some of them might be interesting candidates for explanation of the transgenic phenotype, e.g. Protein disulfide isomerase (PDI) - like 1- 2, and the plastidic pyruvate kinase (key enzyme of the glycolytic pathway; it catalyzes the substrate level phosphorylation of ADP at the expense of phosphoenolpyruvate (PEP), yielding pyruvate and ATP).

**Table 3** - Top 10 proteins, that show a higher abundance in the transgenic line BCS580

<b>Volume Diff.</b>	<b>Protein identification</b>	<b>Taxonomy</b>
6,75	Oleosin S2-2	<i>B. napus</i>
5,18	Oleosin S2-2	<i>B. napus</i>
4,71	Biotin carboxyl carrier protein of acetyl-CoA carboxylase 2, chloroplastic	<i>A. thaliana</i>
3,73	Elongation factor 1-alpha 1	<i>A. thaliana</i>
3,32	60S ribosomal protein L10	<i>E. esula</i>
3,32	Osmotin-like protein	<i>S. lycopersicum</i>
3,18	MLP-like protein 31	<i>A. thaliana</i>
2,74	Oleosin S2-2 O	<i>B. napus</i>
2,72	Oleosin 21.2 kDa	<i>A. thaliana</i>
2,66	Glutathione S-transferase U5	<i>A. thaliana</i>



**Table 4** - Top 10 proteins, that show a lower spot volume in the transgenic line BCS580

<b>Volume Diff.</b>	<b>Protein identification</b>	<b>Taxonomy</b>
10,17	Cruciferin CRU1	<i>B. napus</i>
10,17	Malate dehydrogenase	<i>B. napus</i>
5,94	12S seed storage protein CRU1	<i>A. thaliana</i>
5,94	12S seed storage protein CRU4	<i>A. thaliana</i>
5,94	Cruciferin CRU1	<i>B. napus</i>
5,77	Cruciferin CRU1	<i>B. napus</i>
5,63	Cruciferin CRU4	<i>B. napus</i>
5,63	Napin-2	<i>B. napus</i>
4,89	Elongation factor 1-gamma 1	<i>O. sativa</i>
4,89	Elongation factor Tu, chloroplastic	<i>G. max</i>

Proteins with lower spot volume in the transgenics were dominated by Napin2, Cruciferin1 and Cruciferin4 (5-10 fold reduction). A massive reduction of ~10fold in the transgenics was also observed for malate dehydrogenase, which plays an important role in the TCA cycle and converts malate to oxaloacetate. The protein abundance of PEPC isoforms 1 & 2 was ~ 5fold reduced in the transgenics, indicating some success in down-regulation. Noticeably, CRU1 appeared several times in spots captured from the gels. As published recently, in IEF/SDS – PAGE the chains of cruciferin are separated into different spots (Nietzel *et al*, 2013). In our Coomassie stained gel, it was clearly visible that certain chains show a massive reduction ( $\alpha$  P1,  $\beta$  P2), whereas others exhibited only minor changes ( $\alpha$  P2,  $\alpha$  P3,  $\beta$  P1 + P3) (figure 20).

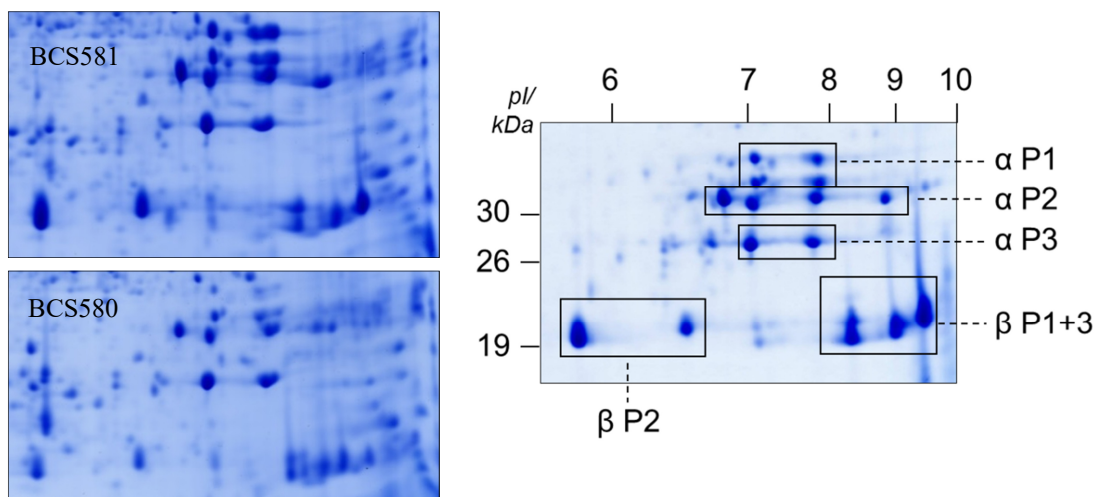


**Figure 20:** Proteome structure of cruciferin chains obtained after separation for pI and kDa in WTS BCS581 and transgenic line BCS580 as well as the published separation of cruciferin chains (Nietzel *et al.*, 2013).

#### 4.2.6 Transcriptomics - Impact of the triple knockdown on gene expression pattern of embryo

##### 4.2.6.1 General aspects

We performed an RNA sequencing analysis in collaboration with Dr. Himmelbach (IPK Gatersleben). The obtained sequencing raw data from transgenic and wildtype plants were processed by Dr. Jörg Schwender (Brookhaven National Laboratory, USA). According to the analysis, expression was detectable for 67.885 (67%) protein encoding genes in *B. napus*. Out of these, 184 genes showed a significant change ( $p < 0.01$ ) and a log2fold change of 2 or higher. In total 90 genes showed a lower abundance in the transgenic line BCS580 and 94 showed an increased transcript abundance. Out of these (due to gene redundancy in *A. thaliana*), 129 genes could be assigned to the Arabidopsis genome (63 down-regulated, 66 up-regulated). Analysis using Mapman software (figure 21) revealed that only very few transcripts matched the central metabolic categories of CHO metabolism, photosynthesis as well as lipid metabolism. Major changes were visible for the category of amino acid metabolism (5 diff expr.), stress related genes (9 diff expr.) and protein synthesis related genes (13 diff expr.). A lot of genes could not be assigned to a certain functional group. Overall we don't see a significant enrichment in any of the categories.

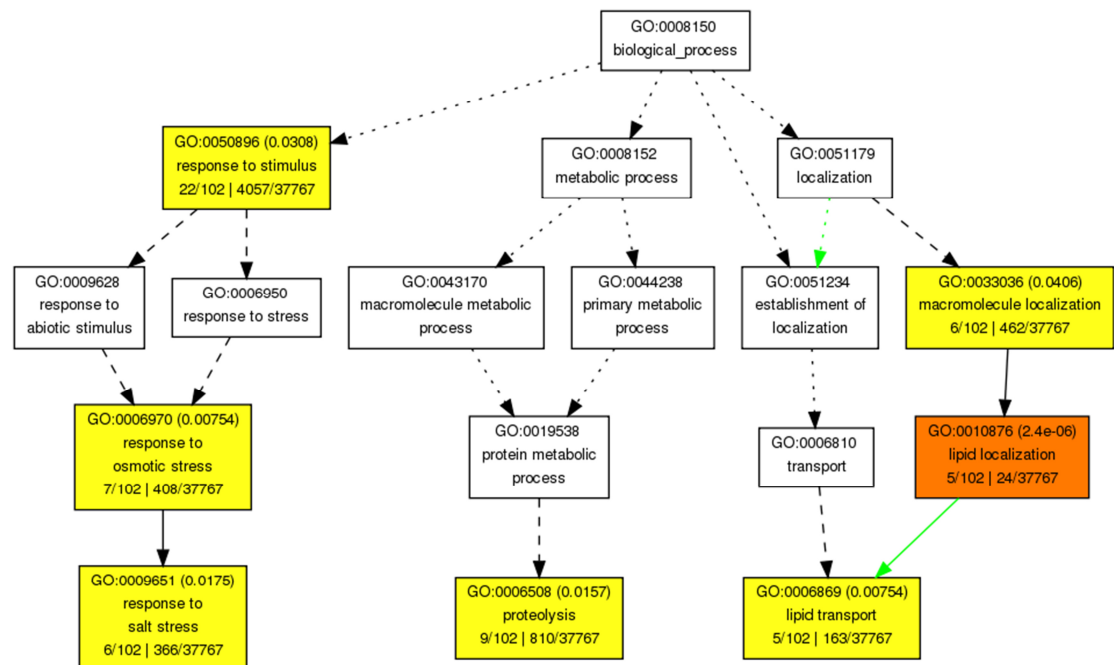
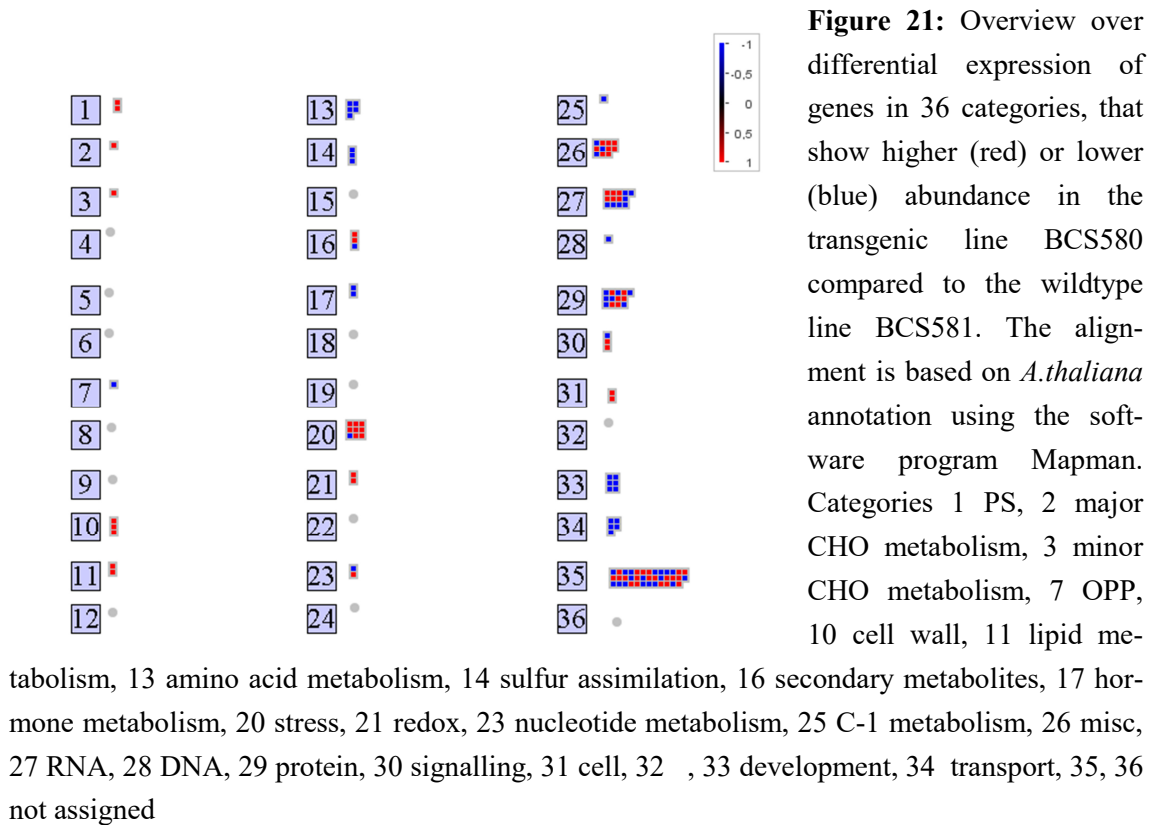


**Figure 22:** GO ontology mapping of the reads regarding biological processes overrepresented in the embryo of the transgenic line BCS580 compared to the WTS BCS581. The threshold was set to log<sub>2</sub>-fold-change >1 and p-value <0.05.

If we consider the GO categories in the reads of genes that are enriched in the embryo of the transgenic line BCS580, we mainly found gene groups associated to lipid localization and transport and also proteolysis (figure 22). Furthermore the GO groups of responses to salt and osmotic stresses showed a read accumulation.

#### 4.2.6.2 Transcript abundance of storage proteins

For the triple transgenic line the expression of storage proteins was found to be dramatically reduced. In comparison to the WTS, 12 *B. napus* gene transcripts annotated as *napin* and 7 annotated as *cruciferin* were significantly reduced with up to 10-fold and an up to 111-fold reduction in read counts. Surprisingly in the WTS ~50% of the total read counts mapped to 25 *napin* and *cruciferin* transcripts. In contrast, the transgenic line showed only 5% of total counts mapping to the same genes. These results corresponded well to the trends seen in proteomic data.

#### 4.2.6.3 Rebalancing of amino acid demands in transgenic plants

Based on the transcript data we estimated the amino acid (AA) demand of embryos for protein biosynthesis. The demands for a particular protein were computed based on multiplying the relative abundance of each amino acid in the protein with normalized RNAseq read counts (read counts divided by the length of the protein encoding mRNA). As shown in figure 23 the need for certain AA shifted clearly in the transgenics. Significant changes ( $p < 0.01$ ) were obtained for alanine, aspartic acid, asparagine, glutamine and serine. The strongest difference was visible for glutamine, which showed a reduction in demand of ~50% in the transgenics compared to the WTS. This corresponded to the shift in the steady state levels of free amino acids: transgenics showed strongly increased levels of glutamine.

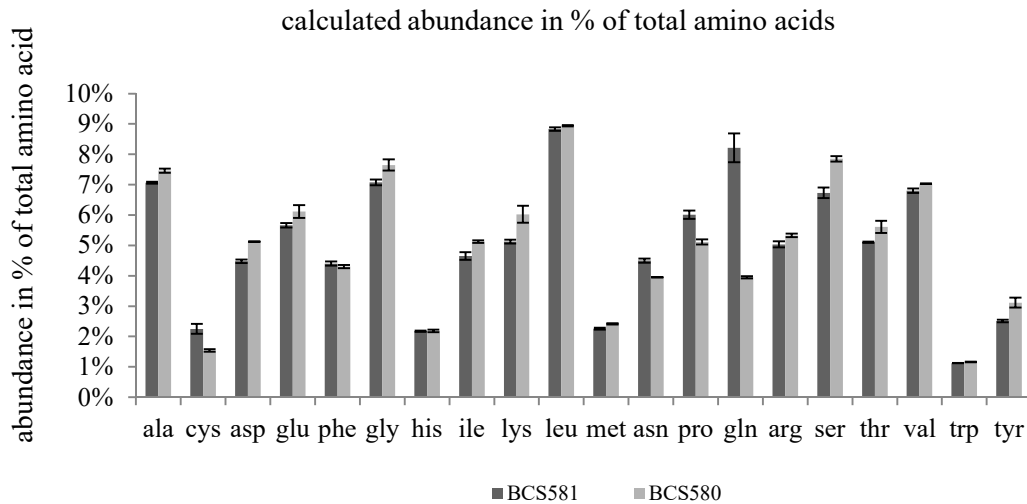


**Figure 23:** Calculated amino acid demands for protein synthesis in the transgenic line BCS580 compared to the WTS based on differential expression of genes, obtained from the RNA Seq data.

#### 4.2.6.4 No significant changes in PEPC transcript abundance in transcriptomics

Previous datasets already revealed that the down-regulation of the PEPC via the RNAi-construct is rather low: neither in real-time PCR analysis nor in enzyme activity measurements we detected strong changes (However, a ~5-fold reduction in protein abundance of PEPC was seen in proteomics). To verify these data, we checked if a decrease in transcript amount of PEPC isoforms was detectable in the transcriptome. While *A. thaliana* encodes for 5 isoforms of PEPC in *B. napus* we have 27 orthologs. About 97% of the reads assigned to PEPC account for the orthologs *pepc1* and *pepc2*. Although transgenics showed a decrease in transcript abundance of about 2-fold, this was not statistically significant.

#### 4.2.6.5 No significant increase in transcript abundance of oleosins in the embryo of the transgenic line BCS580

The proteome data revealed a strong rise of oleosin protein in transgenics. The transcriptomic data also showed an enhanced *oleosin* transcript abundance in embryos of the transgenic plants. However, for none of the 19 genes encoding oleosin isoforms the increase was found to be statistically significant. This might already indicate that the

stimulation of oleosin synthesis rather occurs at the translational level but not at the transcriptional level. In addition multiple members of a family of non-specific lipid transfer proteins were found to be upregulated, most evident for BnaC04g30640D. A subsequently performed real-time PCR analysis on the temporal expression of the oleosin isoforms in transgenic and wildtype embryos, revealed a strong increase in *oleosin* transcript in the transgenic plants from day 32 to 40 (see supplement figure S4).

#### 4.2.6.6 Transcriptomics revealed changes in sulfur metabolism

Out of the 129 genes that show an altered expression, 9 genes belong to the subgroup of sulfur metabolism and transport (Table 5). All of them were down-regulated in the transgenic plant. Multiple genes of the pathway for reduction of sulfate were found significantly downregulated, among them orthologs to an *Arabidopsis* sulfate transporter of the chloroplast envelope (AT5G13550), chloroplastidic isoforms of ATP sulfurylase (AT3G22890), 5'-adenylylsulfate reductase (AT1G62180) and sulfite reductase (AT5G04590). In addition, two orthologs of *Arabidopsis* adenylyl-sulfate kinase (AT2G14750; providing activated sulfate for secondary metabolism synthesis) were downregulated. Also related to sulfur metabolism, Serine acetyltransferase (AT2G17640; an enzyme active in cysteine synthesis), was downregulated. On the proteome level, S-adenosylmethionine synthase (AT4G01850, AT2G36880) was downregulated.

**Table 5:** Overview over differential expressed genes related to sulfur metabolism and transport

log2foldc hange	ortholog in <i>thaliana</i>	A. TAIR gene description
-5,59	AT1G72810	Pyridoxal-5'-phosphate-dependent enzyme family protein
-5,44	AT5G48850	SULPHUR DEFICIENCY-INDUCED 1
-4,74	AT1G04770	Tetratricopeptide repeat (TPR)-like superfamily protein;
-4,36	AT1G36370	serine hydroxymethyltransferase 7 (SHM7)
-3,77	AT1G18570	myb domain protein 51 (MYB51)
-3,76	AT1G62180	5'adenylylphosphosulfate reductase 2
-3,64	AT5G13550	sulfate transporter 4.1
-2,10	AT2G17640	ATSERAT3;1
-2,03	AT3G22890	ATP sulfurylase 1 (APS1 (ATP) activity)

## 4.2.7 Further analysis of transgenic plants

### 4.2.7.1 Transgenic plants show a reduction in sulphur content

The transcriptomic data already revealed a significant enrichment in genes that encode for sulphur metabolism and transport related genes in transgenics. The two sulfur (S) containing amino acids cysteine and methionine contribute to 2.5% (cruciferins) and 10% (napins) of total seed amino acids (Schwenke et al., 1981; Monsalve et al., 1991). We analysed the total S content of seeds using inductively coupled plasma optical emission spectroscopy (ICP-OES) in collaboration with Dr. Kai Eggert (IPK Gatersleben). As shown in figure 24, seeds of the transgenic plants showed a significant reduction in sulphur content at 30 DAP. Same difference was evident for mature seeds (data not shown).

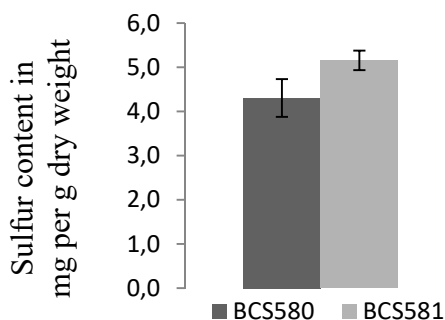


**Figure 24:** The total sulphur content in seeds (30 DAP) was measured by inductively coupled plasma optical emission spectroscopy (ICP-OES) as mg per g dry weight material and minute. Values are mean  $\pm$  SD ( $n = 3$ ). Significance is based on students T-Test ( $p$ -value = 0.038).

### 4.2.7.2 Transgenic seeds show a delayed germination

As the mobilisation of carbon/energy out of storage lipids and the degradation of storage proteins is crucial for proper germination, we tested if transgenics show any defects/delays in germination. The rate of germination of mature seeds of the same harvest of the transgenic line BCS580 and the corresponding WTS BCS581 was determined. After 20 hours the first seeds of both transgenic line and WTS started to germinate (=visible radicle protrusion; figure 25). After 30 hours almost all seeds of the WTS had germinated, while only 50% of the seeds of transgenics had germinated. It took additional 30 hours until about 90 % of the transgenic seeds were germinated. This evidences a clear delay in germination rate.

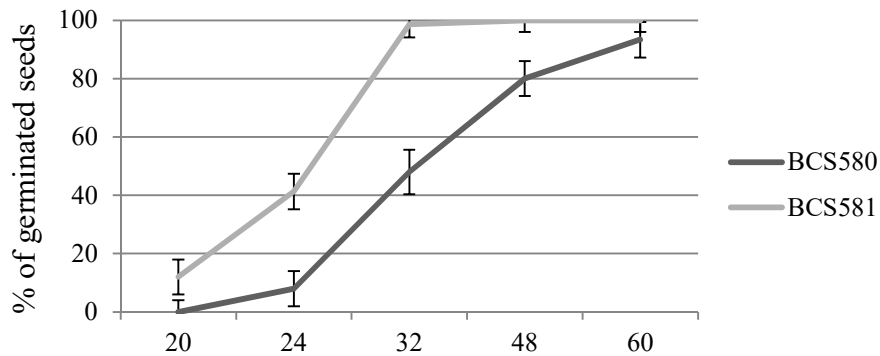


**Figure 25:** Time curve of germination of seeds from transgenic (BCS580) and WTS (BCS581) plants taken from the same batch (growth period). Seeds were

#### 4.2.7.3 Respiratory activity does not differ between transgenic and wildtype plants

Respiration rates of embryos were measured using non-invasive optical oxygen microsensors. Five isolated embryos (30 DAP) were taken for each measurement. Our data indicate that embryos of both transgenic and WT plants have similar respiratory activity (figure 26). The uptake of  $O_2$  ranged between 1.5-2  $\mu\text{mol}$  per mg embryo fresh weight and minute. Differences between transgenics and WTS were not statistically significant. This result corresponds to the (unchanged) pattern in metabolic intermediates related to energy metabolism (LC/MS-data) as well as transcriptome data

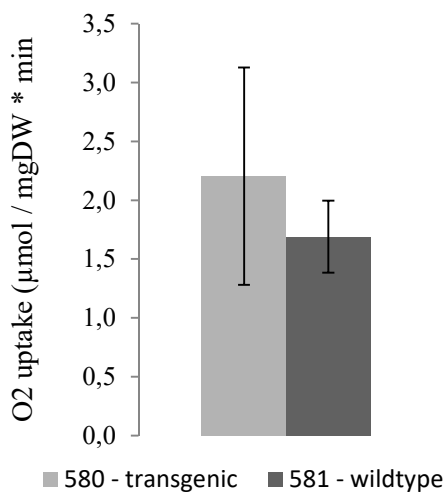


**Figure 26:** Respiration rates measured as uptake of  $O_2$ . (see methods for details) values are means  $\pm$  SD (n = 5).



#### **4.2.7.4 Transgenic and wildtype embryos have similar photosynthetic activity at physiological light conditions**

To check for photosynthetic capacity of seeds (30 DAP) we measured the operation efficiency of photosystem II using PAM fluorescence. The photosynthetic energy transfer occurring within the seed was assessed by the measurement of the linear electron transport rate (ETR). When providing photosynthetic active radiation of 37  $\mu\text{mol}$  quanta per  $\text{m}^2$  per second, the embryos of transgenic and WTS plants reached similar ETR's and showed similar gradients across the seed (figure 27 A & B). For both types of embryos, the seed coat displayed substantially higher levels of ETR than the embryo itself. A slight gradient was also visible for the outer and inner cotyledon, which is in accordance to earlier studies (Borisjuk *et al.*, 2013). We further determined the rapid light response curves for both sample types (figure 27 C). Data indicate that both transgenic and WT embryos possess similar photosynthetic activity at physiological light levels (maximum of 100 PAR that reaches the embryo inside the seed). Some differences between transgenic and wildtype embryos became apparent at higher light levels, which are, however, physiologically less relevant.

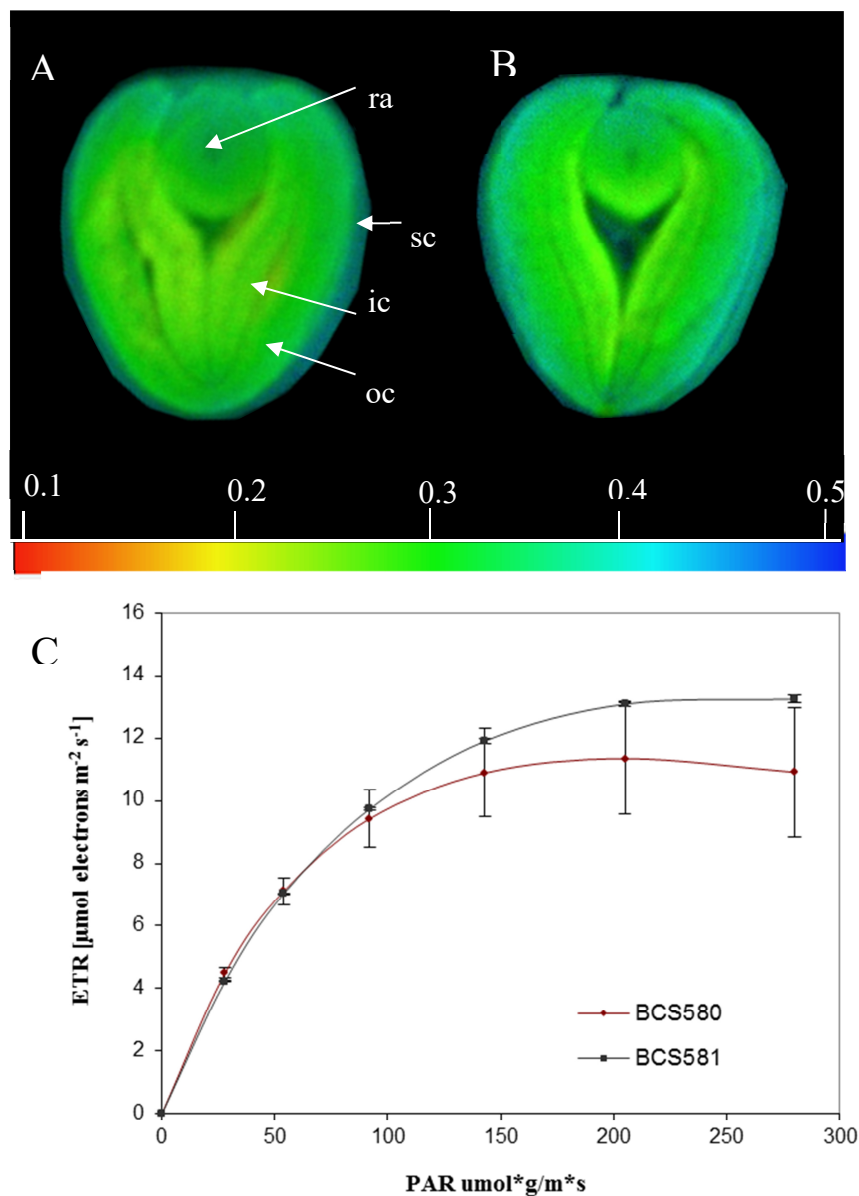


**Figure 27:** Gradients in *B. napus* seed photosynthesis measured by the Imaging-PAM Chlorophyll Fluorometer. The colour-coded map of the effective quantum yield of photosystem II of embryos derived from the transgenic line BCS580 (A) or the corresponding wildtype line BCS581 (B). The distribution of photosynthetic capability across the seed was measured at 37  $\mu\text{mol}$  quanta per  $\text{m}^2$  per second. The diagram (C) shows the rapid light response profiles of the photosynthetic ETR in distinct regions of the seed. Each data point represents the mean  $\pm$  sd ( $n = 10$ ). ic, inner cotyledon; oc, outer cotyledon; ra, radicle; sc, seed coat.

#### 4.2.8 Histology – demonstrating an extraordinary phenotype

Seeds at 50 DAP were prepared for transmission electron microscopy (TEM) and pictures of outer cotyledons were taken. As shown in figure 28, the cells of outer cotyledons of transgenic plants looked abnormal (A, C). Protein storage vacuoles (psv) were clearly visible in wildtype cells, but were smaller or nearly absent in transgenic cells (B, D). Lipid droplets (that usually are found to be attached in an ordered two rowed manner along the cell membrane) were spread across the entire cell in the transgenic plants. Most surprisingly, we observed huge membrane foldings in the cytoplasm of transgenic plants. The cell sizes were comparable between transgenic and wildtype outer cotyledon cells.

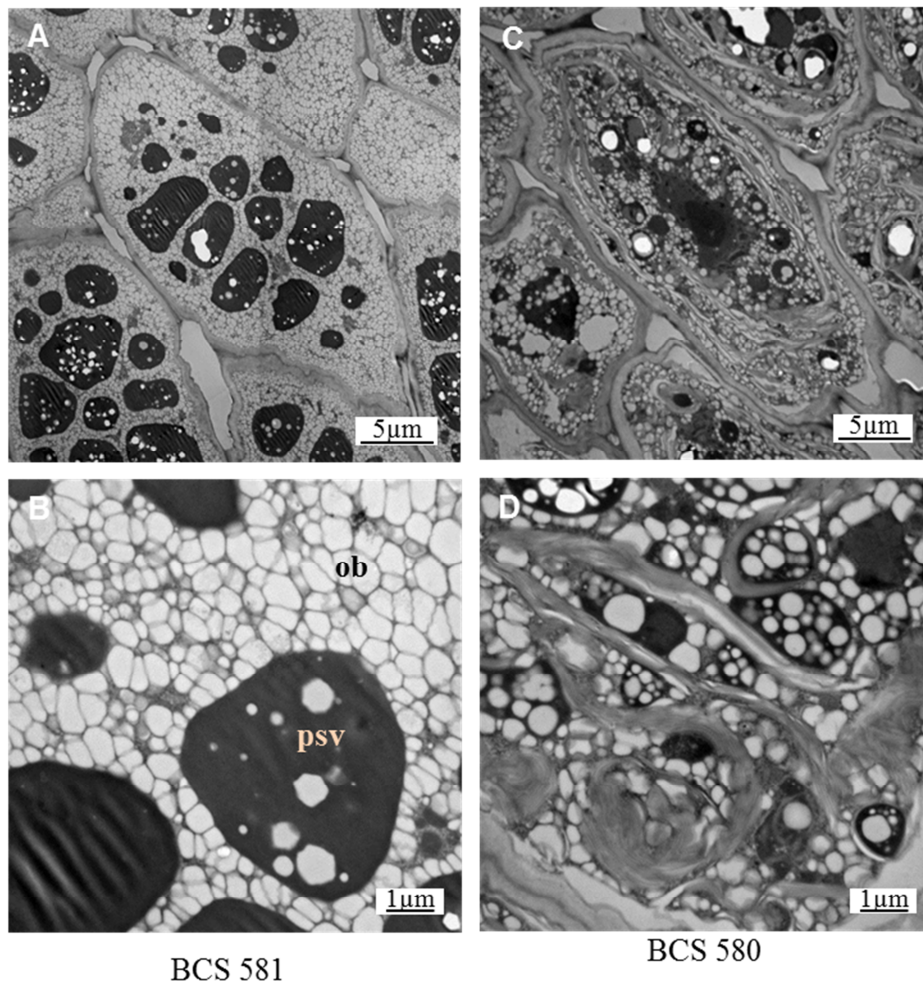


**Figure 28:** TEM - Histology of outer cotyledon cells of seeds (50 DAP) (A, B) overview over the whole cell. (C, D) detailed view to pinpoint interesting aspects. Ob - oil bodies, psv - proteins storage vacuoles

We further performed an immunolabelling of napins, cruciferins and oleosins (figure 29). In WTS, we found a clear localization of cruciferins and napins in protein storage vacuoles that were spread evenly throughout the cell. Oleosin in contrast was localized to the oil bodies that surrounded the storage vacuoles and were directed toward the cell wall. In transgenics, much less labelling of cruciferin and almost no labelling of napin in the storage vacuoles was observed. Oleosins show a much higher labelling intensity as compared to WTS; they clearly localized to the unusual membrane structures expanding toward the inside of the cell.

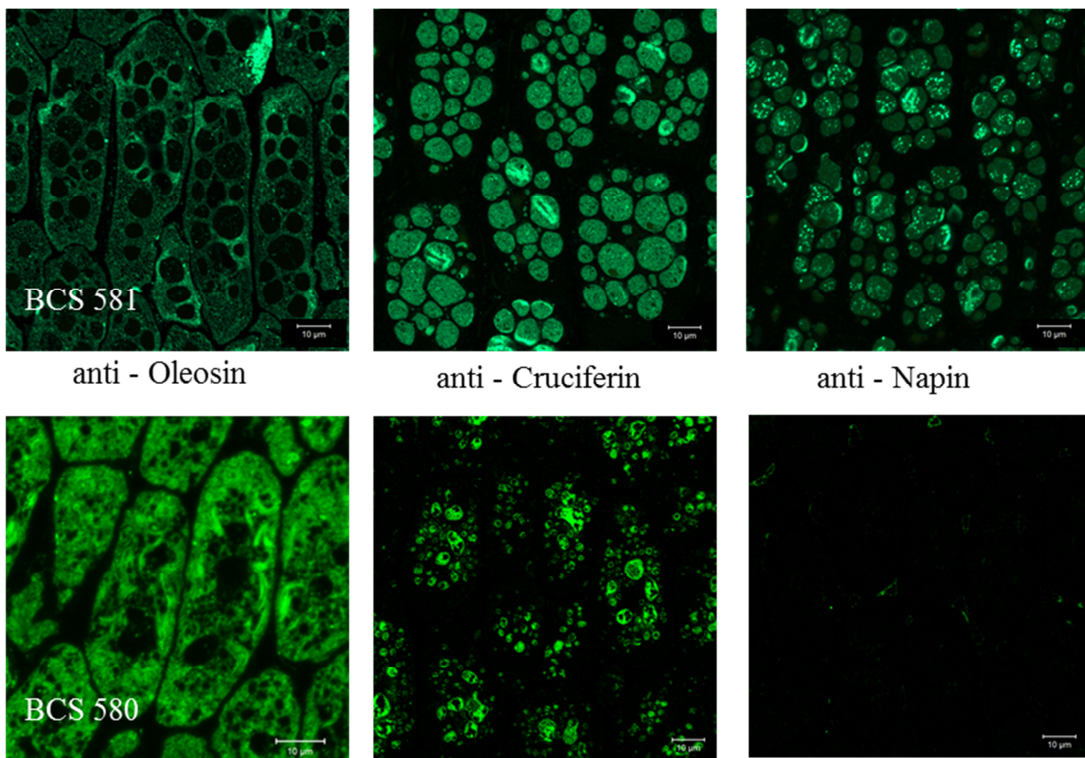


**Figure 29:** Immunostaining of cotyledons cells at almost mature stage of development (50 DAP). The immunolabeling was carried out as described in the MM section. The sections show the distribution of oleosins, cruciferins and napins throughout the cell. Upper row – WTS BCS 581, bottom row – Transgenic line BCS 580

#### 4.2.9 The obtained phenotype in triple knockdown lines is probably not related to the low reduction in PEPC

Above results on the triple knockdown (transgenic) plants indicated a strong repression of the storage proteins napin and cruciferin but a rather low repression of PEPC. To check whether the apparent phenotype relates also to PEPC knockdown – or exclusively to the napin/cruciferin knockdown – we additionally analysed transgenic *B. napus* plants where only PEPC was down-regulated.

##### 4.2.9.1 Low down-regulation effect in *pepc* knockdown lines

To investigate the degree of successful down-regulation in all three *pepc* knockdown lines, RNA of 30 days old embryos was isolated and used for quantitative real-time PCR analysis. Three PEPC isoforms were tested and the same primers were used as in the previous experiment for the triple knockdown lines. As shown in figure 30 the transgenic lines BCS1175 and BCS1177 show a reduction in transcript amount of about log<sub>2</sub> fold -0,5, which means half reduction in PEPC transcript amount compared to their corresponding wildtype. For the line BCS1188 no significant reduction in transcript abundance for the tested PEPC isoforms could be detected. The overall down-regulation thus is rather low, as seen previously in the analysis of the triple construct lines.

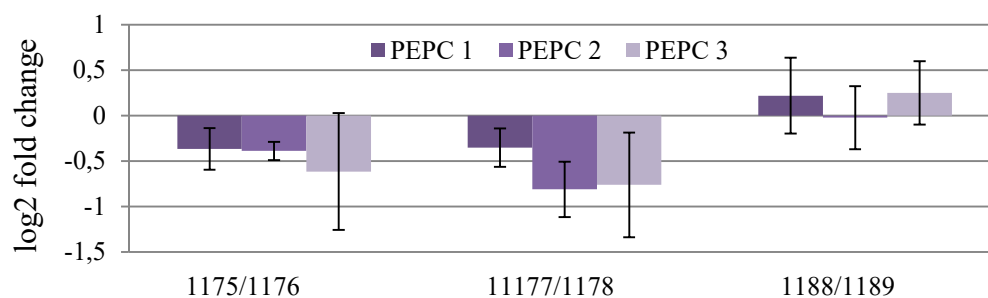


**Figure 30:** Transcript level changes displayed as log<sub>2</sub>fold change of *pepc* genes in embryos of the *pepc* single knockdown line and corresponding wildtype. Total RNA was extracted from the embryos of 30-days-old embryos and the transcript levels of the genes were analyzed by quantitative real-time PCR. The expression level was normalized to that of *BnUBC9*. Values are mean  $\pm$  SD (n = 3).

#### 4.2.9.2 The PEPC enzyme activity was not affected in embryos of *pepc* knockdown lines

We again performed a coupled enzyme activity assay to determine  $V_{max}$  activity of PEPC. Total enzyme extract was prepared from embryos (30 DAP). Data in figure 31 indicate that PEPC enzyme activity was not statistically significantly changed in the transgenics. Enzyme activity ranged between 0.5-1  $\mu\text{mol}$  per g fresh weight and min, which was similar to those obtained in the previous measurement. This clearly indicates that the efficiency of *pepc* down-regulation is rather low.

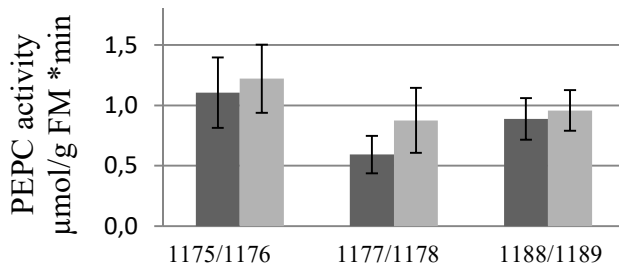


**Figure 31:** Measurement of the  $V_{max}$  PEPC enzyme activity in  $\mu\text{mol/g}$  fresh weight per minute of *pepc* single transgenic lines (grey) compared to their corresponding wildtype (dark grey bars). Values are mean  $\pm$  SD (n=6).

#### 4.2.9.3 Mature seeds of PEPC knockdown plants do not show any changes in seed traits

We measured major seed traits in *pepc* knockdown lines in comparison to their WTS. As shown in figure 21, the total lipid content of mature seeds was comparable among all lines. We also checked for protein content and seed dry weight. In none of these parameters we could find any consistent significant changes in transgenics versus WTS (Supplemental table S6).

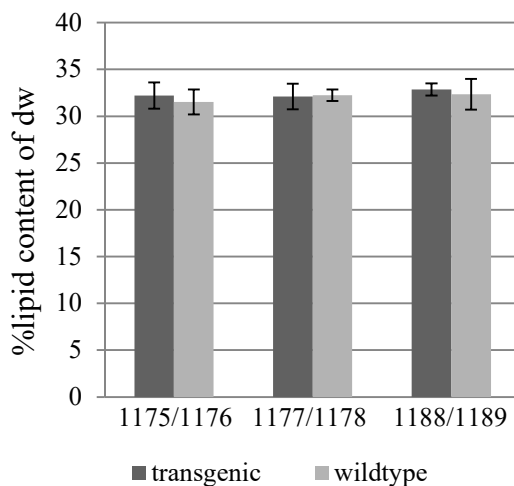


**Figure 32:** Measurement of the lipid content as % of dry weight of intact mature seeds of the three *pepc* single transgenic lines and their corresponding WTS. Values are mean (10 seeds each)  $\pm$  SD (n=3).

## 5.1 Discussion PART I

### 5.1.1 Establishment and evaluation of an isotope labelling technique for developing seeds

A proper isotope labelling technique for developing seeds has at least two goals: (1) it should allow the seed/embryo to grow identical or near to *in vivo* conditions; and (2) it should be able to transfer sufficient label, so that maximum information can be retrieved from the experiment. Many different approaches have been developed to trace the uptake of labelled metabolites and its subsequent metabolic conversion. Initial studies often used  $^{14}\text{C}$ -labelled substrates as the analysis turned out to be pretty sensitive (Keiller & Mathers, 1983; Shields & Paul, 1973; Harris & Jeffcoat, 1972). This has shifted to the use of stable isotopes like  $^{13}\text{C}$  or  $^{15}\text{N}$ . One advantage of stable isotopes is the avoidance of hazards as well as radioactive pollution (Derrien *et al.*, 2003; Ghashghaie & Tcherkez, 2013). Possibly more important is the option to trace the label transfer among metabolites using LC/MS technology. Many approaches describe the labelling of whole plants using  $^{13}\text{CO}_2$  (Bromand *et al.*, 2001; Berg *et al.*, 1991; Svejcar *et al.*, 1990; Thompson, 1996), aiming to study the metabolism of carbohydrates (Meharg, 1994; Warembourg & Kummerow, 1991). To meet (above-mentioned) goal #1, it was the initial idea to label the entire plant or the source leaf with  $^{13}\text{C}$ - $\text{CO}_2$ . However, this did not provide sufficient amounts of  $^{13}\text{C}$ -label toward the seed/embryo (preliminary tests, data not shown). Instead, a previously published incubation method (Morley-Smith *et al.*, 2008) was evaluated and refined. Siliques were excised from the plant and incubated in a medium, containing  $^{13}\text{C}$ -labelled sugar and/or  $^{15}\text{N}$ -labelled amino acids. In this way, we could maintain the environment which seeds/embryos experience *in vivo*. We could also define the quantity and type of sugar taken up by the seed, calculate uptake rates and follow subsequent metabolism. To meet the metabolic *in vivo* scenario, the choice of labelled substrate was important to consider. The majority of studies uses either  $^{13}\text{C}$ -glucose or  $^{13}\text{C}$ -sucrose as carbon source. While  $^{13}\text{C}$ -glucose is generally more affordable in terms of costs, our experiments demonstrated that the use of  $^{13}\text{C}$ -sucrose results in much higher assimilate uptake rates. Sucrose is - as compared to glucose - the preferred, natural transport form of photosynthetically assimilated sugars in higher plants (Ward *et al.*, 1998). It is derived from maternal source organs like leaf or silique and transported via the phloem to the seed coat via distinct sucrose transporters. It was shown in *A. thaliana* that phloem unloading and delivery occurs via the funiculus, which is connected

to the outer integument (Stadler *et al.*, 2005). Studies on *in vitro* culture of early *B. napus* embryos showed, that the supply of sucrose to the growth medium was the carbon source of choice for *in vitro* culture, providing morphologically normal embryos (Slesak & Przywara, 2003). The type of sugar supplied to the seed can also have implications for embryo development. Seeds aged 17 days and older exhibit a much higher sucrose than hexose concentration (Morley-Smith *et al.*, 2008). This is in concert with a fall in acid invertase activity in the liquid endosperm, a decrease in the overall amount of endosperm, and the onset of storage product synthesis in the embryo (Baud *et al.*, 2002; Hill *et al.*, 2003). As a result of my studies, an experimental protocol for silique culture using  $^{13}\text{C}$ -sucrose and with well-defined parameters is now available.

### 5.1.2 The contribution of the silique to the development of the seeds

The main contribution of the silique to the seed development is not only being a shell to protect them from environmental influences, but also to provide carbohydrates and other nutrients (Major and Charnetski, 1976; Singal *et al.*, 1987; Sheoran *et al.*, 1991; Bennett *et al.*, 2011). At the end of maturation, siliques even become the most dominating photosynthetic organ of the *B. napus* plant, due to leaf senescence and leaf area decline (Allen *et al.*, 1971; King *et al.*, 1997; Mogensen *et al.*, 1997; Berry and Spink 2006). Recent studies showed, that siliques of high oil rapeseed lines contributed to the increase in lipid content via superior photosynthetic assimilate production (Hua *et al.*, 2012). Photosynthesis of silique seems to make a large contribution to final seed weight as could be shown in light shading experiments (Singal *et al.*, 1992). In our experimental setup, siliques incubated in  $^{13}\text{C}$ -sucrose containing medium accumulated label up to 48 hours of incubation, and maintained a stable level thereafter (which is in contrast to seeds which steadily accumulated label also for extended time periods). Siliques do obviously rather support the flow of  $^{13}\text{C}$ -sucrose to the seed than store or metabolize it themselves.



### 5.1.3 Quantification and visualization of the $^{13}\text{C}$ label intake of developing seeds

The developing plant embryo receives its nutrition from the surrounding maternal seed coat and endosperm. The molecular mechanisms are still not fully clear, and, in particular, the pathway of carbon delivery remained controversially discussed. Our studies demonstrated that the liquid endosperm accumulates and stores most of the  $^{13}\text{C}$ -sucrose entering the seed (figure 7). This already pinpoints to the important role of the liquid endosperm fraction as sugar storage pool. Besides its function as carbon source, sucrose also plays an important role for osmoregulation (King *et al.*, 1997; Hill *et al.*, 2003; Morley-Smith *et al.*, 2008). The liquid endosperm also showed highest concentrations of  $^{13}\text{C}$ -labelled hexoses (released from sucrose). King *et al.* (1997) showed that hexoses in seeds containing early-cotyledon stage embryos were mainly localized to the liquid endosperm and that sucrose was evenly distributed between seed fractions (embryo and endosperm/seed coat). In our experiments, the unlabeled hexose also showed highest concentration in liquid endosperm. We could furthermore detect various  $^{13}\text{C}$ -labeled metabolites in the seed coat/aleurone layer; they appeared much earlier than in the embryo and liquid endosperm tissue, indicating substantial metabolic activity in this organ.

For the developing dicotyledonous seed like *B. napus*, there still exist opposing assumptions about the pathway of sucrose transfer towards the embryo. The funiculus links the developing seed to the silique. It terminates in the outer integument that lies below the chalazal endosperm, where phloem unloading of sucrose occurs into the outer integument (Stadler *et al.*, 2005). The subsequent pathway to the embryo remains elusive. Some have suggested that the suspensor plays an important role in nutrient supply to the early developing embryo (Kawashima and Goldberg, 2010), but direct evidence is lacking. SUT transporters have been identified in pea (*Pisum sativum*), bean (*Phaseolus vulgaris*) and others, mediating sucrose efflux from seed coat (Ritchie *et al.*, 2003; Zhou *et al.*, 2007). To unravel the sugar transport route in *B. napus*, one needs to visualise the uptake of  $^{13}\text{C}$ -sucrose inside the developing seed. For this purpose, we decided to use mass spectrometry imaging. Siliques were incubated using the developed culture approach (see above) and seeds were sampled at different time points. About 3 hours after start of incubation,  $^{13}\text{C}$ -sucrose was clearly detectable in the branch point of funiculus and outer integument, starting to spread evenly through the first third of the seed; label was detectable in both liquid endosperm and aleurone layer attached to the seed coat. Notably, there was no signal for  $^{13}\text{C}$ -sucrose in the suspensor. Our results do therefore

not provide evidence for the suggested nutrient supply function of suspensor. Some studies state, that pushing and anchoring the embryo into the inner part of the seed, in the surrounding endosperm, is another important function of the suspensor (Yeung and Clutter, 1979). At least for *A. thaliana*, the expression of transporters involved in nutrient transport in suspensor cells was shown (Friml *et al.*, 2003; Hruz *et al.*, 2008). Studies on the suspensor length showed an embryo growth inhibition for shorter suspensors (Babu *et al.*, 2013).

Taken together, I propose a scenario where the phloem-derived sugars spread to the aleurone layer and further to the endosperm. From there, sugars are taken up by the embryo. We did not find support for the proposed sugar transport function of suspensor.

#### **5.1.4 The silique culture approach can be used to model metabolism in contrasting genotypes**

My work demonstrates that silique culture in combination with  $^{13}\text{C}$ -labelling and subsequent LC/MS analytics can be a versatile tool to identify metabolic modes in distinct rapeseed accessions. Exemplarily, I have chosen two contrasting rapeseed genotypes (CR3170 and CR3231), previously characterised by Schwender *et al.* (2014). CR3231 represents a low-oil genotype with compensatory increased starch accumulation compared to the high-oil genotype CR3170. Their siliques were incubated (as described above) and their seeds were analysed. High-oil line CR3170 took up about 20% more  $^{13}\text{C}$ -sucrose than CR3231. Furthermore, the high-oil line was capable of elevated sucrose breakdown/glycolysis, indicated by higher  $^{13}\text{C}$ -labeling in hexoses/hexose-P but less label in sucrose. Sucrose uptake and conversion via glycolysis to fatty acids/lipids is a major metabolic activity in developing embryos of *B. napus* (Baud *et al.*, 2008; Wei *et al.*, 2008). Our experimental data fit to this general activity profile as well as to more specific findings on these two contrasting rapeseed accessions (Schwender *et al.*, 2014). From this one can conclude that the developed silique culture approach is suitable for more widespread applications in plant biochemistry and physiology.

## 5.2 Discussion PART II

### 5.2.1 The triple knockout lines show massive down-regulation of major storage proteins

The generation of triple knockout lines followed the idea that reductions in storage proteins synthesis would favour oil biosynthesis. These two storage compound classes represent competing sinks for both energy and carbon. To achieve an apparent reduction in seed storage proteins, the down-regulation constructs for *cruciferin* and *napin2*, respectively, were set under the seed-specific *napin*-promoter. For napins in rapeseed, the different large and short chains share a high similarity in amino acid composition (Lönerdal & Janson, 1972). Thus, one can expect that a down-regulation in *napin2* will also influence other napins. The napin promoter, used here, was shown to induce a strong seed-specific expression (Stålberg *et al.*, 1996) and to successfully express foreign genes or down-regulate unwanted genes in a seed specific manner in several plants such as *Lesquerella fendleri* (Lin & Chen, 2012), *B. napus* (Hitz *et al.*, 1995) and chili pepper (Subramanyam *et al.*, 2010). In the closely related *A. thaliana*, five At2S gene homologues to napA are described. Four of them are found in a cluster (van der Klei *et al.*, 1993). Sequence alignment revealed that the At2S3 promoter in *A. thaliana* is very similar to the napA promoter (Martin *et al.*, 2008). *Napin* gene expression is regulated at the transcriptional level in a strict temporal and spatial pattern during early and mid seed maturation and reaches very high levels of transcript. Previous studies on the *napA* promoter indicated that the sequences between -152 and +44 are essential for the seed-specific expression pattern in transgenic tobacco plants, and several cis-elements upstream from -152 were found to act as positive or negative regulatory motifs (Stålberg *et al.*, 1993; Ellerström *et al.*, 1996). The *B. napus* napin promoter is known to be controlled by the transcriptional activator ABI3 and ABA (Ezcurra *et al.*, 2000) ABI3 is a key regulator of gene expression during embryo maturation in crucifers (Marion-Poll, 1997; Phillips *et al.*, 1997). The phytohormone abscisic acid (ABA) is the key hormone required throughout the process of seed maturation (Nambara *et al.*, 2003). ABA is necessary both for storage product deposition and for induction of seed dormancy (Phillips *et al.*, 1997).

Our studies on down-regulation of different *B. napus* cruciferin and napin isoforms revealed a high success for all tested transgenic lines from mid to late stages of seed de-

velopment. The transcript amount was reduced up to 1000 - fold for napins and 120 - fold for cruciferins at 45 DAP in transgenic versus wildtype (WT) embryos. Cruciferin1 and cruciferin2 exhibit 70% identity and are of similar size, while cruciferin3 has an extended glutamine rich region in the center of a larger polypeptide that contributes to its divergence from the other family members, with only approximately 50% identity (Lin *et al.*, 2013). The success in down-regulation could further be seen in the proteomics approach (reduction of cruciferin spot volumes from 3-10 fold; for napin2 the spot volume was reduced about 5-6 fold). As mentioned before, five different *B. napus* cruciferins belong to three different families. Recently it has been shown that cruciferin exhibits an octameric structure and the different chains can be separated in an IEF SDS Page (Nietzel *et al.*, 2013). Our Coomassie stained gel clearly showed that certain chains are massively reduced ( $\alpha$  P1,  $\beta$  P2), whereas others exhibit minor changes ( $\alpha$  P2,  $\alpha$  P3,  $\beta$  P1 + P3). It appears likely that the construct used for transformation has preferentially hit certain chains, which in turn lead to an ineffective assembly of the cruciferins.

### 5.2.2 The down-regulation of major storage proteins leads to protein rebalancing

Although the accumulation of specific major storage proteins was significantly reduced in transgenics, the overall seed protein content remained surprisingly stable (~10% reduction as compared to WTS). There are reports on the expression of foreign proteins in plants, where protein rebalancing was observed. For example in rice, the expression of a sulfur rich sunflower protein gene does not alter overall protein content, due to the downregulation of endogenous reserve proteins (Hagan *et al.*, 2003). Also for wheat, there is a report on glutenin overexpression, which causes a compensatory reduction in endogenous prolamins (Scossa *et al.*, 2008). Most of the studies, aiming to manipulate certain protein reserves by enhanced expression of target proteins, lead to a protein rebalancing effect. More recent studies aimed to down regulate unwanted proteins by antisense/RNAi technology. There are reports on the introduction of antisense genes for either napins or cruciferins in *B. napus* that lead to the increase of the other without causing any changes to the overall protein or lipid content, nor fatty acid composition (Kohno-Murase *et al.*, 1994, Kohno-Murase *et al.*, 1995). In *Arabidopsis*, there are studies that deal with seed storage protein mutants, one of them is *ssp1*. A stop codon in *cruciferin3* leads to a repression in cruciferin synthesis and seeds exhibit lower protein

content of ~15% compared to WT. Surprisingly, *spl1* seeds also contain about 15% less oil than those of WT (Lin *et al.*, 2013). Taken together, it is likely that seeds somehow exhibit a function in “sensing” the total protein (nitrogen) content and tending to keep it in balance. Regulation of seed storage protein accumulation likely involves an integrated genetic and physiological network (Golombek *et al.*, 2001; Brocard-Gifford *et al.*, 2003; Elke *et al.*, 2005; Fait *et al.*, 2006). Tight genetic control of storage protein accumulation is also depending on a range of maternal, nutritional and environmental effects (Weber *et al.*, 2005). For example, ABA has been extensively studied to modulate napin/cruciferin levels. Isolated embryos at the beginning of seed storage protein accumulation, cultivated with ABA, aggregated usual levels of seed storage proteins, whereas under absence of ABA, the mRNA levels of seed storage proteins decreased dramatically (Crouch *et al.*, 1985, Finkelstein *et al.*, 1985). Transcriptional regulation of storage product related gene expression is complex. For example in *A. thaliana* the gene FUS3 is known to regulate storage protein synthesis by affecting transcript amounts. Furthermore studies on a *fus3* mutant showed that it also affects lipid and carbohydrate metabolism (Bäumlein *et al.*, 1994). The primary role of these transcription factors (TFs) during seed development involves the control of accumulation of storage reserves and related processes (Kroj *et al.*, 2003; Gutierrez *et al.*, 2007; Santos-Mendoza *et al.*, 2008).

To better understand the protein rebalancing phenotype, we performed a detailed proteome analysis. All together 1124 protein spots could be identified of which 109 showed differential spot volumes. Increased spot volumes in the transgenics became apparent for Oleosin2 (~6-fold increase compared to WT). No other storage proteins were detected to compensate for napins/cruciferins, but some additional changes in enzyme proteins were seen (e.g. biotin carboxyl carrier protein of acetyl-CoA carboxylase 2, glutathione S-transferase, nitrogen regulatory protein, alpha-galactosidase). Unfortunately, our proteomics approach did not account for (rather hydrophobic) membrane associated proteins (Nagaraj *et al.*, 2007). Membrane proteins play important physiological roles and constitute ~20-30% of all open reading frames (ORFs) in fully sequenced genomes (Nam *et al.*, 2009).

### 5.2.3 Protein rebalancing also affected amino acid composition of the seed

To uncover potential changes in seeds amino acid composition, we analysed metabolite and calculated the respective pool sizes. Transgenics showed clear changes in steady state levels of free amino acids compared to WT (more His, Ser, Trp, Val, Arg and Gln, but less Pro). Notably, oleosin proteins comprise a proline knot motif in the hydrophobic domain, which is required for oil body targeting (Abell *et al.*, 1997). The lower protein biosynthetic demands in transgenics are believed to cause the higher abundance of most free amino acids. Amino acid demands were also calculated based on transcript data, indicating that transgenics have ~2-fold lower demands for Gln as compared to WT. This is in accordance with our measurements of (elevated) steady state levels of free Gln.

### 5.2.4 Down-regulation of PEPC is unlikely to contribute to the transgenic phenotype

The enzyme PEPC (one target of the triple knockdown) is responsible for the irreversible conversion of PEP to OAA, enriching the organic acid pool (anaplerotic function), which are subsequently used up by the TCA cycle and/or as precursors for amino acid synthesis (Chollet *et al.*, 1996; Stitt, 1999). Repression of PEPC was proposed to channel carbon from organic acid/amino acid synthesis toward fatty acids/storage lipids. Elevation of its substrate PEP was proposed to allosterically enhance the flux toward acetyl-CoA/fatty acids/TAG (Schwender *et al.*, 2015). Correspondingly, overexpression of PEPC in *Vicia narbonensis* caused an increase in protein content to up to 20% of total dry weight and additionally a higher seed weight of 20-30% (Rolletschek *et al.*, 2004). Furthermore, metabolite profiles of developing embryos revealed a shift of carbon from starch to amino acids and organic acids. In leaves of *A. thaliana*, PEPC1 and PEPC2 turned out to be the most highly expressed isoforms and their activity ranked for around 93% of total PEPC activity in the leaves. The *pepc1/pepc2* double mutant exhibited a severe growth phenotype whereas the single mutants showed no phenotype (Shi *et al.*, 2015). In our approach the RNAi construct for *pepc* was either set under the promoter *FatB4* (lines BCS 566, 568, 570, 572 and 574) or *Ole1At* (lines BCS 576, 578, 580). Both were shown in preliminary studies to work well in seeds. To quantify the success in repressing PEPC in transgenics, we determined gene expression, protein abundance and enzyme activity. The down-regulation of expression of all three tested

*pepc* isoforms in the transgenic plants was rather low (1-4 fold compared to WT). When measuring the maximum catalytic activity ( $V_{\max}$ ) of this enzyme, only two lines (BCS570, BCS580) showed a statistically significant reduction (up to 75% compared to WT), most obvious for line BCS580. PEPC activity is known to be allosterically controlled. Malate, aspartate and glutamate are known as negative regulators, whereas sugar phosphates stimulate PEPC (O'Leary *et al.*, 2011a). As transgenics show significant reduction for malate and oxalacetate, one can exclude negative feedback regulation. Our proteome study revealed a reduction in PEPC protein abundance of  $\sim 70\%$ , confirming the results of the enzyme assay. We also noted a higher abundance of chloroplastic pyruvate kinase ( $PK_c$ ). This is interesting, because PEPC was shown to build an alternative flux mode to  $PK_c$  when combined with malate dehydrogenase and mitochondrial NAD malic enzyme or plastidial NADP malic enzyme, respectively (Schwender *et al.*, 2006). Taken together, the changes related to PEPC are regarded as less significant with respect to the seed phenotype observed in the transgenics.

To confirm this assumption we also analysed transgenic plants, where only PEPC was down-regulated using the same *pepc* RNAi construct. As expected, the knockdown of *pepc* transcript was rather low in all single RNAi lines and enzyme activity was even unchanged between transgenic and wildtype embryos. None of the tested lines showed a reduction in either lipid or protein content nor any other obvious phenotype.

### 5.2.5 Triple knockdown lines accumulate less lipid

Protein storage and oil accumulation do sometimes but not always compensate for each other. For example, in *Arabidopsis* *abi* and *aba* mutants where storage protein content is strongly reduced, oil content does not change (Finkelstein and Somerville, 1990). In the *wri1* mutant, oil is reduced by 80% but storage protein content is similar to that of WT (Focks and Benning, 1998). In two lines of *B. napus* with a 10% difference in oil content there is only a 1% difference in protein content (Li *et al.*, 2006). In our study, the triple knockdown lines showed (to our surprise) a significant reduction in lipid content of  $\sim 15\%$  in all tested lines, whereas the overall protein content was much less affected. Fatty acid analysis showed only minor changes (slightly less oleic acid in favour of linoleic and linolenic acid). The reduction in oleic acid might be related to lower protein abundance of stearyl-acyl carrier protein desaturase in the transgenics. This enzyme is

known to catalyse the first desaturation step on the stearic acid (C18:0) chain (Los & Murata 1998; Kachroo *et al.*, 2007). Studies on soybean identified a quantitative trait loci for seed oil and protein content in recombinant inbred lines (RIL). Seed oil was found to be inversely correlated to protein content (Lark *et al.*, 1994). There are hypotheses according to which the protein-to-oil ratio is generally maintained (e.g. in the *cruciferin3* mutant). Our transgenics do not support this.

### 5.2.6 Possible effects of oleosin on oil body formation

Previous investigations showed, that up to 4% of the seed oil body weight accounts for proteins, mainly oleosins (Huang, 1992; Tzen and Huang, 1992, Jolivet *et al.*, 2004; D'Andréa *et al.*, 2007; Vermachova *et al.*, 2011). Our transgenics show a 6-fold increase in Oleosin2 while TAG content was ~15% lower. This relationship is in contrast to what is generally believed: oleosins correlate with lipid content in a positive manner. Overexpression of the oleosin 3 (OLE3) gene in *S. cerevisiae* resulted in an increased accumulation of diacylglycerols and triacylglycerols. There is a direct role for oleosin3 in the biosynthesis (and mobilization) of plant oils (Parthibane *et al.*, 2011). Overexpression of oleosin in the Pa19 cell culture line *Pimpinella anisum* resulted in higher oil content (Radetzky & Langheinrich 1994). On the other hand, older studies demonstrated that species containing higher amounts of oleosin (e.g. *B. napus*) have generally smaller oilbodies compared to those with lower oleosin content. The content of lipids decreases whereas the protein content increases with increasing oil body diameter (Tzen *et al.*, 1993). Furthermore, low oil lines of maize showed a reduced TAG – to – oleosin ratio, whereas high oil lines had a higher TAG – to – oleosin ratio (Ting *et al.*, 1996). Overexpression of soybean oleosin in transgenic rice leads to an increase of seed lipid content and in more numerous and smaller oil bodies compared to WT, suggesting an inverse relationship between oil body size and oleosin level (Liu *et al.*, 2013). Studies on the *oleosin1* mutant in *A. thaliana* showed a significant decrease in oil content, but an increase in protein accumulation in an almost compensatory manner (Siloto *et al.*, 2006). Ablation of a major oleosin resulted in an aberrant phenotype of embryo cells that contain large oil bodies, which were not observed in normal seeds. Studies on different *A. thaliana* oleosin mutants showed that oil body sizes and distributions differ amongst the single, double, and triple mutant backgrounds (Miquel *et al.*, 2014). They concluded that especially oleosin4 (which is the homolog to *B. napus oleosin2*, which



shows an increase in our study) prevents oil body fusion. This would explain why an elevated level of *B. napus* oleosin2 in our transgenics leads to the formation of more frequent and smaller oil bodies. From a physical point of view, the optimization of intracellular space by compaction is more efficient with very small oil bodies but demands much more membrane surface (Walther and Farese, 2009; Yang *et al.*, 2012). A plausible mechanism for the oil body size reduction is the direct filling or reattachment to the ER, where the TAG content is spread into newly formed oil bodies (Miquel *et al.*, 2014). Overall, the correlation of oleosins to lipid content is controversially discussed, but it seems certain that oleosins have direct impact on oil body size and formation. Probably, a balanced amount of oleosins is necessary to keep an optimal TAG content inside the seed.

### 5.2.7 The transgenics show a massive cellular phenotype

The use of histology provided additional insights into the transgenic phenotype. Staining of protein storage vacuoles unravelled less soluble protein and empty storage vacuoles during early to mid development. Transmission electron microscopy unlocked an extraordinary cellular phenotype: the transgenics show protein storage vacuoles with crystalline structures, while WT comprises voluminous storage vacuoles filled with soluble proteins. The structure of oil bodies was also changed: they were no longer evenly formed and uniformly spread along the plasma membrane but smaller and spread irregularly. Most surprisingly, we observed abnormal membrane appearance and folding inside the cells of transgenics. In regular plant cells, the endomembrane system is composed of the endoplasmic reticulum (ER), golgi stacks, endosomes, and vacuoles. These structures are interconnected with one another and with the continuous membrane of the outer nuclear envelope (Herman *et al.*, 1990; Boevink *et al.*, 1996). Vacuoles, which are the most prominent compartment in the plant cell, may also have a dynamic and complex membrane structure. Studies found that spherical structures consisting of a double membrane were often observed within the lumen of vacuoles and were connected with the vacuolar membrane (Saito *et al.*, 2002; Uemura *et al.*, 2002). They move around within or along the outline of the membrane, mediated by actin filaments but not by microtubules (Uemura *et al.*, 2002). Plant cells have developed unique actin-dependent mechanisms for endomembrane organization (Boevink *et al.*, 1998; Brandizzi *et al.*, 2002). In our transcriptomics dataset we identified candidates assigned to membrane structure formation like an exostosin family protein. One prominent member of this

large family is *katamaril/mur3* which has been reported to interact with actin and to be required for the proper endomembrane organization and for cell elongation. Investigations have been made on an *A. thaliana* mutant, *katamaril* (*kam1*), which has a defect in the organization of endomembranes and actin filaments. The *kam1* plants form abnormally large aggregates that consist of endoplasmic reticulum with actin filaments in the perinuclear region within the cells and are defective in normal cell elongation (Tamura *et al.*, 2005). Unfortunately there are no reports on an overexpression of *katamaril*, but because of its huge influence on intracellular organization, one can assume that elevated abundance of exostosin family protein might contribute to a change in endomembrane formation. Immunostaining of oleosins in our transgenics showed that the membrane structures contain oleosins. The observed increase in oleosins might lead to the formation of more oil-body surface (to utilize the larger amounts of oleosin) but decreases in volume, which eventually might be causative for the observed decrease in seed lipid content.

### **5.2.8 The reduction in sulphur content might additionally contribute to the low oil phenotype**

Beside changes in protein and lipid we detected a change in sulphur metabolism in the transgenics. In higher plants, sulphur is an essential macronutrient for several processes. It is essential for the synthesis of the S-containing amino acids methionine and cysteine as well as for a range of cofactors and prosthetic groups (Hesse and Hoefgen, 2003; Saito, 2004). The seeds of transgenics (line BCS580) show a significant reduction in total sulphur content compared to WTS. This corresponds to the trend of reduction in sulphur-containing metabolites like methionine and glutathione. There is evidence in the literature showing a massive reduction in lipid content for plants grown under sulphur-limiting conditions (Nikiforova *et al.*, 2005). Under sulphur fertilization, the activity of acetyl-CoA carboxylase, the contents of acetyl-CoA, soluble protein, total RNA and sugar were significantly higher in the developing seeds of *Brassica juncea* compared to sulphur starved ones. As a consequence, sulphur fertilized seeds contained much more oil than sulphur starved ones (Fazili *et al.*, 2010). Our transcriptome data unravelled about 8% of the differentially expressed genes belonging to sulphur metabolism and transport, with the most prominent one being ATP sulfurylase 1 (APS1). APS1 is one of the key enzymes in sulphur metabolism and catalyses the first step in sulfate assimilation pathway. It mediates selenate reduction, and promotes Se and sulfur uptake and

assimilation by the following reaction:  $\text{ATP} + \text{sulfate} = \text{diphosphate} + \text{adenylyl 5' phosphosulphate}$ . The latter is further reduced by adenosine 5'-phosphosulfate reductase to sulfite and subsequently by sulfite reductase to sulfide. This sulfide can then be used to form cysteine (Takahashi *et al.*, 2011). A lower abundance of *aps1* transcript as well as the APS1 protein content, in turn lead to a lower metabolism of inorganic sulphur into sulphur containing metabolites. Our transgenics with reduced translation of cruciferins and napins exhibit a lower need for sulphur containing amino acids, especially cysteine. Recent studies showed a connection of sink strength and sulphur metabolism (Tabe & Droux, 2002). Seed tissues are the dominant site of ATP sulfurylase activity during reproductive growth of soybean (Sexton and Shibles, 1999). Beside S-converting enzymes also sulphur transporters can be of significance (Kataoka *et al.*, 2004), and contribute to the phenotype observed here. For example, the sulfate transporter 4.1 that shows a down-regulation in the transgenic line is responsible for the remobilisation of sulfur out of storage vacuoles, where sulfur is stored as sulfate.

### 5.2.9 Factors which might additionally contribute to the transgenic phenotype

We also considered other parameters as contributing to the transgenic phenotype. Although starch content in mature seeds did not differ between transgenics and WT, differences in transient accumulation during development were visible. Mutants of *A. thaliana* with defects in plastidic starch biosynthesis (loss-of-function of plastidic phosphoglucomutase) showed lowered seed oil content, which emphasizes the importance of transient starch as a carbon source supporting seed oil biosynthesis (Periappuram *et al.*, 2000). Our proteomics data revealed a lower abundance of phosphoglucomutase 1 and 2 in transgenics, accompanied by lower levels of transient starch.

Furthermore, germination of seeds of the transgenic lines was compromised. This was not further studied here, but there is sufficient evidence showing a link between proper germination and mobilization of storage reserves (Fu *et al.*, 2005, Soltani *et al.*, 2006). Interestingly, our proteomics approach detected a higher spot volume for 1-Cys peroxiredoxin PER1 in transgenics. This gene/protein is known to inhibit germination under stress conditions. It protects tissues from reactive oxygen species during desiccation and early imbibition, and is involved in protection during dormancy (Haslekas *et al.*, 2003).

Furthermore, biotin carboxyl carrier protein of acetyl-CoA carboxylase 2 (BCCP2) shows a higher spot volume in transgenics (~5fold). BCCP2 is a component of the acetyl-coenzyme A carboxylase (ACCase) complex, which is itself the key enzyme in the *de novo* fatty acid biosynthesis (Roesler *et al.*, 1997; Baud *et al.*, 2003). Notably, overexpression of BCCP2 was shown to inhibit ACCase, resulting in altered oil, protein, and carbohydrate composition in mature *Arabidopsis* seed (Chen *et al.*, 2009). This is in accordance to Thelen & Ohlrogge (2002), where the seed-specific overexpression resulted in seeds with ~3fold reduced ACCase activity and less oil.

### 5.2.10 Transcriptomics and proteomics data show rather low concordance

When comparing the differentially expressed genes/proteins identified by either transcriptomics or proteomics, we found only 5 ATG numbers that were present in both datasets and showed the same pattern of regulation. Four of these show a downregulation in transgenics (AT4G28520/*cruciferin3*; AT5G44120/*cruciferin1*; AT4G27140/*napin1*; At3g22890/ATP sulfurylase 1 (APS1)). In the transcriptomics dataset we also find AT1G62180 as a down-regulated candidate, which encodes 5'adenylylphosphosulfate reductase 2 (APR2). Studies in *A. thaliana* reported that the sulphate content is mainly controlled by the two genes APS1 and APR2 (Koprivova *et al.*, 2013). The remaining top - candidate shows an upregulation in transgenics: At5g08370 encodes for alpha-galactosidase 2 (AGAL2). This enzyme plays a role in various pathways. AGAL2 protein is localized to cell wall/apoplast (Chrost *et al.*, 2007; Floerl *et al.*, 2012), and is important for wall loosening/wall expansion. Furthermore, AGAL2 enzyme activity plays a role in glycerolipid (and galactose) metabolism, e.g. for the formation of glycerol. It has a role in germination (McCleary and Matheson, 1975; Feurtado *et al.*, 2000).



## 6 Outlook

The use of labelling experiments in plant research unravels the opportunity to follow certain metabolic steps in plant physiology. Especially for metabolic flux analyses, the incubation of embryos with defined amounts of labelled compounds is crucial for the overall calculation of metabolic activities (Schwender *et al.*, 2015). Unfortunately the *in vitro* cultivation of embryos often leads to a loss of the phenotype, that is observed, when embryos/seeds grow *in planta*. For that reason, the establishment of a labelling approach, that is near the *in vivo* situation might in future not only enable the trace of substrates, that are naturally delivered by maternal tissue but also improve the results that are obtained by calculated flux analyses. Furthermore the  $^{13}\text{C}$  labelling of intact siliques enables the tracking of carbon atoms throughout the metabolism in near *in vivo* situations, for example into fatty acid and subsequently synthesised TAGs. This might thus give deeper insights into carbon flow to lipids and other storage components and might furthermore allow the comparison between different high and low oil varieties and transgenic lines. Additionally, the cultivation of siliques in sterile incubation medium theoretically allows to grow the seeds until maturity, however this has to be proven in future experiments.

The characterization of a storage protein deficient mutant has led to vital insights towards the regulation of seed storage product synthesis and accumulation. Although the approach has not led to the anticipated increase in seed lipid content, the results obtained contribute to a better understanding of regulation of storage protein accumulation and rebalancing mechanisms occurring in the seed. The complex regulation, beginning with changing amino acid demands, thus lower needs for sulphur and ending in histological relevant phenotypes is a good model to understand protein rebalancing in seeds, with one of the main substituents being Oleosin, which has been reported to be transcriptionally regulated by LEC2 (Che *et al.*, 2009), however LEC2 did not appear to be differentially expressed in our approach. Thus the transgenic lines might help to find other factors controlling Oleosin2 expression. The achieved increase in Oleosin2 protein amount and the resulting cellular phenotype might additionally be interesting in future work, especially when combined with an overexpression of genes related to fatty acid synthesis and TAG assembly and/or oil body trafficking. Because of the extraordinary cell phenotype, the characterized transgenic plants might also be a good model to study membrane expansion and fibre formation.

## Supplement

**Table S 1:** Filtered Masses and potentials of MS/MS transitions in negative mode. DP Declustering Potential, EP Entrance Potential, CE Collision Energy, CXP Collision Cell Exit Potential.

<b>Compound</b>	<b>Q1 mass</b>	<b>Q3 mass</b>	<b>DP</b>	<b>EP</b>	<b>CE</b>	<b>CXP</b>
Acephate	182	141	-40	-10	-18	-25
3-PGA	185	97	-35	-10	-20	-15
3-PGA M+1	186	97	-35	-10	-20	-15
3-PGA M+2	187	97	-35	-10	-20	-15
3-PGA M+3	188	97	-35	-10	-20	-15
PEP	167	79	-35	-10	-14	-5
PEP M+1	168	79	-35	-10	-14	-5
PEP M+2	169	79	-35	-10	-14	-5
PEP M+3	170	79	-35	-10	-14	-5
Glucose	179	89	-50	-10	-12	-10
Glucose M+1	180	89	-50	-10	-12	-10
Glucose M+1 B	180	90	-50	-10	-12	-10
Glucose M+2	181	89	-50	-10	-12	-10
Glucose M+2 B	181	90	-50	-10	-12	-10
Glucose M+2 C	181	91	-50	-10	-12	-10
Glucose M+3	182	89	-50	-10	-12	-10
Glucose M+3 B	182	90	-50	-10	-12	-10
Glucose M+3 C	182	91	-50	-10	-12	-10
Glucose M+3 D	182	92	-50	-10	-12	-10
Glucose M+4	183	90	-50	-10	-12	-10
Glucose M+4 B	183	91	-50	-10	-12	-10
Glucose M+4 C	183	92	-50	-10	-12	-10

---

Glucose M+5	184	91	-50	-10	-12	-10
Glucose M+5	184	92	-50	-10	-12	-10
Glucose M+6	185	92	-50	-10	-12	-10
Fructose	179	89	-55	-10	-12	-8
Fructose M+1	180	89	-50	-10	-12	-10
Fructose M+1 B	180	90	-50	-10	-12	-10
Fructose M+2	181	89	-50	-10	-12	-10
Fructose M+2 B	181	90	-50	-10	-12	-10
Fructose M+2 C	181	91	-50	-10	-12	-10
Fructose M+3	182	89	-50	-10	-12	-10
Fructose M+3 B	182	90	-50	-10	-12	-10
Fructose M+3 C	182	91	-50	-10	-12	-10
Fructose M+3 D	182	92	-50	-10	-12	-10
Fructose M+4	183	90	-50	-10	-12	-10
Fructose M+4 B	183	91	-50	-10	-12	-10
Fructose M+4 C	183	92	-50	-10	-12	-10
Fructose M+5	184	91	-50	-10	-12	-10
Fructose M+5	184	92	-50	-10	-12	-10
Fructose M+6	185	92	-50	-10	-12	-10
Sucrose	341	179	-180	-10	-18	-15
Sucrose M+1	342	179	-180	-10	-18	-15
Sucrose M+1 B	342	180	-180	-10	-18	-15
Sucrose M+2	343	179	-180	-10	-18	-15
Sucrose M+2 B	343	180	-180	-10	-18	-15
Sucrose M+2 C	343	181	-180	-10	-18	-15
Sucrose M+3	344	179	-180	-10	-18	-15
Sucrose M+3 B	344	180	-180	-10	-18	-15
Sucrose M+3 C	344	181	-180	-10	-18	-15
Sucrose M+3 D	344	182	-180	-10	-18	-15
Sucrose M+6	347	179	-180	-10	-18	-15
Sucrose M+6 B	347	180	-180	-10	-18	-15
Sucrose M+6 C	347	181	-180	-10	-18	-15



---

Sucrose M+6 D	347	182	-180	-10	-18	-15
Sucrose M+6 E	347	183	-180	-10	-18	-15
Sucrose M+6 F	347	184	-180	-10	-18	-15
Sucrose M+6 G	347	185	-180	-10	-18	-15
Sucrose M+12	353	185	-180	-10	-18	-15
Hex-P	259	97	-50	-10	-16	-19
Hex-P M+1	260	97	-50	-10	-16	-19
Hex-P M+2	261	97	-50	-10	-16	-19
Hex-P M+3	262	97	-50	-10	-16	-19
Hex-P M+4	263	97	-50	-10	-16	-19
Hex-P M+5	264	97	-50	-10	-16	-19
Hex-P M+6	265	97	-50	-10	-16	-19
Succinate M+4	121	76	-35	-10	-18	-5
Succinate M+3 A	120	76	-35	-10	-18	-5
Succinate M+3 B	120	75	-35	-10	-18	-5
Succinate M+2 A	119	75	-35	-10	-18	-5
Succinate M+2 B	119	74	-35	-10	-18	-5
Succinate M+1 A	118	74	-35	-10	-18	-5
Succinate M+1 B	118	73	-35	-10	-18	-5
Succinate	117	73	-35	-10	-18	-5
Malate	133	115	-60	-10	-16	-7
Malate M+4	137	119	-60	-10	-16	-7
Malate M+3	136	118	-60	-10	-16	-7
Malate M+2	135	117	-60	-10	-16	-7
Malate M+1	134	116	-60	-10	-16	-7
Citrate	191	87	-55	-10	-24	-5
Citrate M+6	197	90	-55	-10	-24	-5
Citrate M+5	196	90	-55	-10	-24	-5
Citrate M+5 B	196	89	-55	-10	-24	-5
Citrate M+4	195	90	-55	-10	-24	-5
Citrate M+4 B	195	89	-55	-10	-24	-5
Citrate M+4 C	195	88	-55	-10	-24	-5

Citrate M+3	194	90	-55	-10	-24	-5
Citrate M+3 B	194	89	-55	-10	-24	-5
Citrate M+3 C	194	88	-55	-10	-24	-5
Citrate M+3 D	194	87	-55	-10	-24	-5
Citrate M+2	193	89	-55	-10	-24	-5
Citrate M+2 B	193	88	-55	-10	-24	-5
Citrate M+2 C	193	87	-55	-10	-24	-5
Citrate M+1	192	88	-55	-10	-24	-5
Citrate M+1 B	192	87	-55	-10	-24	-5

**Table S 2:** Primers used for Oleosin real-time PCR

<b>Gene name</b>	<b>Sequence 5' → 3'</b>
Oleosin S1-1 fwd	ACAGGATTCATGGCGTCAGG
Oleosin S1-1 rev	CATCTTTTGTCTCTGCCCC
Oleosin S2-1 fwd	GGTTATGGTGGTCGTGCTGA
Oleosin S2-1 fwd	GATAGCGGCCGGGACAATAA
OleosinS2-2 fwd	GCTGGACTCACTCTAGCCGG
OleosinS2-2 fwd	CTTAGCATAGTCCAATTGCTC
Oleosin S3 fwd	CATAACCAGCCGTGACCAGT
Oleosin S3 rev	AGGGTGAGACTGGAGAGGAC
Oleosin S4 fwd	TCCTCTTCAGCCCGGTCATA
Oleosin S4 rev	CTGCCCCATTCCTTTTCCCT
Oleosin 5 fwd	TCATCACTGGGTTTCCTTGCC
Oleosin 5 rev	TGGTGTTGCTGATGGACTCC

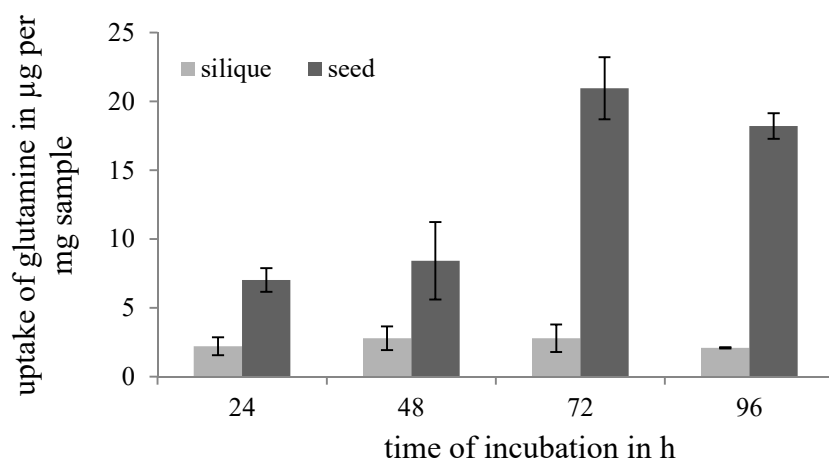


**Figure S 1:** Uptake of <sup>15</sup>N glutamine into 1 mg of siliques or seeds that were incubated in a solution containing 20mM of <sup>15</sup>N gklutamine for 24 to 96 hours.

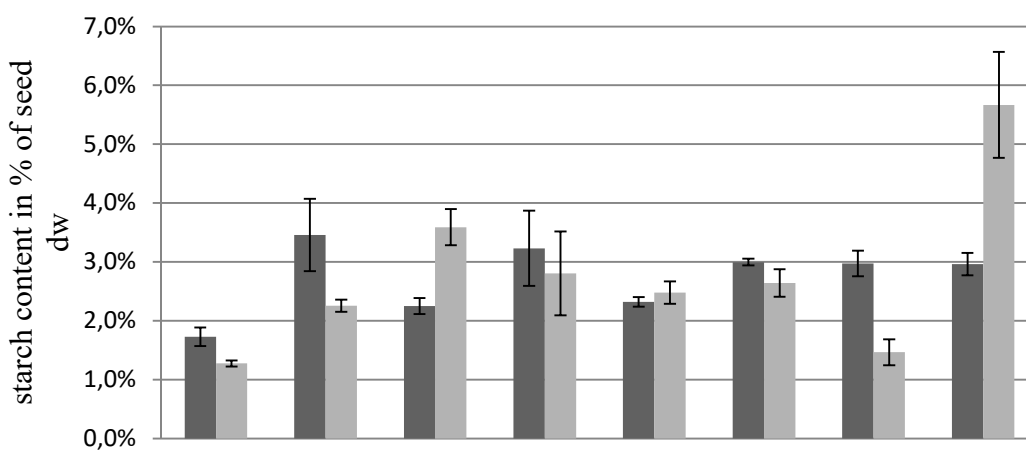


**Figure S 2:** Starch content in % of the seed dry weight in mature seeds of all tested transgenic lines.

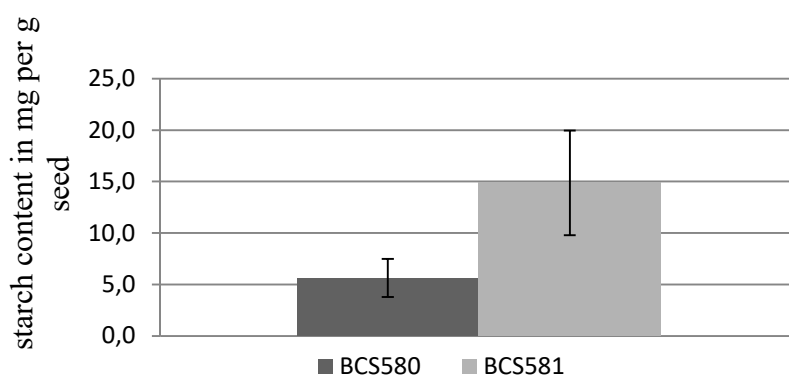


**Figure S 3:** Starch content in mg per g embryo dw at 37 DAP

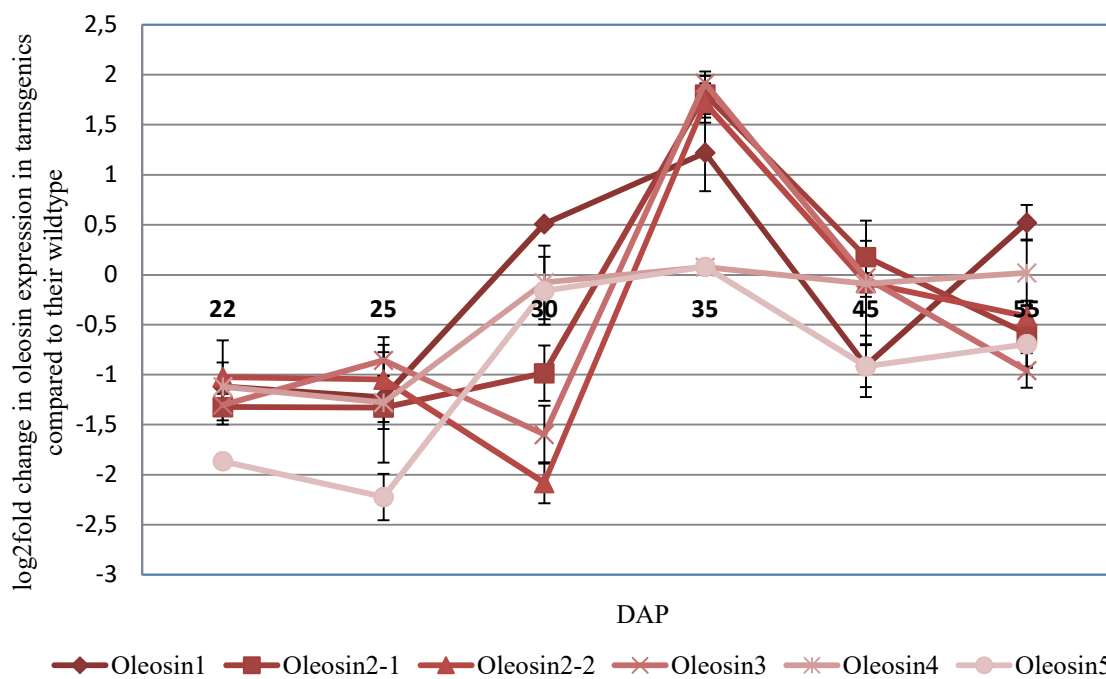


**Figure S 4:** Temporal expression profile of oleosins in transgenic lines compared to their wildtype.

**Table S 3:** Proteins with higher spot volume in the transgenic line (BCS580)

Volume Diff.	Protein name	Taxonomy
6,75	Oleosin S2-2	<i>B. napus</i>
5,18	Oleosin S2-2	<i>B. napus</i>
4,71	Biotin carboxyl carrier protein of acetyl-CoA carboxylase 2, chloroplastic	<i>A. thaliana</i>
3,73	Elongation factor 1-alpha 1	<i>A. thaliana</i>
3,32	60S ribosomal protein L10	<i>E. esula</i>
3,32	Osmotin-like protein	<i>S. lycopersicum</i>
3,18	MLP-like protein 31	<i>A. thaliana</i>
2,74	Oleosin S2-2 O	<i>B. napus</i>
2,72	Oleosin 21.2 kDa	<i>A. thaliana</i>
2,66	Glutathione S-transferase U5	<i>A. thaliana</i>
2,66	Ribulose-phosphate 3-epimerase, chloroplastic (Fragment)	<i>S. tuberosum</i>
2,56	Nitrogen regulatory protein P-II homolog	<i>A. thaliana</i>
2,35	Beta-galactosidase 3	<i>A. thaliana</i>
2,35	Probable serine protease EDA2	<i>A. thaliana</i>
2,32	Isopentenyl-diphosphate Delta-isomerase II	<i>A. thaliana</i>
2,25	Alpha-galactosidase	<i>C. arabica</i>
2,25	UDP-sulfoquinovose synthase, chloroplast precursor	<i>A. thaliana</i>
2,19	Importin subunit alpha-1	<i>A. thaliana</i>
2,19	Protein disulfide isomerase-like 1-2	<i>A. thaliana</i>
2,19	Pyruvate kinase isozyme A, chloroplastic	<i>N. tabacum</i>

**Table S 4:** Proteins with lower spot volume in the transgenic line (BCS580)

Volume Diff.	Protein name	Taxonomy
10,17	Cruciferin CRU1	<i>B. napus</i>
10,17	Malate dehydrogenase	<i>B. napus</i>
5,94	12S seed storage protein CRU1	<i>A. thaliana</i>
5,94	12S seed storage protein CRU4	<i>A. thaliana</i>
5,94	Cruciferin CRU1	<i>B. napus</i>
5,77	Cruciferin CRU1	<i>B. napus</i>
5,63	Cruciferin CRU4	<i>B. napus</i>
5,63	Napin-2	<i>B. napus</i>
4,89	Elongation factor 1-gamma 1	<i>O. sativa</i>
4,89	Elongation factor Tu, chloroplastic	<i>G. max</i>
4,89	Probable monodehydroascorbate reductase, cytoplasmic isoform 3	<i>A. thaliana</i>
4,89	S-adenosylmethionine synthase	<i>B. rapa</i>
4,89	S-adenosylmethionine synthase 2	<i>N. tabacum</i>
4,89	S-adenosylmethionine synthase 3	<i>S. lycopersicum</i>
4,53	Methylenetetrahydrofolate reductase 1	<i>A. thaliana</i>
4,53	Probable phosphoglucomutase, cytoplasmic 1	<i>A. thaliana</i>
4,53	Probable phosphoglucomutase, cytoplasmic 2	<i>A. thaliana</i>
4,53	Pyruvate decarboxylase isozyme 1 (Fragment)	<i>N. tabacum</i>
4,35	Cruciferin CRU1	<i>B. napus</i>
4,35	Succinyl-CoA ligase [GDP-forming] subunit alpha-1, mitochondrial	<i>A. thaliana</i>
4,22	Biotin synthase	<i>A. thaliana</i>
4,22	Fructose-bisphosphate aldolase, cytoplasmic isozyme	<i>S. oleracea</i>
4,22	Fructose-bisphosphate aldolase, cytoplasmic isozyme	<i>C. arietinum</i>

---

4,15	Cruciferin CRU1	<i>B. napus</i>
4,08	Branched-chain-amino-acid aminotransferase-like protein 2	<i>A. thaliana</i>
3,97	Glutathione S-transferase U17	<i>A. thaliana</i>
3,96	Eukaryotic translation initiation factor 3 subunit H	<i>A. thaliana</i>
3,96	Probable UDP-arabinopyranose mutase 5	<i>A. thaliana</i>
3,96	Spermidine synthase	<i>C. arabica</i>
3,96	Thylakoid lumenal 33.6 kDa protein (Fragment)	<i>S. oleracea</i>
3,77	Aldo-keto reductase family 4 member C9	<i>A. thaliana</i>
3,77	Cruciferin CRU1	<i>B. napus</i>
3,77	Malate dehydrogenase 1, mitochondrial	<i>A. thaliana</i>
3,77	Malate dehydrogenase, chloroplastic	<i>A. thaliana</i>
3,77	Phosphopantothenate--cysteine ligase 2	<i>A. thaliana</i>
3,77	Unknown protein 1 (Fragment)	<i>V. rotundifolia</i>
3,65	Chalcone synthase 1	<i>S. alba</i>
3,65	Peptidyl-prolyl cis-trans isomerase CYP40	<i>A. thaliana</i>
3,64	4-alpha-glucanotransferase DPE2	<i>A. thaliana</i>
3,51	Allergen Bra j 1-E	<i>B. juncea</i>
3,51	Cruciferin	<i>B. napus</i>
3,51	Napin	<i>B. napus</i>
3,51	Napin-3	<i>B. napus</i>
3,51	Unknown protein 1 (Fragment)	<i>V. rotundifolia</i>
3,46	Cruciferin CRU1	<i>B. napus</i>
3,45	Phosphoenolpyruvate carboxylase 1	<i>A. thaliana</i>
3,45	Phosphoenolpyruvate carboxylase 2	<i>A. thaliana</i>
3,45	Probable E3 ubiquitin-protein ligase ARI12	<i>A. thaliana</i>
3,05	Alpha-L-fucosidase 2	<i>A. thaliana</i>
3,05	Alpha-xylosidase	<i>A. thaliana</i>

3,05	Unknown protein 1 (Fragment)	<i>V. rotundifolia</i>
3,01	Peptidyl-prolyl cis-trans isomerase CYP20-3, chloroplastic	<i>A. thaliana</i>
2,96	Annexin D2	<i>A. thaliana</i>
2,96	L-lactate dehydrogenase	<i>Z. mays</i>
2,96	Ribulose biphosphate carboxylase large chain	<i>A. magnifica</i>
2,96	Transcription factor Pur-alpha 1	<i>A. thaliana</i>
2,95	Cruciferin CRU1	<i>B. napus</i>
2,95	Malate dehydrogenase 1, mitochondrial	<i>A. thaliana</i>
2,95	Serine acetyltransferase 5	<i>A. thaliana</i>
2,91	3-ketoacyl-CoA thiolase 2, peroxisomal	<i>A. thaliana</i>
2,91	Citrate synthase 3, peroxisomal	<i>A. thaliana</i>
2,91	Unknown protein 1 (Fragment)	<i>V. rotundifolia</i>
2,91	ATP sulfurylase 1, chloroplastic	<i>A. thaliana</i>
2,91	Glutamate-1-semialdehyde 2,1-aminomutase, chloroplastic	<i>B. napus</i>
2,91	Probable sarcosine oxidase	<i>A. thaliana</i>
2,87	Beta-glucosidase 18	<i>A. thaliana</i>
2,82	Beta-glucosidase 18	<i>A. thaliana</i>
2,64	3-ketoacyl-CoA thiolase 2, peroxisomal	<i>A. thaliana</i>
2,64	Citrate synthase 3, peroxisomal	<i>A. thaliana</i>
2,62	Cruciferin CRU1	<i>B. napus</i>
2,62	Probable protein phosphatase 2C 39	<i>A. thaliana</i>
2,55	Ran-binding protein 1 homolog a	<i>A. thaliana</i>
2,55	Sedoheptulose-1,7-bisphosphatase, chloroplastic	<i>A. thaliana</i>
2,54	Catalase-3	<i>A. thaliana</i>
2,54	Cruciferin CRU1	<i>B. napus</i>
2,54	NADP-dependent glyceraldehyde-3-phosphate dehydrogenase	<i>A. thaliana</i>



---

2,46	Elongation factor Tu, mitochondrial	<i>A. thaliana</i>
2,46	Glutamate-1-semialdehyde 2,1-aminomutase, chloroplastic	<i>B. napus</i>
2,46	LL-diaminopimelate aminotransferase, chloroplastic	<i>A. thaliana</i>
2,46	30S ribosomal protein S5, chloroplastic	<i>A. thaliana</i>
2,46	Cruciferin CRU1	<i>B. napus</i>
2,46	Cruciferin PGCRURSE5	<i>R. sativus</i>
2,43	Cruciferin CRU4	<i>B. napus</i>
2,43	Napin-B	<i>B. napus</i>
2,33	3-ketoacyl-CoA thiolase 5, peroxisomal	<i>A. thaliana</i>
2,33	Aspartate aminotransferase P2, mitochondrial (Fragment)	<i>L. angustifolius</i>
2,33	Aspartate aminotransferase, chloroplastic	<i>A. thaliana</i>
2,28	Cruciferin	<i>B. napus</i>
2,28	Peptidyl-prolyl cis-trans isomerase CYP20-3, chloroplastic	<i>A. thaliana</i>
2,28	Proteasome subunit beta type-6	<i>A. thaliana</i>
2,27	L-ascorbate peroxidase 1, cytosolic	<i>A. thaliana</i>
2,27	Proteasome subunit alpha type-6-B	<i>A. thaliana</i>
2,27	Triosephosphate isomerase, cytosolic	<i>A. thaliana</i>
2,26	Cruciferin	<i>B. napus</i>
2,26	Cruciferin CRU1	<i>B. napus</i>
2,26	Cruciferin CRU4	<i>B. napus</i>
2,26	Proteasome subunit beta type-7-A	<i>A. thaliana</i>
2,17	Cruciferin BnC1	<i>B. napus</i>
2,17	Cruciferin CRU1	<i>B. napus</i>
2,17	Unknown protein 1 (Fragment)	<i>V. rotundifolia</i>
2,13	Actin-depolymerizing factor 2 - Petunia hybrida (Petunia)	<i>P. hybrida</i>
2,13	Actin-depolymerizing factor 3 - Arabidopsis	<i>A. thaliana</i>

	thaliana (Mouse-ear cress)	
2,13	Glycine-rich RNA-binding protein GRP1A	<i>S. alba</i>
2,13	MLP-like protein 329	<i>A. thaliana</i>
2,11	Cruciferin	<i>B. napus</i>
2,11	Cruciferin BnC1	<i>B. napus</i>
2,11	Cruciferin CRU1	<i>B. napus</i>

**Table S 5:** Amino acid sequences of seed storage proteins

Amino acid	Napin short chain	Napin large chain	Cruciferin	Oleosin
<b>Ala (A)</b>	10.0%	3.3%	6.7%	<b>9.0%</b>
<b>Arg (R)</b>	7.5%	5.5%	5.6%	<b>4.8%</b>
<b>Asn (N)</b>	0.0%	2.2%	5.8%	<b>1.1%</b>
<b>Asp (D)</b>	0.0%	0.0%	4.0%	<b>4.8%</b>
<b>Cys (C)</b>	5.0%	6.6%	1.0%	<b>0.0%</b>
<b>Gln (Q)</b>	<b>17.5%</b>	<b>24.2%</b>	<b>12.3%</b>	4.3%
<b>Glu (E)</b>	2.5%	3.3%	3.8%	<b>3.7%</b>
<b>Gly (G)</b>	7.5%	5.5%	10.7%	<b>12.2%</b>
<b>His (H)</b>	5.0%	2.2%	2.0%	<b>2.1%</b>
<b>Ile (I)</b>	2.5%	4.4%	4.8%	<b>4.3%</b>
<b>Leu (L)</b>	5.0%	7.7%	8.3%	<b>11.2%</b>
<b>Lys (K)</b>	7.5%	4.4%	3.0%	<b>3.7%</b>
<b>Met (M)</b>	2.5%	0.0%	1.2%	<b>2.1%</b>
<b>Phe (F)</b>	5.0%	1.1%	4.0%	<b>1.6%</b>
<b>Pro (P)</b>	10.0%	11.0%	5.0%	<b>4.8%</b>
<b>Ser (S)</b>	7.5%	4.4%	7.7%	<b>7.4%</b>
<b>Thr (T)</b>	0.0%	5.5%	3.8%	<b>8.0%</b>
<b>Trp (W)</b>	5.0%	0.0%	1.0%	<b>0.5%</b>
<b>Tyr (Y)</b>	0.0%	2.2%	2.2%	<b>4.8%</b>
<b>Val (V)</b>	<b>0.0%</b>	<b>6.6%</b>	<b>6.9%</b>	<b>9.6%</b>

**Table S 6:** Seed relevant traits for the tested PEPC single transgenic line (grayed) and the corresponding WTS.

	Seed dry weight in mg	Protein content in %
BCS1175	5,19±0,52	35,23 ±1,98
BCS1176	5,89±0,12	34,31±0,62
BCS1177	5,67±0,19	31,02±6,42
BCS1178	5,52±0,33	35,30±0,45
BCS1188	5,81±0,10	32,94±3,28
BCS1189	5,57±0,01	31,77±4,56

## References

- Abell, B.M., Holbrook, L.A., Abenes, M., Murphy, D.J., Hills, M.J. and Moloney, M.M.** (1997) Role of the proline knot motif in oleosin endoplasmic reticulum topology and oil body targeting. *Plant Cell*, 9, 1481–1493.
- Allen, E.J., Morgan, D.G. and Ridgman, W.I.** (1971) A physiological analysis of the growth of oilseed rape. *J. Agric. Sci.* 77, 339–341.
- Andre C., Froehlich JE., Moll MR., Benning C.** (2007) A heteromeric plastidic pyruvate kinase complex involved in seed oil biosynthesis in *Arabidopsis*. *Plant Cell* 19 2006–2022
- Andriotis V.M., Pike M.J., Kular B., Rawsthorne S., Smith A.M.** (2010). Starch turnover in developing oilseed embryos. *New Phytol.* 187: 791–804.
- Auger B., Marnet N., Gautier V., Maia-Grondard A., Leprince F., Renard M., Guyot S., Nesi N., Routaboul JM.** (2010). A detailed survey of seed coat flavonoids in developing seeds of *Brassica napus L.* *Journal of Agricultural and Food Chemistry* ;58:6246-6256.
- Bates P. D., Durrett T. P., Ohlrogge J. B., Pollard M.** (2009). Analysis of acyl fluxes through multiple pathways of triacylglycerol synthesis in developing soybean embryos. *Plant Physiol.* 150 55–72. 10.1104/pp.109.137737
- Bates P. D., Browse J.** (2011). The pathway of triacylglycerol synthesis through phosphatidylcholine in *Arabidopsis* produces a bottleneck for the accumulation of unusual fatty acids in transgenic seeds. *Plant J.* 68, 387–399 10.1111/j.1365-3113X.2011.04693.x
- Baud S., Boutin JP., Miquel M., Lepiniec L., Rochat C.** (2002) An integrated overview of seed development in *Arabidopsis thaliana* ecotype WS. *Plant Physiol Biochem* 40: 151–160
- Baud S., Guyon V., Kronenberger J., Wulleme S., Miquel M., Caboche M., Lepiniec L., Rochat C** (2003) Multifunctional acetyl-CoA carboxylase 1 is essential for very long chain fatty acid elongation and embryo development in *Arabidopsis*. *Plant J*33: 75–86
- Baud S., Wulleme S., Dubreucq B., de Almeida A., Vuagnat C., Lepiniec L., Miquel M., Rochat C.** (2007) Function of plastidial pyruvate kinases in seeds of *Arabidopsis thaliana*. *Plant J* 52 405–419

- Baud, S., Dubreucq, B., Miquel, M., Rochat, C. and Lepiniec, L.** (2008) Storage reserve accumulation in Arabidopsis: metabolic and developmental control of seed filling. In *The Arabidopsis Book* (Last, R.L., ed). Rockville, MD: American Society of Plant Biologists, pp. 1–24
- Baud S., Lepiniec L.** (2009). Regulation of de novo fatty acid synthesis in maturing oilseeds of Arabidopsis. *Plant Physiol. Biochem.* 47: 448–455
- Bäumlein, H., Braun, H., Kakhovskaya, I.A. and Shutov, A.D.** (1995) Seed storage proteins of spermatophytes share a common ancestor with desiccation proteins of fungi. *J. Mol. Evol.* 41, 1070–1075.
- Bennett E.J., Roberts J.A., Wagstaff C.** (2011) The role of the pod in seed development: strategies for manipulating yield. *New Phytologist* ;190:838-853.
- Berg J D., Hendrix P F., Chang W X. and Dillard A L.** (1991) A labelling chamber for <sup>13</sup>C enrichment of plant tissue for decomposition studies. *Agric. Ecosyst. Environ.* 34, 421–425.
- Berry, P.M. and Spink, J.H.** (2006). A physiological analysis of oilseed rape yields: Past and future. *Journal of Agricultural Science, Cambridge* 144, 381-392.
- Berth M., Moser F., Kolbe M., Bernhardt J** (2007). The state of the art in the analysis of two-dimensional gel electrophoresis images. *Applied Microbiology and Biotechnology* 76, 1223–1243.
- Boevink, P., Santa Cruz, S., Hawes, C., Harris, N., and Oparka, K.J.** (1996). Virus-mediated delivery of the green fluorescent protein to the endoplasmic reticulum of plant cells. *Plant J.* 10, 935–941.
- Boevink, P., Oparka, K., Cruz, S.S., Martin, B., Betteridge, A., and Hawes, C.** (1998). Stacks on tracks: The plant Golgi apparatus traffics on an actin/ER network. *Plant J.* 15, 441–447.
- Borisjuk L., Neuberger T., Schwender J., Heinzl N., Sunderhaus S., Fuchs J., et al.** (2013). Seed architecture shapes embryo metabolism in oilseed rape. *Plant Cell* 25 1625–1640 10.1105/tpc.113.111740
- Boughton B. A., Thinagaran D., Sarabia D., Bacic A., Roessner U.** (2015). Mass spectrometry imaging for plant biology: a review. *Phytochem. Rev.* 14, 1–44. 10.1007/s11101-015-9440-2
- Brandizzi, F., Snapp, E.L., Roberts, A.G., Lippincott-Schwartz, J., and Hawes, C.** (2002). Membrane protein transport between the endoplasmic reticulum and the Golgi in tobacco leaves is energy dependent but cytoskeleton independent: Evidence from selective photobleaching. *Plant Cell* 14, 1293–1309.

- Brocard-Gifford, I., Lynch, T., and Finkelstein, R.** (2003). Regulatory networks in seeds integrating developmental, ABA, sugar and light signaling. *Plant Physiol.* 131, 78–92.
- Bromand B, Whalen JK, Janzen HH, Schjoerring JK, Ellert BH.** (2001) A pulse-labelling method to generate C-13-enriched plant materials. *Plant and Soil.* 235:253–257.
- Brown RC., Lemmon BE., Nguyen H., Olsen O-A.** (1999) Development of endosperm in *Arabidopsis thaliana*. *Sex Plant Reprod* 12: 32–42
- Cernac A., Benning C.** (2004). WRINKLED1 encodes an AP2/EREB domain protein involved in the control of storage compound biosynthesis in *Arabidopsis*. *Plant J.* 40: 575–585
- Chan A., Belmonte M.** (2013). Histological and ultrastructural changes in canola (*Brassica napus*) funicular anatomy during the seed lifecycle. *Botany* 91, 671–679.
- Chen X., Steed A., Travella S., Keller B., Nicholson P.** (2009) *Fusarium graminearum* exploits ethylene signaling to colonize dicotyledonous and monocotyledonous plants. *New Phytologist.* 182:975–983.
- Chollet R., Vidal J., O’Leary MH.** (1996) Phosphoenolpyruvate carboxylase: a ubiquitous, highly regulated enzyme in plants. *Annu Rev Plant Physiol Plant Mol Biol* 47:273–298
- Chrispeels, M.J., Higgins, T.J.V., and Spencer, D.** (1982). Assembly of storage protein oligomers in the endoplasmic reticulum and processing of the polypeptides in the protein bodies of developing pea cotyledons. *J. Cell Biol.* 93, 306-313.
- Chrost B., Kolukisaoglu U., Schulz B., Krupinska K.** (2007) An  $\alpha$ -galactosidase with an essential function during leaf development. *Planta* 225: 311–320
- Colditz F., Nyamsuren O., Niehaus K., Eubel H., Braun H.-P., Krajinski F.** (2004). Proteomic approach: identification of *M. truncatula* proteins induced in roots after infection with the pathogenic oomycete *A. euteiches*. *Plant Mol. Biol.* 55, 109–120  
10.1007/s11103-004-0499-1
- Crouch ML., Sussex IM.** (1981) Development and storage-protein synthesis in *Brassica napus* L. embryos in vivo and in vitro. *Planta* 153: 64-74
- Crouch ML, Tenbarger K, Simon A, Finkelstein R, Scofield S & Solberg L** (1985) Storage protein mRNA levels can be regulated by abscisic acid in *Brassica* embryos. In: van Vloten-Doting L, Groot GSP & Hall TC (Eds) *Molecular Form and Function of Plant Genome* (pp 555–566). Plenum Press, New York

- D'Andréa S, Jolivet P, Boulard C, Larré C, Froissard M, Chardot T** (2007) Selective one-step extraction of *Arabidopsis thaliana* seed oleosins using organic solvents. *J Agric Food Chem* 55: 10008–10015
- Derrien A, Zheng B, Osterhout JL, Ma YC, Milligan G, Farquhar MG, Druey KM.** (2003) Src-mediated RGS16 tyrosine phosphorylation promotes RGS16 stability. *J Biol Chem* 278:16107–16116
- Dyer, J.M. and Mullen, R.T.** (2008) Engineering plant oils as high-value industrial feedstocks for biorefining: the need for underpinning cell biology research. *Physiol. Plant.* 132, 11–22.
- Eastmond PJ.** (2006) SUGAR-DEPENDENT1 encodes a patatin domain triacylglycerol lipase that initiates storage oil breakdown in germinating *Arabidopsis* seeds. *Plant Cell* 18: 665–675
- Elke GR, Blackmore D, Offler CE, Patrick JW** (2005) Increased capacity for sucrose uptake leads to earlier onset of protein accumulation in developing pea seeds. *Funct Plant Biol* 32: 997–1007
- Ellerström, E., Stålberg, K., Ezcurra, I. and Rask, L.** (1996) Functional dissection of a napin gene promoter: identification of promoter elements required for embryo and endosperm specific expression. *Plant Mol. Biol.* 32, 1019-27
- Ezcurra I, Ellerström M, Wycliffe P, Stålberg K, Rask L** (1999) Interaction between composite elements in the napA promoter: Both the B-box ABA-responsive complex and the RY/G complex are necessary for seed-specific expression. *Plant Mol Biol* 40: 699–709
- Ezcurra I, Wycliffe P, Nehlin L, Ellerstrom M, Rask L** (2000). Transactivation of the *Brassica napus* napin promoter by ABI3 requires interaction of the conserved B2 and B3 domains of ABI3 with different cis-elements: B2 mediates activation through an ABRE, whereas B3 interacts with an RY/G-box. *Plant J* 24: 57–66
- Fait A, Angelovici R, Less H, Ohad I, Urbanczyk-Wochniak E, Fernie AR, Galili G** (2006) *Arabidopsis* seed development and germination is associated with temporally distinct metabolic switches. *Plant Physiol* 142: 839–854
- Fazili IS , Masoodi M , Ahmad S , Jamal A , Khan JS and Abdin MZ** (2010) Interactive effect of sulfur and nitrogen on growth and yield attributes of oilseed crops (*Brassica campestris l.* and *eruca sativa mill.*) differing in yield potential. *J Plant Nutr* 33(8): 1216-1228
- Feurtado JA.** (1999).  $\alpha$ -Galactosidase and  $\beta$ -mannoside mannohydrolase in tomato seeds (*Lycopersicon esculentum Mill. cv. Glamour*) and fruit (*L. esculentum Mill. cv. Trust*). MSc thesis, Department of Botany, University of Guelph, Canada.

- Finkelstein, R., Tenberge, K., Shumway, J., and Crouch, M.** (1985). Role of abscisic acid in maturation of rapeseed embryos. *Plant Physiol.* 78 630–636.
- Finkelstein, R., and Somerville, C.** (1990). Three classes of abscisic acid (ABA)-insensitive mutations of *Arabidopsis* define genes that control overlapping subsets of ABA responses. *Plant Physiol.* 94, 1172–1179.
- Floerl S., Majcherczyk A., Possienke M., Feussner K., Tappe H., Gatz C., et al.** (2012). *Verticillium longisporum* infection affects the leaf apoplastic proteome, metabolome, and cell wall properties in *Arabidopsis thaliana*. *PLoS ONE* 7:e31435 10.1371
- Focks N, Benning C** (1998) wrinkled1: a novel, low-seed-oil mutant of *Arabidopsis* with a deficiency in the seed-specific regulation of carbohydrate metabolism. *Plant Physiol* 118: 91–101
- Friml J, Vieten A, Sauer M, Weijers D, Schwarz H, Hamann T, Offringa R, Jürgens G** (2003) Efflux-dependent auxin gradients establish the apical-basal axis of *Arabidopsis*. *Nature* 426: 147–153
- Fu Q., Wang B. C., Jin X., Li H. B., Han P., Wei K. H., Zhang X. M., Zhu Y. X.** (2005) Proteomic analysis and extensive protein identification from dry, germinating *Arabidopsis* seeds and young seedlings. *J. Biochem. Mol. Biol.* (1):650–660.
- Ghashghaie J, Tcherkez G.** (2013). Isotope ratio mass spectrometry technique to follow plant metabolism: principles and applications of  $^{12}\text{C}/^{13}\text{C}$  isotopes. *Advances in Botanical Research: metabolomics coming of age with its technological diversity*, chap. 8, vol. 67. Academic Press, Elsevier, 378–405.
- Gillingham LG, Harris-Janz S, Jones PJ** (2011). Dietary monounsaturated fatty acids are protective against metabolic syndrome and cardiovascular disease risk factors. *Lipids.* 46(3):209-28.
- Golombek S, Rolletschek H, Wobus U, Weber H** (2001) Control of storage protein accumulation during legume seed development. *J Plant Physiol* 158: 457–464
- Goto-Inoue N., Hayasaka T., Zaima N., Nakajima K., Holleran W. M., Sano S., et al.** (2012). Imaging mass spectrometry visualizes ceramides and the pathogenesis of Dorfman-Chanarin syndrome due to ceramide metabolic abnormality in the skin. *PLoS ONE* 7:e49519. 10.1371/journal.pone.0049519
- Grabherr, M.G., Haas, B.J., Yassour, M., Levin, J.Z., Thompson, D.A., Amit, I., Adiconis, X., Fan, L., Raychowdhury, R., Zeng, Q. et al.** (2011) Full-length transcriptome assembly from RNA-Seq data without a reference genome. *Nat. Biotechnol.* 2011; 29: 644–652



- Guerche P, Tire C, De Sa FG, De Clercq A, Van Montagu M, Krebbers E** (1990) Differential expression of the Arabidopsis 2S albumin genes and the effects of increasing gene family size. *Plant Cell* 2: 469–478
- Gutierrez, L.; Van Wuytswinkel, O.; Castelain, M. & Bellini, C.** (2007). Combined networks regulating seed maturation. *Trends in Plant Science*, Vol.12, No.7, pp. 294-300, ISSN 1360-1385
- Hagan N. D., Upadhyaya N., Tabe L. M., Higgins T. J.** (2003). The redistribution of protein sulfur in transgenic rice expressing a gene for a foreign, sulfur-rich protein. *Plant J.* 34, 1–11. 10.1046/j.1365-313X.2003.01699.x
- Harris, G.P. and Jeffcoat, B.,** (1972). Distribution of  $^{14}\text{C}$ -labelled assimilates in flowering carnation plants. *J. Hortic. Sci.*, 47 : 25--35.
- Harwood JL.** (1996). Recent advances in the biosynthesis of plant fatty acids. *Biochimica et Biophysica Acta* 1301: 7–56
- Haslekas, C., Viken, M.K., Grini, P.E., Nygaard, V., Nordgard, S.H., Meza, T.J. and Aalen, R.B.** (2003) Seed 1-cysteine peroxiredoxin antioxidants are not involved in dormancy, but contribute to inhibition of germination during stress. *Plant Physiol.* 133, 1148–1157.
- Hay, J. O., Shi, H., Heinzl, N., Hebbelmann, I., Rolletschek, H., & Schwender, J.** (2014). Integration of a constraint-based metabolic model of *Brassica napus* developing seeds with  $^{13}\text{C}$ -metabolic flux analysis. *Frontiers in Plant Science*, 5, 724.
- HeneenWK, KarlssonG, Brismar K, Gummeson PO, Marttila S, Leonova S, Carlsson AS, Bafor M, Banas A, Mattsson B, et al.** (2008) Fusion of oil bodies in endosperm of oat grains. *Planta* 228: 589–599
- Herman, E.M., Tague, B.W., Hoffman, L.M., and Kjemtrup, S.E.** (1990). Retention of phytohemagglutinin with carboxyterminal tetrapeptide KDEL in the nuclear envelope and the endoplasmic reticulum. *Planta* 182, 305–312.
- Hesse H, Hoefgen R.** (2003). Molecular aspects of methionine biosynthesis in *Arabidopsis* and potato. *Trends in Plant Science* 8, 259–262.
- Hill L. M., Morley-Smith E. R., Rawsthorne S.** (2003) Metabolism of sugars in the endosperm of developing seeds of oilseed rape. *Plant Physiol.* 1316(1):228–236.
- Hills M.J.** (2004) Control of storage product synthesis in seeds. *Current Opinion in Plant Biology* Volume 7, Issue 3, Pages 302–308.
- Hitz, W.D., Mauvis, C.J., Ripp, K.G., Reiter, R.J., DeBonte, L., and Chen, 2.** (1995). The use of cloned rapeseed genes for cytoplasmic fatty acid desaturases and the plastid acyl-ACP thioesterases to alter relative levels of polyunsaturated and saturated

fatty acids in rapeseed oil. In *Rapeseed Today and Tomorrow: Proceedings of the Ninth International Rapeseed Congress*, 4-7 July, 1995, Cambridge, United Kingdom, D. Murphy, J. MacLeod, and D.S. Kimber, eds (Cambridge, UK: Organizing Committee of the Ninth International Rapeseed Congress), pp. 470-472.

**Hruz, T., et al.** (2008). Genevestigator V3: a reference expression database for the meta-analysis of transcriptomes. *Adv. Bioinformatics*.2008, 420747.

**Hsieh K, Huang AHC** (2004) Endoplasmic reticulum, oleosins, and oils in seeds and tapetum cells. *Plant Physiol* 136: 3427–3434

**Hua W, Li RJ, Zhan GM, Liu J, Li J, Wang XF, Liu GH, Wang HZ.** (2012) Maternal control of seed oil content in *Brassica napus*: the role of silique wall photosynthesis. *The Plant Journal* 69:432-444.

**Huang, A.H.C.** (1992). Oilbodies and oleosins in seeds. *Annu. Rev. Plant Physiol. Plant Mol. Biol.* 43, 177–200.

**Huang, A.H.C.** (1996). Oleosins and oil bodies in seeds and other organs. *Plant Physiol* 110: 1055–1061

**Jako C, Kumar A, Wei Y, Zou J, Barton DL, Giblin EM, Covello PS, Taylor DC.** (2001) Seed-specific over-expression of an *Arabidopsis* cDNA encoding a diacylglycerol acyltransferase enhances seed oil content and seed weight. *Plant Physiol* 126: 861–874

**Jolivet, P., Roux, E., d'Andrea, S., Davanture, M., Negroni, L., Zivy, M., and Chardot, T.** (2004). Protein composition of oilbodies in *Arabidopsis thaliana* ecotype WS. *Plant Physiol. Biochem.* 42501–509.

**Kachroo, A., Shanklin, J., Whittle, E., Lapchyk, L., Hildebrand, D., and Kachroo, P.** (2007). The *Arabidopsis* stearyl-acyl carrier protein-desaturase family and the contribution of leaf isoforms to oleic acid synthesis. *Plant Mol. Biol.* 63:257–271

**Kang D, Gho SG, Suh M, Kang C.** (2002) Highly Sensitive and Fast Protein Detection with Coomassie Brilliant Blue in Sodium Dodecyl Sulfate-Polyacrylamide Gel Electrophoresis. *Bull. Korean Chem. Soc.* 11:1511–1512.

**Kataoka T, Watanabe-Takahashi A, Hayashi N, Ohnishi M, Mimura T, Buchner P, Hawkesford MJ, Yamaya T, Takahashi H.** (2004). Vacuolar sulphate transporters are essential determinants controlling internal distribution of sulphate in *Arabidopsis*. *The Plant Cell* 16:2693–2704.

**Kawashima, T. and Goldberg, R.B.** (2010) The suspensor: not just suspending the embryo. *Trends In Plant Science* 15, 23-30.

**Keiller, D.R. and Mathers, J.C.,** (1983). Preparation of 14 Carbon-Labelled Plant Material for liquid Scintillation Counting. *Int. J. App Radiat. Isotopes*, 34, pp.1479-1481.

- Kelly, A.A., van Erp, H., Quettier, A.L., Shaw, E., Menard, G., Kurup, S., and Eastmond, P.J.** (2013). The sugar-dependent 1 lipase limits triacylglycerol accumulation in vegetative tissues of *Arabidopsis*. *Plant Physiol.* 162: 1282–1289
- Kennedy E. P.** (1961). Biosynthesis of complex lipids. *Fed. Proc.* 20 934–940.
- Khan D., Millar JL., Girard IJ et al.** (2015). Transcriptome atlas of the *Arabidopsis* funiculus—a study of maternal seed subregions. *The Plant Journal* 82, 41–53.
- Klodmann J., Sunderhaus S., Nimtz M., Jansch L., Braun HP** (2010). Internal architecture of mitochondrial complex I from *Arabidopsis thaliana*. *The Plant Cell* 22, 797–810.
- Kim MJ, Yang SW, Mao HZ, Veena SP, Yin JL, Chua NH.** (2014) Gene silencing of Sugar-dependent 1 (JcSDP1), encoding a patatin-domain triacylglycerol lipase, enhances seed oil accumulation in *Jatropha curcas*. *Biotechnol Biofuels* 7: 36.
- Kimber, D.S. and D.I. McGregor.** (1995). The species and their origin, cultivation and world production. In: *Brassica Oilseed; Production and Utilization*. (Eds.): D.S. Kimber and D.I. McGregor. Centre for Agriculture and Biosciences International, University Press, Cambridge, pp. 1-7.
- King, S.P., Lunn, J.E., and Furbank, R.T.** (1997). Carbohydrate content and enzyme metabolism in developing canola siliques. *Plant Physiol.* 114, 153–160.
- Kohno-Murase, J., Murase, M., Ichikawa, H. and Imamura, J.** (1994) Effects of antisense napin gene on seed storage compounds in transgenic *Brassica napus* seeds. *Plant Mol. Biol.* 26, 1115–1124.
- Kohno-Murase J, Murase M, Ichikawa H, Imamura J.** (1995) Improvement in the quality of seed storage protein by transformation of *Brassica napus* with an antisense gene for cruciferin. *Theoretical and Applied Genetics* 91:627-631.
- Koprivova A., Giovannetti M., Baraniecka P., Lee B. R., Grondin C., Loudet O., et al.** (2013). Natural variation in the ATPS1 isoform of ATP sulfurylase contributes to the control of sulfate levels in *Arabidopsis*. *Plant Physiol.* 163 1133–1141.
- Krebbers E, Seurinck J, Herdies L, Cashmore A, Timko M.** (1988) Four genes in two diverged subfamilies encode the ribulose-1,5-bisphosphate carboxylase small subunit polypeptides of *Arabidopsis thaliana*. *Plant Mol Biol.* 11:745–759.
- Kroj, T., Savino, G., Valon, C., Giraudat, J., and Parcy, F.** (2003). Regulation of storage protein gene expression in *Arabidopsis*. *Development* 130 6065–6073.
- Langmead B, Salzberg S.** (2012) Fast gapped-read alignment with Bowtie 2. *Nature Methods.* 9:357-359.

- Lark, K.G., Orf, J., Mansur, L.M.** (1994) Epistatic expression of quantitative trait loci (QTL) in soybean [*Glycine max* (L.) Merr.] determined by QTL association with RFLP alleles. *Theor. Appl. Genet.* 88:486–489.
- Lee, W.S., Tzen, J.T.C., Kridl, J.C., Radke, S.E., and Huang, A.H.C.** (1991). Maize oleosin is correctly targeted to seed oil bodies in *Brassica napus* transformed with the maize oleosin gene. *Proc. Natl. Acad. Sci. USA* 88 6181–6185.
- Lee Y. J., Perdian D. C., Song Z. H., Yeung E. S., Nikolau B. J.** (2012). Use of mass spectrometry for imaging metabolites in plants. *Plant J.* 70, 81–95. doi:10.1111/j.1365-3113.2012.04899.x
- Leprince, O., vanAelst, A.C., Pritchard, H.W., and Murphy, D.J.** (1998). Oleosins prevent oil-body coalescence during seed imbibition as suggested by a low-temperature scanning electron microscope study of desiccation-tolerant and -sensitive oilseeds. *Planta* 204 109–119.
- Li RJ, Wang HZ, Mao H, Lu YT, Hua W.** (2006) Identification of differentially expressed genes in seeds of two near-isogenic *Brassica napus* lines with different oil content. *Planta.* 224:952–962.
- Li, B. and Dewey, C. N.** (2011). RSEM: accurate transcript quantification from RNA-Seq data with or without a reference genome. *BMC Bioinformatics.* 12:323.
- Li-Beisson Y., Shorrosh B., Beisson F., Andersson M., Arondel V., Bates P., et al.** (2010). Acyl-lipid metabolism. *Arabidopsis Book* 8 e0133. doi:10.1199/tab.0133
- Lin L, Liu YG, Xu X, Li B** (2003). Efficient linking and transfer of multiple genes by a multigene assembly and transformation vector system. *Proc Natl Acad Sci USA* 100: 5962–5967
- Lin JT, Chen GQ** (2012) Identification of minor acylglycerols less polar than triricinolein in castor oil by mass spectrometry. *J Am Oil Chem Soc* 89:1773–1784
- Lin Y., Pajak A., Marsolais F., McCourt P., Riggs C. D.** (2013). Characterization of a cruciferin deficient mutant of *Arabidopsis* and its utility for overexpression of foreign proteins in plants. *PLoS ONE* 8:e64980. doi:10.1371/journal.pone.0064980
- Liu WX., Hua Liang Liu, Le Qing Qu** (2013). Embryo-specific expression of soybean oleosin altered oil body morphogenesis and increased lipid content in transgenic rice seeds *Theoretical and Applied Genetics* Volume 126, Issue 9, pp 2289-2297
- Livak KJ, Schmittgen TD** (2001) Analysis of relative gene expression data using real-time quantitative PCR and the  $2^{-\Delta\Delta C(T)}$  Method. *Methods* 25 (4): 402–408.

- Lönnerdal, B. & Janson, J.-C.** (1972). Studies on Brassica seed proteins: I. The low molecular weight proteins in rapeseed. Isolation and characterization. *Biochimica et Biophysica Acta (BBA)-Protein Structure*, 278(1), pp. 175-183
- Lorenz C., Rolletschek H., Sunderhaus S., Braun HP.** (2014). *Brassica napus* seed endosperm — Metabolism and signaling in a dead end tissue. *Journal of Proteomics* 108, 382–426.
- Los DA., Murata N.** (1998). Structure and expression of fatty acid desaturases. *Biochimica et Biophysica Acta* 1394: 3–15.
- Lutziger I., Oliver DJ.** (2000). Molecular evidence of a unique lipoamide dehydrogenase in plastids: analysis of plastidic lipoamide dehydrogenase from *Arabidopsis thaliana*. *FEBS Lett* 484:12–16.
- Mailer R.** (2009). Grain quality. In: McCaffery D, Potter T, Marcroft S, Pritchard F (Eds). *Canola best practice management guide for south-eastern Australia*. Grains Research and Development Corporation, New South Wales, Australia pp 7-10.
- Major, D.J. and Charnetski, W.A.** (1976) Distribution of 14carbon-labelled assimilates in flowering plants of oilseed rape (*Brassica napus L.*). *Can. J. Plant Sci.* 58, 783–787.
- Marion-Poll A.** (1997) ABA and seed development. *Trends Plant Sci.*, 2 447-448
- Martin N, Wernersson J, Valsecchi I, Ezcurra I, Rask L.** (2008) bHLH and bZIP factors target the G-box of the RY/G cluster in the seed storage protein *napA* promoter. Manuscript
- McCleary BV, Matheson NK.** (1975). Galactomannan structure and b-mannanase and b-mannosidase activity in germinating legume seeds. *Phytochemistry* 14, 1187–1194
- Meharg AA.** (1994). Integrated tolerance mechanisms – constitutive and adaptive plant- responses to elevated metal concentrations in the environment. *Plant, Cell & Environment* 17: 989–993.
- Mendham, N. J.; Salisbury, P. A.** (1995) Physiology: crop development, growth and yield. In: Kimber, D.; McGregor, D. I. (Eds.). *Brassica oilseeds: production and utilization*. Cambridge: CAB. p. 11-64
- Mihr C., Braun HP.** (2003) Proteomics in plant biology. In: Michael P . ed. *Handbook of proteomics methods* . Totowa: Humana, 409–416.
- Miquel, M., Trigui, G., d'Andrea, S., Kelemen, Z., Baud, S., Berger, A., Deruyffelaere, C., Trubuil, A., Lepiniec, L. and Dubreucq, B.** (2014). Specialization

of oleosins in oil body dynamics during seed development in *Arabidopsis* seeds. *Plant Physiol* 164(4): 1866-1878.

**Mogensen, V.O., Jensen, C.R., Mortensen, G., Andersen, M.N., Schjoerring, J.K., Thage, J.H. and Koribidis, J.** (1997) Pod photosynthesis and drought adaptation of field grown rape (*Brassica napus* L.). *Eur. J. Agron.* 6, 295–307.

**Möller B., Weijers D.** (2009). Auxin control of embryo patterning. *Cold Spring Harb. Perspect. Biol.* 1:a001545. 10.1101

**Morley-Smith E.R., Pike M.J., Findlay K., Köckenberger W., Hill L.M., Smith A.M., Rawsthorne S.** (2008). The transport of sugars to developing embryos is not via the bulk endosperm in oilseed rape seeds. *Plant Physiol.* 147: 2121–2130

**Murphy D.J., Cummins I.** (1989). Biosynthesis of seed storage products during embryogenesis in rapeseed, *Brassica napus*. *Plant Physiol.* 135 3–69. 10.1016/S0176-1617(89)80225-1

**Nagaraj S, Lei Z, Watson B, Sumner L, Gallardo K, Dumas-Gaudot E, Recorbet G, Robert F, Thiery O, Valot B, Mathesius U, Triplett E.** (2007) In: *The Medicago truncatula handbook*. Mathesius U, Journet EP, Sumner LW, editors. ISBN 0–9754303–1–9

**Nakabayashi K, Okamoto M, Koshiha T, Kamiya Y, Nambara E** (2005) Genome-wide profiling of stored mRNA in *Arabidopsis thaliana* seed germination: epigenetic and genetic regulation of transcription in seed. *Plant J* 41: 697–709

**Nam HJ, Jeon J, Kim S.** (2009) Bioinformatic approaches for the structure and function of membrane proteins. *BMB Rep.* 30;42(11):697-704.

**Nambara E., Marion-Polla A.** (2003) ABA action and interactions in seeds. *Trends Plant Sci.* 8(5):213-7.

**Napier J. A.** (2007) The production of unusual fatty acids in transgenic plants. *Annu. Rev. Plant Biol.*, 58, 295–319.

**Neuhoff V., Stamm R., Eibl H** (1985). Clear background and highly sensitive protein staining with coomassie blue dyes in polyacrylamide gels: a systematic analysis. *Electrophoresis* 6, 427–448.

**Neuhoff V., Stamm R., Pardowitz I., Arold N., Ehrhardt W., Taube D** (1990). Essential problems in quantification of proteins following colloidal staining with coomassie brilliant blue dyes in polyacrylamide gels, and their solution. *Electrophoresis* 11, 101–117.

**Nietzel T., Dudkina NV, Haase C, Denolf P, Semchonok DA, Boekema EJ, Braun HP, Sunderhaus S.** (2013) The native structure and composition of the cruciferin complex in *Brassica napus*. *J Biol Chem.* 2013 Jan 25;288(4):2238-45

**Nikiforova VJ,**

**Kopka J, Tolstikov V, Fiehn O, Hopkins L, Hawkesford MJ, Hesse H, Hoeffgen R** (2005) Systems rebalancing of metabolism in response to sulfur deprivation, as revealed by metabolome analysis of *Arabidopsis* plants. *Plant Physiol* 138: 304–318

**O’Leary, B., Park, J. and Plaxton, W.C.** (2011) The remarkable diversity of plant PEPC (phosphoenolpyruvate carboxylase): recent insights into the physiological functions and post-translational controls of non-photosynthetic PEPCs. *Biochem. J.* 436, 15–34.

**O’Neill CM., Gill S., Hobbs D., Morgan C. and Bancroft I.** (2003). Natural variation for seed lipid traits in *Arabidopsis thaliana* *Phytochemistry* 64: 1077-1090

**Parthibane V., Rajakumari S., Venkateshwari V., Iyappan R., Rajasekharan R.** (2012). Oleosin is bifunctional enzyme that has both monoacylglycerol acyltransferase and phospholipase activities. *J. Biol. Chem.* 287 1946–1954. 10.1074/jbc.M111.309955

**Periappuram, C., Steinhauer, L., Barton, D.L., Taylor, D.C., Chatson, B., and Zou, J.** (2000). The plastidic phosphoglucomutase from *Arabidopsis*. A reversible enzyme reaction with an important role in metabolic control. *Plant Physiol.* 122 1193–1199.

**Perry HJ, Harwood JW.** (1993) Radiolabeling studies of acyl lipids in developing seeds of *Brassica napus*: use of [<sup>14</sup>C]acetate precursor. *Phytochemistry.* 33:329–333.

**Perry HJ, Bligny R, Gout E, Harwood JL** (1999) Changes in Kennedy pathway intermediates associated with increased triacylglycerol synthesis in oil-seed rape. *Phytochemistry* 52: 799-804

**Peukert M., Matros A., Lattanzio G., Kaspar S., Abadía J., Mock H.-P.** (2012). Spatially resolved analysis of small molecules by matrix-assisted laser desorption/ionization mass spectrometric imaging (MALDI-MSI). *New Phytol.* 193, 806–815. 10.1111/j.1469-8137.2011.03970.x

**Phillips J, Artsaenko O, Fiedler U, Horstmann C, Mock H-P, Muentz K, Conrad U.** (1997) Seed-specific immunomodulation of abscisic acid activity induces a developmental switch. *EMBO J.* 16:4489–4496.

**Post-Beittenmiller D, Jaworski JG, Ohlrogge JB.** (1991) In vivo pools of free and acylated acyl carrier proteins in spinach: evidence for sites of regulation of fatty acid biosynthesis. *J Biol Chem.*;266:1858–1865.

- Post-Beittenmiller D, Roughan G, Ohlrogge J.** (1992) Regulation of plant fatty acid biosynthesis: analysis of acyl-CoA and acyl-acyl carrier protein substrate pools in spinach and pea chloroplasts. *Plant Physiol.* ;100:923–930.
- Radetzky, R. and Langheinrich, U.** (1994) Induction of accumulation and degradation of the 18.4-kDa oleosin in a triacylglycerol-storing cell culture of anise (*Pimpinella anisum* L.). *Planta* 194: 1-8.
- Rawsthorne S.** (2002) Carbon flux and fatty acid synthesis in plants. *Prog Lipid Res* 41: 182-196
- Ritchie R.J., Fieuw-Makaroff S., Patrick J.W.** (2003). Sugar retrieval by coats of developing seeds of *Phaseolus vulgaris* L. and *Vicia faba* L. *Plant Cell Physiol.* 44: 163–172.
- Roberts A., et al.** (2011) Improving RNA-Seq expression estimates by correcting for fragment bias. *Genome Biol.*12:R22.
- Rödin J., Ericson M. L., Josefsson L. G. and Rask L.** (1990), Characterization of a cDNA clone encoding a *Brassica napus* 12 S protein (cruciferin) subunit. *J. Biol. Chem.* 265, 2720-2723.
- Roesler KR, Shintani D, Savage L, Boddupalli S, Ohlrogge JB.** (1997) Targeting of the *Arabidopsis* homomeric acetyl-coenzyme A carboxylase to *Brassica napus* seed plastids. *Plant Physiol.* 113:75–81
- Rolletschek H, Borisjuk L, Radchuk R, Miranda M, Heim U, Wobus U, Weber H** (2004) Seed-specific expression of a bacterial phosphoenolpyruvate carboxylase in *Vicia narbonensis* increases protein content and improves carbon economy. *Plant Biotechnol J* 2: 211–219
- Rolletschek H, Fuchs J, Friedel S, Börner A, Todt H, Jakob PM, Borisjuk L.** (2015). A novel non-invasive procedure for high-throughput screening of major seed traits. *Plant Biotech J* 13: 188-199
- Roughan PG.** (1997) Stromal concentrations of coenzyme A and its esters are insufficient to account for rates of chloroplast fatty acid synthesis: evidence for substrate channelling within the chloroplast fatty acid synthase. *Biochem J.*;327:267–273.
- Ruuska, S.A., and Ohlrogge, J.B.** (2001). Protocol for small-scale RNA isolation and transcriptional profiling of developing *Arabidopsis* seeds. *Biotechniques* 31, 752–758.
- Saito, C., Ueda, T., Abe, H., Wada, Y., Kuroiwa, T., Hisada, A., Furuya, M., and Nakano, A.** (2002). A complex and mobile structure forms a distinct subregion within the continuous vacuolar membrane in young cotyledons of *Arabidopsis*. *Plant J.* 29, 245–255.



- Saito, K.** (2004). Sulfur assimilatory metabolism. The long and smelling road. *Plant Physiol.* 136 2443–2450.
- Santos-Mendoza M, Dubreucq B, Baud S, Parcy F, Caboche M, Lepiniec L.** (2008). Deciphering gene regulatory networks that control seed development and maturation in *Arabidopsis*. *Plant J* 54: 608–620
- Sasaki Y. and Nagano Y.** (2004), Plant acetyl-CoA carboxylase: structure, biosynthesis, regulation, and gene manipulation for plant breeding. *Biosci. Biotechnol. Biochem.* 68, 1175 – 1184
- Schmidt M. A., Herman E. M.** (2008). The collateral protein compensation mechanism can be exploited to enhance foreign protein accumulation in soybean seeds. *Plant Biotechnol. J.* 6 832–842 10.1111/j.1467-7652.2008.00364.x
- Schwender J, Ohlrogge J, Shachar-Hill Y.** (2004). Understanding flux in plant metabolic networks. *Current Opinion in Plant Biology* 7, 309–317
- Schwender J., Shachar-Hill Y., Ohlrogge J. B.** (2006). Mitochondrial metabolism in developing embryos of *Brassica napus*. *J. Biol. Chem.* 281, 34040–34047
- Schwender J.** (2008). Metabolic flux analysis as a tool in metabolic engineering of plants. *Current Opinion in Biotechnology* 19,131–137
- Schwender J., König C., Klapperstück M., Heinzl N., Münz E., Hebbelmann I., et al.** (2014). Transcript abundance on its own cannot be used to infer fluxes in central metabolism. *Front. Plant Sci.* 5:668 10.3389/fpls.2014.00668
- Schwender J, Hebbelmann I, Heinzl N, Hildebrandt T, Naik D, Rogers A, Klapperstück M, Braun H-P, Schreiber F, Denolf, P, Borisjuk L, Rolletschek H.** (2015). Quantitative multilevel analysis of central metabolism in developing oilseeds of *Brassica napus* during *in vitro* culture. *Plant Physiology* 168: 828-848.
- Scossa F., Laudencia-Chinguanco D., Anderson O. D., Vensel W. H., Lafiandra D., D'Ovidio R., et al.** (2008). Comparative proteomic and transcriptional profiling of a bread wheat cultivar and its derived transgenic line overexpressing a low molecular weight glutenin subunit gene in the endosperm. *Proteomics* 8, 2948–2966. 10.1002/pmic.200700861
- Sexton PJ, Shibles RM** (1999). Activity of ATP sulfurylase in reproductive soybean. *Crop Science* 39:131-135.
- Sheen, J.** (1999). C4 gene expression. *Annu. Rev. Plant Physiol. Plant Mol. Biol.* 50, 187–217.
- Sheoran IS, Sawhney V, Babbar S, Singh R.** (1991). *In vivo* fixation of CO<sub>2</sub> by attached pods of *Brassica campestris* L. *Annals of Botany* 67, 425–428.

- Shi J, Yi K, Liu Y, Xie L, Zhou Z, Chen Y, Hu Z, Zheng T, Liu R, Chen Y, et al.** (2015) Phosphoenolpyruvate carboxylase in Arabidopsis leaves plays a crucial role in carbon and nitrogen metabolism. *Plant Physiol* 167: 671–681
- Shields, J.A., Paul, E.A.** (1973). Decomposition of C14 labelled plant material under field conditions. *Can. J. Soil Sci.* 53, 297-306.
- Shimada, T.L., Shimada, T., Takahashi, H., Fukao, Y. and Hara-Nishimura, I.** (2008) A novel role of oleosins in freezing tolerance of oilseeds in Arabidopsis thaliana. *Plant J.* 55, 798–809.
- Siloto, R.M.P., Findlay, K., Lopez-Villalobos, A., Yeung, E.C., Nykiforuk, C.L. and Moloney, M.M.** (2006) The accumulation of oleosins determines the size of seed oil-bodies in Arabidopsis. *Plant Cell* 18, 1961–1974.
- Singal, H.R., Sheoran, I.S. and Singh, R.** (1987) Photosynthetic carbon fixation characteristics of fruiting structures of Brassica campestris L. *Plant Physiol.* 83, 1043–1047.
- Singal, H.R., I.S. Sheoran and R. Singh.** (1992). Photosynthetic contribution of pods towards seed yield in Brassica. *P. Indian Natl. Sci. Acad.*, 58: 365-370.
- Slesak, H., Przywara, L.,** (2003). The effect of carbohydrate source on the development of Brassica napus L. immature embryos in vitro. *Acta Biol. Crac. Ser. Bot.* 45, 183–190.
- Snowdon R., Lühs W. and Friedt W.** (2007) Oilseed rape. *In: Kole C. (ed.) Genome mapping and molecular breeding in plants, vol. 2: Oilseeds*, Springer, Berlin Heidelberg, pp. 55–114.
- Soltani, A., M. Gholipour and E. Zeinali,** (2006). Seed reserve utilization and seedling growth of wheat as affected by drought and salinity. *Environ. Exp. Bot.*, 55: 195-200.
- Sosulski, F.W. & G.I. Imafidon.** (1990). Amino acid composition and nitrogen-to-protein conversion factors for animal and plant foods. *J. Agric. Food. Chem.*, 38: 1351-1356.
- Stadler, R., Lauterbach, C., and Sauer, N.** (2005). Cell-to-cell movement of green fluorescent protein reveals post-phloem transport in the outer integument and identifies symplastic domains in Arabidopsis seeds and embryos. *Plant Physiol.* 139: 701–712.
- Stålberg K, Ellerstrom M, Josefsson L-G, Rask L** (1993) Deletion analysis of a 2S seed storage protein promoter of Brassica napus in transgenic tobacco. *Plant Mol Biol* 23: 671–683
- Stålberg K., Ellerstöm M., Ezcurra I., Ablov S., Rask L.** (1996). Disruption of an overlapping E-box/ABRE motif abolished high transcription of the napA storage-protein promoter in transgenic Brassica napus seeds. *Planta* 199 515–519.

- Stitt M.** (1999). Nitrate and the regulation of primary metabolism, allocation and growth. *Current Opinion in Plant Science* 2, 178–186.
- Subramanyam K, Sailaja KV, Subramanyam K, Rao DM, Lakshmidevi K** (2010) Ectopic expression of an osmotin gene leads to enhanced salt tolerance in transgenic chilli pepper (*Capsicum annum* L.). *Plant Cell Tissue Organ Cult* 105:181–192
- Suzuki M., M.G. Ketterling, D.R. McCarty.** (2005) Quantitative statistical analysis of cis-regulatory sequences in ABA/VP1- and CBF/DREB1-regulated genes of *Arabidopsis*. *Plant Physiol*, 139, pp. 437–447
- Svejar T.J., Boutton T.W. & Trent J.D.** (1990) Assessment of carbon allocation with stable carbon isotope labeling. *Agronomy Journal* 82, 18–21.
- Tabe L, Droux M** (2002) Limits to sulfur accumulation in transgenic Lupin seeds expressing a foreign sulfur-rich protein. *Plant Physiol*. 128, 1137–1148.
- Takahashi H., Kopriva S., Giordano M., Saito K., Hell R.** (2011). Sulfur assimilation in photosynthetic organisms: molecular functions and regulations of transporters and assimilatory enzymes. *Annu. Rev. Plant Biol.* 62 157–184
- Tamura K., Shimada T., Kondo M., Nishimura M., Nishimura I. H.** (2005). KATAMARI1/MURUS3 is a novel Golgi membrane protein that is required for endomembrane organization in *Arabidopsis*. *Plant Cell* 17, 1764–1776. doi:10.1105/tpc.105.031930
- Tauchi-Sato K, Ozeki S, Houjou T, Taguchi R, Fujimoto T** (2002). The surface of lipid droplets is a phospholipid monolayer with a unique fatty acid composition. *J Biol Chem* 277: 44507–44512
- Thelen, J.J. and Ohlrogge, J.B.** (2002) Metabolic engineering of fatty acid biosynthesis in plants. *Metab. Eng.* 4, 12–21.
- Thelen, J.J. and Ohlrogge, J.B.** (2002) Both antisense and sense expression of biotin carboxyl carrier protein isoform 2 inactivates the plastid acetyl-coenzyme A carboxylase in *Arabidopsis thaliana*. *Plant J.* 32, 419–431.
- Theodoulou FL, Eastmond PJ.** (2012). Seed storage oil catabolism: a story of give and take. *Current Opinion in Plant Biology* 15, 322–328.
- Thompson R B** (1996) Pulse-labelling a cover crop with <sup>13</sup>C to follow its decomposition in soil under field conditions. *Plant Soil* 180, 49–55.
- Ting, J.T.L., Lee, K.Y., Ratnayake, C., Platt, K.A., Balsamo, R.A., and Huang, A.H.C** (1996). Oleosin genes in maize kernels having diverse oil contents are constitutively expressed independent of oil contents: size and shape of intracellular oilbodies are determined by the oleosins oils ratio. *Planta* 199: 158–165

- Trapnell, C., Pachter, L. & Salzberg, S.** (2009) TopHat: discovering splice junctions with RNA-Seq. *Bioinformatics* 25, 1105–1111.
- Turnham, E. and Northcote, D.H.** (1983) Changes in the activity of acetyl-CoA carboxylase during rape-seed formation. *Biochem. J.* 15, 223–229.
- Tzen JT, Huang AH.** (1992) Surface structure and properties of plant seed oil bodies. *J Cell Biol.* 117(2):327–335.
- Tzen JT, Lie GC, Huang AH.** (1992) Characterization of the charged components and their topology on the surface of plant seed oil bodies. *J Biol Chem.* 5;267(22):15626–15634.
- Tzen, J.T.C, Cao, Y.Z., Laurent, P., Ratnayake, C. and Huang, A.H.C.** (1993) Lipids, proteins, and structure of seed oil bodies from diverse species. *Plant Physiol.* 101:267-276.
- Uemura, T., Yoshimura, S.H., Takeyasu, K., and Sato, M.H.** (2002). Vacuolar membrane dynamics revealed by GFP-AtVam3 fusion protein. *Genes Cells* 7,743–753.
- Van der Klei H., Van Damme J., Casteels P., Krebbers E.** (1993) A fifth 2S albumin isoform is present in *Arabidopsis thaliana*. *Plant Physiol.* 1016(1):1415–1416.
- van Erp H, Kelly AA, Menard G, Eastmond PJ** (2014) Multigene engineering of triacylglycerol metabolism boosts seed oil content in *Arabidopsis*. *Plant Physiol* 165: 30–36
- Vanhercke T, El Tahchy A, Shrestha P, Zhou XR, Singh SP, Petrie JR.** (2013) Synergistic effect of WRI1 and DGAT1 coexpression on triacylglycerol biosynthesis in plants. *FEBS Lett* 587: 364–369
- Vermachova M, Purkrtova Z, Santrucek J, Jolivet P, Chardot T, Kodicek M** (2011) New protein isoforms identified within *Arabidopsis thaliana* seed oilbodies combining chymotrypsin/trypsin digestion and peptide fragmentation analysis. *Proteomics* 11:3430–3434
- Vigeolas H, Waldeck P, Zank T, Geigenberger P.** (2007) Increasing seed oil content in oil-seed rape (*Brassica napus* L.) by over-expression of a yeast glycerol-3-phosphate dehydrogenase under the control of a seed-specific promoter. *Plant Biotechnol J* 5: 431–441
- Walther T.C., Farese R.V., Jr** (2012). Lipid droplets and cellular lipid metabolism. *Annu. Rev. Biochem.* 81:687–714 10.1146/annurev-biochem-061009-102430
- Ward JM, Kühn C, Tegeder M, Frommer WB** (1998) Sucrose transport in higher plants. *Int Rev Cytol* 178 41–71

- Warembourg F. R. & Kummerow J.** (1991) in Carbon Isotope Techniques. (eds. Coleman D. C., & Fry B.) 11–37 (Academic Press, Inc., San Diego)
- Weber H, Heim U, Borisjuk L, Wobus U** (1995) Cell-type specific, coordinate expression of two ADP-glucose pyrophosphorylase genes in relation to starch biosynthesis during seed development in *Vicia faba* L. *Planta* 195: 352–361
- Weber H., Borisjuk L., Wobus U.** (2005). Molecular physiology of legume seed development. *Annu. Rev. Plant Biol.* 56 253–279  
10.1146/annurev.arplant.56.032604.144201
- Wei Y, Dong M, Huang ZY, Tan DY** (2008). Factors influencing seed germination of *Salsola affinis*, a dominant annual halophyte inhabiting the deserts of Xinjiang, China. *Flora*. 203:134–140.
- Weselake RJ, Shah S, Tang M, Quant PA, Snyder CL, Furukawa-Stoffer TL, Zhu W, Taylor DC, Zou J, Kumar A, et al.** (2008) Metabolic control analysis is helpful for informed genetic manipulation of oilseed rape (*Brassica napus*) to increase seed oil content. *J Exp Bot* 59: 3543–3549
- Weselake RJ, Taylor DC, Rahman MH, Shah S, Laroche A, McVetty PB, Harwood JL.** (2009) Increasing the flow of carbon into seed oil. *Biotechnol Adv* 27: 866–878
- West MAL, Harada JJ** (1993) Embryogenesis in higher plants: an overview. *Plant Cell* 5: 1361-1369
- Wilfling F, Wang H, Haas JT, Krahmer N, Gould TJ, Uchida A, Cheng JX, Graham M, Christiano R, Frohlich F, Liu X, Buhman KK, Coleman RA, Bewersdorf J, Farese RV Jnr, Walther TC.** (2013). Triacylglycerol synthesis enzymes mediate lipid droplet growth by relocalizing from the ER to lipid droplets. *Developmental Cell* 24:384–399.
- Wobus, U., and Weber, H.** (1999). Seed maturation: Genetic programmes and control signals. *Curr. Opin. Plant Biol.* 2, 33–38.
- Yang L., Ding Y., Chen Y., Zhang S., Huo C., Wang Y., Yu J., Zhang P., Na H., Zhang H., et al.** (2012). The proteomics of lipid droplets: structure, dynamics, and functions of the organelle conserved from bacteria to humans. *J. Lipid Res.*
- Yatsu IY, Jacks TJ** (1972) Spherosome membranes. Half-unit membranes. *Plant Physiol* 49: 937-943
- Yeung EC, Clutter ME.**(1979) Embryogeny of *Phaseolus coccineus*: the ultrastructure and development of the suspensor. *Can J Bot.* 57:120–136. doi: 10.1139/b79-021.

---

**Zhou Y., Qu H., Dibley K.E., Offler C.E., Patrick J.W. (2007).** A suite of sucrose transporters expressed in coats of developing legume seeds includes novel pH-independent facilitators. *Plant J.* 49: 750–764.

## Appendix

### Curriculum Vitae

Name	Christina König
Date of Birth	03.03.1987
Place of Birth	Nauen
Citizenship	Citizen of Germany

---

### School Education

1993-1994	Primary School in Radegast
1994-1997	Primary School in Köthen
1997-1999	Förderstufe „Naumannschule“ Köthen
1999-2006	“Ludwigsgymnasium Köthen“ - Qualification A-level

---

### Academic education

Oct 2006 – May 2012	<p>Student at the Martin Luther Universität Halle - Wittenberg – Diploma in Biology /Department of Plant Genetics</p> <p>Thesis: „Etablierung der <i>Agrobacterium tumefaciens</i> – vermittelten Virus - basierten Expression von Typ - III - Effektoren aus <i>Xanthomonas campestris pv. vesicatoria in planta</i>“</p>
Sept 2012 – Juni 2016	<p>PhD Student at the Leibniz Institute for Plant Genetics and Crop Plant Research in the Research Group of NMR and Assimilate Allocation, Dr. Ljudmilla Borisjuk in cooperation with the Leibniz Universität Hannover, Institute of Plant Genetics, Department of Plant-Proteomics, Prof. Dr. Hans-Peter Braun</p>

## List of publications

Schwender J, **König C**, Klapperstück M, Heinzl N, Munz E, Hebbelmann I, Hay J O, Denolf P, Bodt S D, Redestig H, Caestecker E, Jakob P M, Borisjuk L, Rolletschek H (2014)

Transcript abundance on its own cannot be used to infer fluxes in central metabolism.  
*Front. Plant Sci.* 5 - 668

## Conference contributions

### **29. Tagung der Molekularbiologie der Pflanzen** - Dabringhausen Februar 2016

Poster: „The use of <sup>13</sup>C-labelling in unravelling organspecific functions in developing rapeseed”

### **28. Tagung der Molekularbiologie der Pflanzen** – Dabringhausen Februar 2015

Lecture: „What transcriptomics can tell us about metabolic phenotypes: a case study based on the oilseed rape embryo”

### **Plant Science Student Conference** – Halle (Saale) Mai 2013

Poster: „Molecular and metabolic characterization of seed metabolism in oilseed rape (*Brassica napus*)”